

Report Number CCEER-93-05

**Effects of Hinge Restrainers  
on the Response of the  
San Gregorio Bridge  
during the Loma Prieta Earthquake**

Emmanuel M. Maragakis  
M. "Saïid" Saïidi  
Shiping Feng  
Linda Flournoy

Prepared for

**California Department of Transportation  
National Science Foundation  
and Nevada Department of Transportation**

**Center for Civil Engineering Earthquake Research  
Department of Civil Engineering  
University of Nevada  
Reno, Nevada 89557**

July 1993

## Abstract

The primary objective of this study is to study the effects of cable restrainers on the nonlinear seismic response of the San Gregorio Bridge. The computer program NEABS-86 was used in the nonlinear analyses.

The earthquake analyses focus on the relative displacements at the hinges, the restrainer stresses, and the abutment forces in both the longitudinal and the transverse directions of the bridge. The peak ground acceleration of the earthquake input, the seismic retrofit, the restrainer gap, and the hinge gap were varied. It was found that, in general, the cable restrainer system reduces the hinge responses in both the longitudinal and the transverse directions. Also found was that, when a zero restrainer gap is assumed, the hinge responses change significantly. It is recommended that the restrainer design be based on cases with both zero and non-zero restrainer gaps, to encompass all the critical forces, stresses and displacements.

Finally, some design methods for the longitudinal restrainer cable at intermediate hinges of the bridge were evaluated. A modified "Dynamic-Caltrans" design procedure was tested preliminarily, and showed some promising results.

## Acknowledgements

The study presented in this report was part of a project which has been mainly funded by the California Department of Transportation. Additional funds were provided by the National Science Foundation and the Nevada Department of Transportation (NDOT). The financial support of all the funding agencies is particularly acknowledged.

Mr. Mark Yashinsky, the Caltrans project monitor is thanked for providing valuable information and comments. Messrs Jim Roberts, the Caltrans Chief Bridge Engineer and Jim Gates, a Caltrans senior Bridge Engineer are also thanked for their close interaction with the principal investigators.

The support of Dr. S. C. Liu, the program manager at the National Science Foundation and the assistance of Mr. Floyd Marcucci, the Chief Bridge Engineer at NDOT and Mr. R. Obisanya, a staff engineer at Caltrans were much appreciated.

Mr. Saber Abdel-Ghaffar, a Doctoral student, and Mr. Dan O'Connor, a research engineer, are thanked for their valuable input to the modeling aspects of the study.

# Chapter 1

## Introduction

### 1.1 Background

Since the 1971 San Fernando Earthquake, the California Department of Transportation (Caltrans) has installed numerous earthquake restrainers as a retrofit measure on existing highway bridges throughout the state to avoid excessive displacements at hinges during strong earthquakes. Many other states are in the process of installing hinge restrainers to upgrade the seismic performance of their bridges. The design of restrainers has been based on a relatively simple equivalent static analysis method. No systematic study has yet been performed to evaluate the effectiveness of the restrainers in reducing or preventing damage.

During the Loma Prieta earthquake of October 17, 1989, many highway bridges with cable restrainers were subjected to relatively severe earthquake excitations. The availability of damage inspection reports of these bridges and earthquake records from strong-motion instruments in the area, presented an opportunity for a detailed evaluation of the role of the restrainers on the response of the bridges during the earthquake. A research project was awarded to the University of Nevada, Reno to perform such a study (Ref. 1). In this report, the analysis of one of the bridge,

the San Gregorio Bridge, is presented in detail.

## 1.2 Objective

The purpose of this report is to present the results of the analysis of the nonlinear response of the San Gregorio Bridge to the 1989 Loma Prieta earthquake. A nonlinear three-dimensional mathematical model of the San Gregorio bridge was developed based on the initial construction plans and the retrofit design information. The results which are primarily discussed in this report, are the response of the bridge with and without the restrainers and the effects of changes in the restrainer gap on the bridge performance during the earthquake. Also included in the report is the redesign of the restrainers using a more elaborate method.

Both the longitudinal and transverse responses of the San Gregorio bridge were considered in the cases studied. The focus of the earthquake analysis of the bridge was on the relative displacements at the hinges, the restrainer stresses, the abutment forces, and the pier ductility demands. Earthquake records with different peak accelerations were used to ensure that the effects of the ground motion variation are incorporated in the study.

## Chapter 2

### Bridge Description and Damage Summary

#### 2.1 Description

The San Gregorio Bridge, shown in Figure 2.1, is located in San Mateo County, about thirteen miles south of Half Moon Bay on Highway 1. Built in 1940, the bridge is a five-span reinforced concrete structure with an overall length of 265 feet and a height of 56 feet. The bridge elevation is higher at the south abutment than at the north abutment. The average vertical grade is 6 percent.

The deck section consists of a 8.125-inch thick reinforced concrete slab and three 20-inch wide rectangular girders with variable depth spaced on 10.5-foot centers. The maximum depth of the girders is 8.25 feet at the center of the bent and the minimum depth is 4.25 feet at the middle of the span. Typical cross-sections of the deck are shown in Figure 2.2. The two end spans are 42 feet long and the three middle spans are 59 feet long. The diaphragms are 10 inch thick at the abutments and 18 inch thick at the bents and at the midpoint of the middle span. The diaphragms located at the intermediate expansion hinges are 12 inch thick.

There are two basic types of bents supporting the

superstructure which are shown in Figure 2.3. The three columns at bent 2 are reverse-tapered rectangular columns, with the smallest section at the column base. Bents # 3, 4 and 5 consist of three tapered columns connected by diaphragms at the top and resting on 15 feet high walls. Both, the column and the wall, are tapered. Each column of bent #2 is connected to its concrete foundation by four No. 6 steel bars. The wall at bent 3, 4 and 5 is connected to its concrete foundation by thirty No. 6 steel bars.

Three expansion joints located in two end spans and the middle span (span 3 from the left) divide the bridge in four parts. The second span is continuous over bent 2 and bent 3 with cantilever section of 15 feet at the end span on its left and 44 feet at the middle span on its right. The fourth span continues over bents #4 and #5 with cantilever sections of 15 feet at both the right end span on its right and the middle span on its left. In the third span, the cantilever sections from the second span and fourth span rest on the expansion hinge. Each end span consists of a deck section simply supported on the expansion joint at one end and on concrete seats at each abutment on the other end.

The intermediate expansion joints are located at mid-height of the deck section, and have a gap of 1 inch at the joint seat. The intermediate hinge joints consist of two opposing 8 inch by 6 inch by 0.75 inch steel angles with an overall seat width of 8 inches, held in place by ten 0.375-inch diameter shear bolts. A detail of

the hinge is shown in Figure 2.4.

The seat-type abutments consist of a concrete seat of 30-inch and 7 feet wide, and a 12-inch, an approximately 7.6 foot high concrete backwall, and 5-foot long wingwalls located at either side of the backwall at a 4.8 to 12 batter. An expansion joint gap of 2 inch exists between the abutment backwall and the bridge deck. A detail of the abutment is shown in Figure 2.5.

## **2.2 Seismic Retrofit**

Damage from 1971 San Fernando Earthquake showed that bridges were especially susceptible to collapse caused by joint pulling apart, therefore, the California Department of Transportation (CALTRANS) has been retrofitting highway bridges with limiting movement of the superstructure. The San Gregorio Bridge was retrofitted in 1982. The general plans of the retrofit are shown in Figure 2.6.

Two sets of restrainer cables were installed at each intermediate hinge, to prevent the superstructure from falling off the joint seats in the event of a strong earthquake. Each cable unit consists of a 17.2-foot long 3/4-inch diameter steel cable with swaged ends and turnbuckle. Each restrainer set consists of seven cable units and goes through a 6 inch hole cored through the diaphragm at the hinge seat and the nearest bent. The turnbuckles

were initially torqued to 20 foot-pounds to remove slack in the cables, then they were untightened by 4 turns and the jam nuts were tightened. The cable restrainers are shown in Figure 2.7.

At each intermediate expansion hinge, two 3" steel pipes were installed as transverse shear keys. Each pipe shear key was filled with concrete and was contained in a 3.75 inch diameter of cored hole through the hinge diaphragm. The one end of the pipe was anchored at the hinge seat by using 1/2" deep anchorage plate. The detail of the pipe shear key is shown in Figure 2.7.

Three reinforced concrete shear pedestals were installed under the girder ends at each abutment to restrain movement in the transverse direction. Each shear pedestal contains two shear blocks, one on either side of the superstructure girder. An expansion gap of 1 inch exists between the shear blocks and the girder. One 0.75 inch cable was installed at each shear block. The cable went through hole cored through the girders at the deck end and embedded in the concrete abutment seat. The pedestal detail is shown as Figure 2.8.

### **2.3 Damage from the Loma Prieta Earthquake**

The 1989 Loma Prieta earthquake caused extensive damage in the San Francisco Bay Area. Caltrans engineers conducted preliminary inspections of more than 1500 bridge structures in the area

affected by the earthquake. The San Gregorio bridge is located approximately 40 miles from the epicenter and suffered some damage.

During the earthquake both abutments were damaged. According to CALTRANS report (Ref. 1), there were 1/8 inch wide diagonal cracks on the face of Abutment 1 starting at the top corner of the curtain walls and extending down through the weep holes and across face of the abutment. There were diagonal cracks on the left and right curtain walls at abutment 1. The joint seal at Abutment 1 had failed.

There were 1/4 inch wide diagonal cracks on the face of Abutment 6 starting at the top corner of the curtain walls and extending through the weep holes and across the face of the abutment. There were 1/16 inch wide diagonal cracks on the outside face of the left and right curtain walls at Abutment 6. The left and right curtain walls at Abutment 6 cracked at the top corner between the abutment backwall and curtain wall. The cracks on top of the curtain walls were up to 1.5 inch wide. There were no signs of instability or settlement of the curtain walls. There were incipient spalls (up to 20 square feet) on the right side of the Abutment 6 curtain backwall and the spalls were on both sides of the backwall and were near the corner of the abutment backwall and the curtain wall. There was an incipient spall (up to 5 square feet) on the front left side of the Abutment 6 backwall and the spall was near the corner of the abutment backwall and curtain

wall.

Another spall (3' long x 2' high x 2" deep) with exposed reinforcement was found near ground on the north side of bent 5. There was no damage reported at the other bents or the superstructure of the bridge. Also the damage report made no mention of any damage to the intermediate hinges or the restrainer cables.

## Chapter 3

### Description of Computer Models

#### 3.1 General

To evaluate the seismic response of the bridge and determine the effects of the retrofit restrainers, two types of analysis were performed in this study: a modal analysis to determine basic dynamic characteristics of the San Gregorio bridge, and an earthquake response analysis to evaluate the performance of the restrainers. Since the modal analysis is linear and the earthquake analysis is nonlinear, two different mathematical models of the San Gregorio Bridge were developed.

#### 3.2 Simplifying Assumptions

For ease in implementing the computer models, certain simplifying assumptions were made:

1. The bridge superstructure lies on 8000-foot radius horizontal curve, which was ignored in the analyses.

2. The San Gregorio Bridge has a superelevation of 2 percent to accommodate high speed traffic on the horizontal curve; the superelevation was neglected in the models.

3. The depth of the superstructure varies parabolically in the longitudinal direction. To model the parabolic variation of the

depth, prismatic beam elements with different depth were used as shown in Figure 3.1. Similar elements were used to model the tapered columns and the walls (Figure 3.1).

4. There are five construction joints in the superstructure of the bridge which were neglected in the models.

### **3.3 Linear Model**

The San Gregorio Bridge modal analysis was performed using the program Images-3D (Ref. 2). Images-3D is a three-dimensional general-purpose Finite Element Analysis package for IBM and compatible personal computers. Images-3D has several linear elements and a nonlinear spring element. The program can perform dynamic analyses including modal analysis as well as time-history and spectrum analyses.

The finite element model of the San Gregorio Bridge for the Images-3D analysis consisted of 77 nodes and 82 linear-elastic beam elements. Figure 3.2 illustrates the finite element mesh and shows the node numbering scheme.

Table 3-1 lists the material properties of the portland cement concrete used in the analysis of the San Gregorio Bridge.

The cross-section of the deck, shown in Figure 2.2, consists of a slab 8.125 inches thick by 31.2 feet wide, with three girders

measuring 20 inches wide and having variable length. Five, six and seven straight beam elements were used to model the two end and intermediate spans as shown in Fig. 3.2. The elements have different cross sectional properties because of the variable height of the girders. The sectional properties of the deck beam elements are listed in Table 3-2.

Bent 2 consists of three reverse-tapered columns which are deeper at the top. Each of bents 3, 4 and 5 consists of three reverse-tapered columns supported by one wall. Each column in the bent is modelled with three linear-elastic beam elements and each wall in the bent is modelled as one beam element. These beam elements were sized to the average cross sectional properties. Table 3-2 lists the properties used in the analysis.

Since the beam elements of the superstructure lie on the center line of the deck, it was necessary to use rigid beam elements to connect the superstructure to the columns. At the top of the walls of bents 3,4 and 5, rigid elements were used to connect the columns to the walls. The cross-sectional properties for these rigid elements were chosen to be 10 times as the cross sectional properties of their neighboring elements.

The seat-type abutments were modeled by roller supports allowed to translate in the longitudinal direction. All the intermediate hinges were modeled by using pin connections at nodes

4, 40, and 74. The retrofit restrainers were not included in the linear analysis.

### **3.4 Nonlinear Model**

The NEABS time-history analysis model of the San Gregorio Bridge consists of 85 nodes, 82 linear-elastic straight beam elements, 31 expansion joint elements and 3 five-spring nonlinear biaxial bending elements. Figure 3.3 illustrates the finite element mesh and shows the node numbering scheme.

The material properties of the portland cement concrete used for each of the concrete element types is listed in Table 3-1.

The cross sectional properties of the 82 linear-elastic straight beam elements of the nonlinear model were the same as those of the linear modal analysis and they are shown in Table 3-2.

To represent the hysteretic behavior in the plastic hinge region at the base of the bents, three non-linear five-spring elements (Ref. 3) were employed at the bottom of the walls of bents 3, 4 and 5. Since the steel bars along the weak axis of the wall bottom extend through the center of the cross section, there is no moment resistant capacity about the local weak-axis of the wall bottom. Therefore, the moments about the local weak-axis of the wall bottom were released to form a pin connection about this local

axis and the five-spring element carried moment in one direction only. The section properties used for the five-spring elements are listed in Table 3-3. The four No. 6 steel bars at each column bottom of bent 2 provide a very small moment resistant capacity which can be ignored in the analysis. Therefore, a two-way pin connection was assumed at each column bottom of bent 2.

The three expansion joints are located in the two end and the center spans as described in Chapter 2. The design hinge gap is 1.0 inch and the seat width is 7 inches at every hinge. There are ten 0.375-inch diameter shear bolts holding in place two opposing steel angles. During the 1982 seismic retrofit, two sets of cable restrainers and two pipe shear keys were installed across each expansion joint to limit longitudinal and transverse relative displacements of the hinge respectively.

The expansion hinges are modeled with several expansion joint elements: one element to model cable restrainers, and others to model the shear bolts and the pipe shear keys. Because the restrainer element is capable of one-way tensile loading only, two restrainer elements are required to model a two-way member such as the shear bolts and pipe shear keys. The modeling of the cables, the shear bolts and the pipe shear keys at the hinge are shown in Figure 3.4.

The cable restrainer properties, listed in Table 3-4, were

calculated according to the Caltrans Guidelines (Ref.4), using a yield stress,  $F_y$ , equal to 176.1 ksi, an area of 0.222 in<sup>2</sup>, and a modulus of elasticity of 10,000 ksi.

The restrainer properties for the shear bolts are also listed in Table 3-4. Because the information regarding the shear bolts did not appear on the construction plans, A307 type bolts were assumed and the shear yield force was obtained from Ref. 5.

The shear strength of the pipe shear key itself is 142.2 kips, which is larger than the bearing capacity of the surrounding concrete. Therefore, the shear yield force of the shear key was considered to be equal to the concrete bearing resistance (see Table 3-4). The bearing area was calculated by multiplying 30% of the circumference of the pipe by an effective bearing length of 6.25 in. (Ref. 4). The pipe stiffness was calculated assuming the pipe to be a beam with two fixed ends including both flexural and shear deformations.

The expansion hinge elements were also employed to model the abutments, the piles supporting the abutments, the backwalls and the retrofit shear blocks as shown in Figure 3.5. Properties for these elements are listed in Table 3-4.

According to the Caltrans Guidelines (Ref. 4), a soil stiffness of 200 kips/in/ft and a maximum effective soil stress of

7.7 ksf were used for the stiffness and yield forces of the abutments, respectively. Because of a 7.6-foot backwall height, a 7.6/8 reduction factor was used to lower the allowable soil stiffness and bearing capacities which are based on a 8 ft deep soil.

A stiffness of 40 kips/in/pile and an ultimate shear capacity of 40 kips/pile were used for the stiffness and yield forces of each one of the twelve piles supporting the abutment, respectively.

Two expansion joint elements acting in opposite direction were used to simulate the retrofit shear blocks under the girders at the end of the deck. The transverse-acting shear blocks were modeled as a restrainer cable with the same stiffness and strength properties as the concrete block. The spring parameter of the expansion element was used to simulate the cables connecting the deck end and the abutment concrete seat at the shear block. The deck end node is free to translate in the longitudinal direction.

### **3.5 Input Earthquake Records**

The epicenter of the Loma Prieta earthquake was located approximately 40 miles from the San Gregorio Bridge.

Accelerograms from the nearest strong-motion station, the Springs Reservoir Pulgas Water Temple in Upper Crystal (CSMIP

station number 58378), were used as the ground motion input for the NEABS earthquake analysis of the San Gregorio Bridge (Ref.6). This station was located approximately 44 miles from the earthquake epicenter. Figures 3.6 and 3.7 show the north and east components of the acceleration records, respectively. The peak acceleration values in the north and east components are estimated at 16 percent and 9 percent of the acceleration of gravity, respectively.

Since the deck center line of the San Gregorio Bridge was oriented 22.9 degree to the north direction, the north component of the acceleration record was applied longitudinally to the bridge and the east component was applied transversely to the bridge.

The earthquake records were normalized to three peak ground acceleration (PGA) combinations for the earthquake analysis: the first PGA combination was 0.16g and 0.09g, with a scale factor of 1.0, in the longitudinal and transverse directions of the bridge respectively; the second PGA combination was 0.32g and 0.18g, with a scale factor of 2.0 and the third was 0.6g and 0.34g, with a scale factor 3.75. In all the PGA combinations the first acceleration is applied in the longitudinal direction and the second in the transverse.

### **3.6 Analysis Cases**

To evaluate the effectiveness of retrofit, two earthquake

response analyses of the bridge were performed for each PGA combination: the first case with retrofit and the second case without retrofit. In the cases with retrofit, the specified restrainer gap of 0.75 in was used based on information obtained from the construction drawings and the Caltrans Guidelines (Ref. 4). In these calculations, the initial cable restrainer gap of 0.75 in. corresponds to the "hottest ambient temperature" (Ref. 4). The corresponding hinge and abutment gaps were 1.0 in. and 2.0 in., respectively. There were no cables at the abutment hinges.

During the extreme low ambient temperature, the restrainer gap is expected to become very small and even approach zero. To determine the influence of the initial restrainer gap on the earthquake response of the bridge, the case with restrainer gap of 0.0 in. was analyzed for each PGA level. In these cases the corresponding hinge and abutment gaps became 1.75 in. and 2.375 in., respectively.

## Chapter 4

### Results and Observations

#### 4.1 General

During the 1989 Loma Prieta earthquake, the San Gregorio Bridge experienced minor structural damage to the superstructure and bents and a moderate level of damage to both abutments.

To evaluate the effectiveness of the retrofit restrainer system installed across the intermediate hinges and the abutment expansion joints in 1982, a modal analysis and a nonlinear earthquake analysis were conducted using programs Images-3D and NEABS, respectively. The linear and nonlinear models for analyses are described in Chapter 3.

The nonlinear response history analysis of the bridge was performed using the computer program NEABS-86 (Ref. 7). The results of the dynamic and earthquake response analyses conducted for the San Gregorio Bridge are discussed in this section. The primary points of the discussion are the earthquake response of the San Gregorio Bridge during the Loma Prieta Earthquake, the effects of the presence of the seismic retrofit of the bridge and the effects of the reduction in the restrainer gap representing the bridge conditions during the extreme high and low temperatures.

## 4.2 Modal Analysis

A modal analysis, using Images-3D, was conducted to evaluate basic dynamic characteristics of the bridge. The natural periods and frequencies calculated from the analysis are shown in Table 4-1. The first mode is in the longitudinal direction and the next two are in the transverse direction.

Based on the calculated frequencies, and using standard structural dynamics techniques (Ref. 8), the Rayleigh damping coefficients were calculated, by assuming a damping factor equal to 5%. The values of the mass-proportional and stiffness-proportional damping factors are shown in Table 4-2.

## 4.3 Earthquake Analysis

As mentioned in Chapter 3, the accelerograms obtained from the nearest strong-motion station have peak ground accelerations (PGA) approximately equal to 0.16g in the north-south component and 0.09g in the east-west component. In the earthquake analysis, the north component of the record was used as the input ground motion in the longitudinal direction of the bridge, while the east component was used as the input in the transverse direction.

To evaluate the dynamic response and the damage of the San Gregorio Bridge during the earthquake, three PGA combinations were

employed in the earthquake analysis: 0.16g and 0.09g; 0.32g and 0.18g; 0.60g and 0.34g. In these combinations, the larger PGA components were applied in the longitudinal direction of the bridge model and the smaller in the transverse direction of the bridge.

#### 4.3.1 Bridge Displacement Responses

Figures 4.1 through 4.3 show the general responses of the bridge due to the three PGA combinations of the input ground motions. The selected displacements occurred at node 4 at the center of the left end span of the bridge, node 22 at the center of the first frame (the second span of the bridge) and node 62 at the center of the second frame (the fourth span of the bridge). These nodes are shown in Figure 3.3.

Both the maximum longitudinal and transverse displacements were dependent on the PGA combinations of the input ground motion. The maximum displacements in the longitudinal direction of the bridge were less than 2.10 inches, 3.50 inches and 6.20 inches for the three PGA combinations from low to high level, respectively. The maximum displacements in the transverse direction in the bridge were less than 1.90 inches, 3.20 inches and 8.40 inches for the three PGA combinations. The general waveform of the envelopes is nearly identical, with differences in peak values depending on the PGA combination of the input ground motion.

The maximum displacements were sensitive to the location of the node in the superstructure. Since node 4 is located in the end span, which is simply supported on the first bridge frame at the hinge and on the abutment, only the friction between the deck and the abutment and the retrofit element restrain the segment movement. It can be seen from Figures 4.1-4.3 that the bridge responses at the end span (node 4) were in general larger than the responses at intermediate spans (node 22 and 62) regardless of the PGA combinations. This is the case in both the longitudinal and transverse directions. The transverse displacement differences among the segments, however, were larger than the longitudinal displacement differences. Frame 1 has significantly larger transverse displacement responses than frame 2. The reasons for this are, a) the left bent (bent 2) of frame 1 consists of three columns which are pinned at the bottom, and b) frame 1 has higher elevation than frame 2 and therefore its supporting columns are more flexible.

The moments about the local weak-axis of the bottom of the bent were released to form the pin connection in the analysis, therefore, only displacement ductilities in the transverse direction of the bridge were calculated. The displacement ductility of the bent due to the earthquake is calculated by:

$$D_y = d_{\max}/d_e \quad (1)$$

in which,  $d_{\max}$  is the maximum displacement of the bent in the

transverse direction, and  $d_e$  is elastic displacement corresponding. The displacement  $d_e$  is determined by:

$$d_e = \int m\Phi dx + \int v\gamma dx \quad (2)$$

In the above equation  $m$ ,  $v$  are the virtual internal moment and shear respectively, produced by a unit force applied at top of the bent, while  $\Phi$ ,  $\gamma$  are the curvature and the shear angle which are determined by the following equations:

$$\Phi = M/EI \quad (3)$$

$$\gamma = V/GA \quad (4)$$

where  $M$ ,  $V$  are the bending moment and shear force, respectively. The displacement ductilities in the transverse direction of the bridge due to the three PGA combinations are shown in the Table 4-3. From this table it can be seen that the transverse ductilities of all bents due to the PGA combination of 0.16g and 0.09g were less than 1.0. This indicates that the bents performed adequately and did not yield. In the case of a PGA combination of 0.32g and 0.18g, the displacement ductilities of bents 3 and 5 were 1.27 and 1.10, respectively, which indicates that the bents may have suffered some minor damage during an earthquake with this PGA level. The ductilities of bents 3, 4 and 5 were 2.12, 1.38 and 1.93, respectively, due to the PGA combinations of 0.60g and 0.34. The displacement ductility demand of bents 3 and 5 indicates that the bents may have experienced a moderate level of damage in this

PGA combination.

A minor structural damage at bent 5 was reported during the Loma Prieta earthquake. No report was made concerning any damage at the bottom of the bents 3 and 4, possibly because these areas are below the water level and therefore they are not directly visible. Considering the displacement response and the intermediate hinge and abutment behavior (discussed later), the analysis with the PGA combination of 0.32g in the longitudinal direction and 0.16 in the transverse direction produced a bridge response which is more consistent with the observed damage.

#### 4.3.2 Response of Intermediate Hinges

Figure 4.4 shows the longitudinal and the transverse relative displacement response histories at hinge 3 due to the PGA combination of 0.32g and 0.18g, when the restrainer gap is 0.75 inches. A positive value in the longitudinal response indicates that the two segments of the superstructure adjacent to the hinge move away from each other. A negative value of 1.0 inch indicates closure of the hinge gap and negative values beyond 1.0 inches are the artificial results of the impact modeled with a finite stiffness. Corresponding force responses at hinge 3 are shown in Figure 4.5.

It can be seen from the figures that during the earthquake,

the cable restrainer in the longitudinal direction experienced tension several times, when the relative hinge movement exceeded the restrainer gap 0.0625 ft. The maximum cable force was far below the yield force. The relative displacement in the transverse direction was larger than the displacement in the longitudinal direction. The maximum shear force in the transverse pipe restrainer reached the yield force in all the cases studied with the seismic retrofit, because of the large stiffness and the relative small yield force of the pipe restrainers.

Shown in the Figure 4.6 are the maximum longitudinal and transverse relative displacements at the intermediate hinges due to the three PGA combinations of the input ground motion. Also shown are the cable restrainer forces for the same cases. Note that in these figures the PGA combinations are denoted by their larger component. Based on these responses the following remarks can be made:

- 1) The maximum relative movements in both the longitudinal and transverse directions increased with larger PGA values of the ground motion.

- 2) The maximum transverse relative displacements at hinges 1 and 3 were larger than at hinge 2 in all the cases studied because the movements of the end span can be restrained only by the friction between the deck and the abutment and the retrofit element at the hinge.

- 3) In most cases hinges 1, 3 have larger longitudinal relative

displacements than hinge 2, except in the case of 0.60g and 0.34g PGA combination.

4) The maximum transverse relative displacements were larger than the longitudinal relative displacements in all the cases studied because of the gap impact effect and the movement restriction from the abutments in the longitudinal direction of the bridge.

5) The maximum longitudinal relative displacement, 3.88 inch at hinge 2 due to the PGA combination of 0.60g and 0.34g was very close to the movement limit of 4 in. at the hinge.

6) The maximum restrainer forces in the longitudinal direction were below the force limit of 492 kips in all cases. However, the maximum cable force at hinge 2 due to the PGA combination of 0.60g and 0.34g was close to 96 percent of this limit. It should be noted, that the cable yield force of 492 kips was calculated based on the allowable longitudinal relative displacement of 4 in. at the hinges.

7) The maximum forces of shear pipes reached the yield force in the all study cases.

8) Since no observed damage to the intermediate hinge was reported in the Loma Prieta earthquake, the analysis with the lower PGA combinations such as the 0.32g and 0.18g produced bridge responses which are more consistent with the actual behavior of the bridge in the Loma Prieta earthquake.

### 4.3.3 Response of Abutment Expansion Joints

The relative displacements of Abutment 6 (nodes 84 and 85 in Figure 3.3) due to a PGA combination of 0.32g and 0.18g are shown in Figure 4.7 when the restrainer gap at the intermediate hinge was 0.75 in. The hinge gap at both bridge abutments is 0.167 ft.. The corresponding force responses at abutment 6 are shown in Figure 4.8.

A positive value of the longitudinal relative displacement indicates that the superstructure moved toward the abutment backwall and the back fill soil. If the positive value is larger than the size of the gap (0.167 ft.), the abutment backwall, abutment back fill and abutment piles are activated. In order to model the transverse gap of a 1.0 in. between the shear blocks and the deck, a restrainer gap of 1.0 in. was used for the cable elements modeling the shear blocks in the transverse direction of the bridge.

The small positive relative displacements at the abutments indicate that the abutments helped to reduce the deck movements in the longitudinal direction. The hinge gap at abutment 6 closed three times, while the maximum force of the back fill soil was 1110 kips, which was below the abutment yield force of 1996 kips.

The maximum transverse relative displacement exceeded the gap

between the shear block and the deck, while the force of the shear block reached the yield force of 105.2 kips.

Shown in Figure 4.9 are the maximum forces of the abutment back fill soil and the forces of the abutment piles due to the three PGA combinations of the input ground motion. The yield forces are 1996 kips and 480 kips for the abutment back fill and the abutment piles, respectively. Also shown are the maximum transverse relative displacements at the abutments for the same study cases. The following general observations can be made from this figure:

1) The abutment forces were sensitive to the PGA combinations of the ground motion. The larger PGA combinations resulted in larger abutment responses.

2) The PGA combination of 0.60g and 0.34g caused yielding at both the back fill and piles of abutment 1 and the back fill of abutment 6. A moderate to serious damage is expected at this PGA level.

3) The forces at both abutments due to a PGA combination of 0.32g and 0.18g were below the yield level and the abutment movements were relatively small. This type of response may result in some minor damage and is consistent with the observed behavior of the bridge during the Loma Prieta earthquake.

4) The zero force at abutment 6 due to the 0.16g and 0.09g PGA combination indicates that the maximum longitudinal displacement at this abutment was less than the hinge gap.

Therefore, at this PGA combination there is not impact between the bridge deck and the abutments.

5) The analysis results indicated that the abutment backwall reached the yield force level in all study cases. This is due to the small value of the yield force of the backwall.

6) The maximum transverse relative displacements at both abutments 1 and 6 exceeded the gap of 0.083 ft. between the shear blocks and the superstructure.

7) The forces at the shear blocks reached their yield level regardless of the input PGA combination because of their high stiffness and the low yield forces. The force level may be reasonable for the evaluation of the shear block damage.

Based on the bridge responses presented above, one can see that the case with a PGA combination of longitudinal 0.32g and transverse 0.18g resulted in responses which are more consistent with the observed damage during the Loma Prieta earthquake. The analysis for a PGA combination of 0.60g and 0.34g, on the other hand, resulted in serious structural damage of the bridge.

#### **4.4 Effects of Seismic Retrofit**

Restrainers are used in bridges to limit relative hinge displacements below an allowable level. The performance of restrainers is considered to be satisfactory when the displacement is kept below the allowable limit without any yielding of the

restrainers and any damage to the hinge region. Also important are the movements at the abutments and the resulting forces because of the close interaction of abutments and hinge displacements, even when abutments are not equipped with restrainers.

To determine the effectiveness of the seismic retrofit, two earthquake responses of the bridge were evaluated for each of the three PGA combination of the ground motions: the first case with the seismic retrofit and the second case without the retrofit. The first PGA combination is 0.16g and 0.09g in the longitudinal and transverse directions of the bridge, respectively. The second PGA combination is 0.32g and 0.18g and the third is 0.60g and 0.34g.

#### 4.4.1 General Response of the Bridge

Figures 4.10 through 4.12 show the typical displacement response comparisons of the San Gregorio bridge for the cases with and without seismic retrofit due to a PGA combination of 0.32g and 0.18g. The selected longitudinal and transverse responses occurred at node 4 in the end span, node 22 at the center of the first frame and node 62 at the center of the second frame (see Figure 3.3). Both longitudinal and transverse displacement responses of the bridge were insensitive to the seismic retrofit, except for the transverse displacement of node 4 at the end span. The end span is simply supported at the abutment and the hinge of the frame, therefore, only friction can restrain transverse displacement of

the end span if the seismic retrofit is not present. The seismic retrofit at the abutment and the intermediate hinge reduced the transverse displacement at the end span and changed the frequency content of its response.

Figure 4.13 shows the comparisons of the relative displacement response histories at hinge 2 in the cases with and without seismic retrofit due to the second PGA combination (0.32g, 0.18g). The seismic retrofit reduced the relative displacements at the hinge in both the longitudinal and the transverse directions. The cable force response history and pipe force response history in the case when the retrofit is present are shown in Figure 4.14. It can be seen that during the earthquake, the cable restrainer experienced tension several times when the opening of the hinge gap exceeded 0.0625 ft. The maximum cable force was significantly below the yield force. The pipe restrainer carried the shear force in the transverse direction. Since the pipe key has relatively high stiffness and low yield strength, the pipe force reached the yield load during the earthquake.

For the same cases, the comparisons of the relative displacement histories at abutment 1 are shown in Figure 4.15. The maximum longitudinal relative displacements were not affected significantly by the presence of the seismic retrofit, while the response waveforms in the cases with and without the retrofit were nearly identical. However, the transverse response histories in the

two cases are significantly different. The maximum relative displacement in the case with seismic retrofit was 0.182 ft, which was 55 percent lower than the maximum relative displacement of 0.405 ft. in the case without the retrofit. There are also significant differences in the transverse response waveforms. The seismic retrofit changed the low frequency of the transverse relative displacements at the abutment hinge to a high frequency relative displacement response because of the added stiffness of the shear blocks and the cables connecting the girders to the abutments. The back fill forces at abutment 1 in the two cases are shown in Figure 4.16. The maximum values in the two cases were almost the same, but the response histories are different since the force was sensitive to the relative displacement at the abutment hinge. The shear blocks under the girders yielded during the earthquake because of their large stiffness and their relatively low yield force. The maximum force in the connecting cable was 15.9 kips, which was far below the cable yield force (39.1 kips).

#### 4.4.2 Response of Intermediate Hinges

Shown in Figure 4.17 are the maximum longitudinal relative displacements of the two segments of the superstructure adjacent to each hinge in the cases with and without seismic retrofit due to three PGA combinations. The maximum transverse relative displacements of the hinges are shown in Figure 4.18. The following general remarks can be made based on these figures:

1) Both the longitudinal and the transverse maximum relative movements at the hinges increased in all the cases as the PGA of the input ground motion increased.

2) The longitudinal relative hinge displacements were sensitive to the seismic retrofit. The cable restrainers effectively reduced the longitudinal relative displacements at the hinges and this was true regardless of the PGA combination of the input ground motion.

3) The permissible longitudinal relative displacement at the hinge is 4.0 inches. It can be seen that this limit was not reached in the cases with and without the retrofit when the input PGA in the longitudinal direction was 0.16g or 0.32g. For the input with a PGA combination of 0.60g and 0.34g, however, the longitudinal relative displacements at hinges 1 and 3 in the case without the retrofit were 3.94 inches and 3.83 inches, respectively. These values are very close to the displacement limit of 4 in.. The longitudinal relative displacement at hinge 2 exceeded the allowable limit. On the other hand, when the seismic retrofit was present the PGA combination of 0.60g and 0.34g caused relative displacements at hinges 1 and 3 which were far below the displacement limit of 4 in.. In the same case, the maximum longitudinal relative displacement at hinge 2 was 3.88 inches which is barely below the limit.

4) The pipe restrainers were also effective in reducing the transverse relative displacements at hinges, but their

effectiveness depended on the PGA level. In the cases with a higher PGA input the restrainers were more effective than in the case with a lower PGA input. In all the cases, the pipe restrainers reached the yield forces because of the high stiffness and the relatively low yield force of the pipes.

5) As it can be seen in Fig. 4.6 (c), the cable restrainer forces increased depending on the input PGA. In all the cases the cable forces were below the cable force limit of 492 kips. However, the cable force at hinge 2 in the case of a PGA combination of 0.60g and 0.34g was close to 96 percent of this limit.

#### 4.4.3 Abutment Expansion Joints

The maximum abutment back fill and pile forces in the longitudinal direction of the bridge are shown in Figures 4.19 and 4.20, respectively. The yield forces for the abutment back fill and the piles are 1996 kips and 480 kips, respectively. The seismic retrofit reduced the abutment forces in the cases with a PGA combination of 0.16g or 0.32g in the longitudinal direction. In the case with 0.60g and 0.34g PGA combination, the abutment back fill yielded regardless of the retrofit presence. The pile forces at the abutments also reached the yield force level, except for the pile force at abutment 6 in the case with the seismic retrofit.

The maximum transverse relative displacements at the abutment hinges are shown in Figure 4.21. The following remarks can be made:

1) The abutment transverse relative displacements in the cases without the seismic retrofit were sensitive to the PGA level of the input ground motion. The transverse relative displacements in the case with the seismic retrofit also increased with the PGA level but at a smaller rate than in the cases without the retrofit.

2) The shear blocks under the girders and the cables connecting the girders to the abutments, effectively reduced the transverse relative displacements at the abutment hinges, but their effectiveness depended on the PGA level. The restrainers in the cases with a higher PGA input were more effective than in the cases with a lower PGA input. In all the cases, the shear blocks reached the yield force level due to their high stiffness and their relatively low yield force level. In the case with a PGA combination of 0.60g and 0.34g, the forces in the connecting cables reached 93 percent of the cable yield force of 39.1 kips. In the other cases, however, the cable forces were far below the yield force.

#### **4.5 Effects of Reduction in Restrainer Gap**

One of the primary factors considered in the San Gregorio Bridge study was to determine the effects of reducing the restrainer gap. According to Caltrans Design Aids (Ref. 4), a restrainer gap of 0.75 inches is assumed to be the maximum required when a bridge is fully expanded due to thermal action at the hottest ambient temperature. A non zero restrainer gap means, that

the restrainers would have no tensile force until the restrainer was stretched and the positive relative displacement of the hinge is equal to the restrainer gap. The restrainer gap, however, may reduce to very small value during low temperatures due to the contraction of the superstructure.

To evaluate the influence of the reduction in the restrainer gap on the bridge response, analytical studies with zero restrainer gap at the bridge expansion hinge were performed for each PGA combination of the input ground motion. Comparison between the results from the cases with 0.75 inch restrainer gap and with 0 inch restrainer gap were made in order to identify the importance of the restrainer gap value.

#### 4.5.1 General Response of the Bridge

Figures 4.22 through 4.24 show the typical displacement response comparison of the San Gregorio Bridge in the cases with a non-zero restrainer gap and with zero restrainer gap due to a PGA combination of 0.32g and 0.18g. The selected longitudinal and transverse responses occurred at node 4 in the segment at the end span of the bridge, node 22 at the center of the first frame and node 62 at the center of the second frame. It can be seen that the longitudinal displacement responses of the bridge were insensitive to the restrainer gap and the longitudinal displacement responses were almost identical in the cases with the non-zero and zero

restrainer gaps. The transverse displacement responses also showed minor influence of the restrainer gap on the bridge response, except that the maximum displacement at node 4 in the zero restrainer gap case was larger than that in the case with a restrainer gap of 0.75 inches.

Figure 4.25 shows the comparison of the relative displacement response histories at hinge 2 in the cases with zero and non-zero restrainer gaps due to the PGA combination of longitudinal 0.32g and transverse 0.18g. The positive value of the longitudinal relative displacement in the case with the non-zero restrainer gap was larger than the displacement with zero restrainer gap. This is because the cables in the non-zero gap case were not activated until the hinge movement reached the value of the restrainer gap (0.75 in.). The negative value of the longitudinal relative displacement in the case with non-zero restrainer gap was smaller than the displacement in the case of zero restrainer gap. This is because when the restrainer gap is zero the hinge gap is larger. This allows more negative relative displacements of the segments of the superstructure which are adjacent to the hinge.

The comparison of the cable force responses at hinge 2 due to a PGA combination of 0.32g and 0.18g is shown in Figure 4.26. The cable forces at the hinge were sensitive to the reduction in the restrainer gap. The cables in the case with zero restrainer gap experienced tension more times than in the non-zero gap case. In

the former case the cable force level was larger than that in the latter case, even though the positive relative displacement at the hinge in the zero restrainer gap case was smaller than in the non-zero gap case as it was discussed previously. The transverse pipe force responses at hinge 2 for the two gap cases are shown in Figure 4.27. The pipe force reached the yield load in both cases.

For the same cases, the comparisons of the relative displacement histories at abutment 1 are shown in Figure 4.28. The peak longitudinal relative displacement for the case with zero restrainer gap was approximately 3.5 inches, compared to 3.4 inches for the case with 0.75 in. gap. The peak transverse relative displacements were 2.9 inches and 2.2 inches for the cases with zero and non-zero restrainer gaps, respectively. In this figure, a positive displacement represents a close of the abutment hinge. The forces of the abutment back fill for two restrainer gap cases are shown in Figure 4.29. The peak force for the case with zero restrainer gap was approximately 425 kips, which was smaller than the force of 822 kips, for the case with non-zero restrainer gap. This is because the increase in the abutment hinge gap in the case with zero restrainer gap allowed more movement of the superstructure before the abutment hinge gap was closed. In the transverse direction, the shear block forces reached their yield load for both zero and non-zero restrainer gap cases.

#### 4.5.2 Intermediate Hinges

Shown in Figure 4.30 are the maximum longitudinal relative displacements of the two segments of the superstructure adjacent to each hinge for the cases with 0.75 in. and 0 in. restrainer gaps due to the three PGA combinations of the input ground motion. The maximum transverse relative displacements of the hinges are shown in Figure 4.31. The following general observations can be made based on these figures:

1) The maximum longitudinal relative displacements for the case with non-zero restrainer gap were larger than in the case with zero restrainer gap. The only exception was the maximum relative displacements of hinges 1 and 3, due to a PGA combination of longitudinal 0.60g and transverse 0.34g.

2) The maximum transverse relative displacements had slight difference between the cases with zero and non-zero restrainer gaps.

3) Both the longitudinal and the transverse relative displacements at the hinges increased with larger PGA combinations of the input ground motion, regardless of the restrainer gap values.

4) The maximum allowable longitudinal displacement at the hinges is 4 inches (limit 1 in Fig. 4.30) when the restrainer gap is 0.75 inches and 3.25 inches (limit 2 in Fig. 4.30) when the restrainer gap is zero. In the case of a PGA combination of 0.60g and 0.34g, the maximum longitudinal relative displacement, 3.88

inches, at hinge 2 for the non-zero restrainer gap case was close to limit 1. The maximum longitudinal relative displacement, 3.62 inches, at hinge 2 for zero restrainer gap exceeded limit 2 and would potentially lead to the collapse of the superstructure. Note, that the maximum value, 3.62 inches, in the zero restrainer gap case was smaller the maximum value of 3.88 inches in the non-zero restrainer gap.

5) The maximum relative displacements at hinges 1 and 3 due to a PGA combination of 0.60g and 0.34g had almost equal values (Fig. 4.30). However, in the case of zero restrainer gap they were very close to their corresponding maximum allowable displacement limit (Fig. 4.30).

The maximum cable restrainer forces in the zero and non-zero restrainer gap cases are shown in Figure 4.32. It can be seen that the restrainer forces were sensitive to the restrainer gap. A reduction in the restrainer gap generally increased the magnitude of cable force. This was true regardless of the PGA combination of the input ground motion. The maximum force at hinge 2 in the zero restrainer gap case reached the yield load due to the PGA combination of 0.60g and 0.34g. The shear pipe forces in the transverse direction reached their yield load in all the cases.

#### 4.5.3 Abutment Expansion Joints

The maximum abutment back fill and pile forces in the

longitudinal direction of the bridge are shown in Figures 4.33 and 4.34, respectively. The yield forces for the abutment back fill and the piles are 1996 kips and 480 kips, respectively. The figures indicate the following:

- 1) The larger openings at the abutments in the zero restrainer gap case generally resulted in smaller forces in the abutment back fill soil and abutment piles. The only exception was the pile force at abutment 6, which was slightly less than the force in the non-zero case due to a PGA combination of 0.60g and 0.34g.

- 2) The maximum abutment forces increased depending on the PGA combination of the input ground motion, regardless of the magnitude of the restrainer gap.

- 3) The force of the abutment back fill soil at abutment 6 reached the yield load in both the zero and non-zero restrainer gap cases due to a PGA combination of 0.60g and 0.34g. For the same cases, the pile force at abutment 6 was below the yield load since the piles have a relatively lower stiffness and larger yield displacement limits than the abutment back fills.

The maximum transverse relative displacement at the abutment hinges are shown in Figure 4.35. The following remarks can be made:

- 1) The abutment transverse relative displacements varied depending on the magnitude of the restrainer gap.

- 2) The maximum transverse relative movement at the abutments

increased depending on the PGA of the ground motion in both zero and non-zero restrainer gap cases.

3) Based on the relative displacements, the forces in the shear blocks under the girders reached their yield load in all the cases.

## Chapter 5

### Study of Restrainer Design

#### 5.1 General

The design methods for the longitudinal restrainer system at the intermediate hinges of the bridge are evaluated in this chapter. The primary steps taken in this study were:

- 1) The current Caltrans method (Ref. 4), which is an equivalent linear static analysis method, was used to design the longitudinal hinge restrainers in the San Gregorio Bridge.

- 2) Several nonlinear response history analyses of the San Gregorio Bridge were performed. In these calculations, no retrofit restrainer system was considered in the bridge model and three selected earthquake records were used. Based on results from these dynamic time history analyses, the required longitudinal hinge restrainers were determined by following the current Caltrans guidelines. This method is referred in this report as the "Dynamic-Caltrans" method. It should be noted that the difference between the "Dynamic-Caltrans" and the original Caltrans methods is that in the former the displacements are calculated by using a nonlinear analysis, while in the latter they are calculated by using an equivalent static analysis method.

- 3) Three different longitudinal cable restrainer retrofit cases were studied. In the first case, the retrofit consists of the

existing cables in the San Gregorio Bridge, in the second case the cables were calculated based on the Caltrans method (step 1) and in the third case they were calculated based on the "Dynamic-Caltrans" method performed in the second step. For each retrofit case, the earthquake analyses of the bridge were carried out using three earthquake records.

4) The number of the longitudinal cables calculated in step 2, was modified to meet the allowable relative displacement limit at the intermediate hinges of the bridge.

## **5.2 Input Earthquake Records**

Three earthquake records were used in this study. These were the north-south component of 1940 El-Centro earthquake, the north-south component of the 1954 Eureka earthquake, and the east-west component of the 1989 Loma Prieta earthquake recorded at the Saratoga station. All the records were normalized to a peak ground acceleration (PGA) of 0.7g, and were only applied in the longitudinal direction of the San Gregorio Bridge.

## **5.3 Number of Cables in Study Cases**

Table 5-1 shows a summary of the number of restrainers from three different cases. One case is the existing longitudinal cables in the San Gregorio Bridge, the others are the cable calculated by using the current Caltrans and the "Dynamic-Caltrans" procedures.

Two restrainer sets were used in each intermediate hinge and 3/4-in diameter cable restrainers were used for all the cases. Note that the abutments had no restrainers.

The longitudinal cable design based on the current Caltrans method is shown in Table 5-2. In this table,  $D_{eq}$  and  $D_r$  represent the equivalent earthquake deflection of the unrestrained system and the permissible restrainer deflection, respectively. In the current Caltrans method, the specified restrainer gap of 0.75 in. is for the "hottest ambient temperature". The corresponding hinge gap and abutment gap for the San Gregorio Bridge are 1.0 in. and 2.0 in., respectively. The allowable maximum relative movement at hinge is 4.0 in. The fourth column of Table 5-2 shows the actual number of required cables based on the current Caltrans method, while the fifth column shows the recommended number of cables for the retrofit design.

In the "Dynamic-Caltrans" procedure, the earthquake deflection of an unrestrained system,  $D_{eq}$ , is obtained from the dynamic analysis and then the cable design follows the Caltrans method. Figure 5.1 shows the longitudinal relative displacements at the intermediate hinges of the San Gregorio Bridge under the selected three earthquake records. In the analyses, no longitudinal cable restrainers at the hinges were considered. An extreme low ambient temperature was assumed in these cases, therefore, a zero restrainer gap was used and the corresponding hinge and abutment

motions.

2) The cable system from the current Caltrans method (see Table 5-1), resulted in maximum relative displacements at the hinges which were less than the response of the unrestrained San Gregorio Bridge (Fig. 5.1). The relative displacements at hinges 2 and 3, however, were still larger than the allowable limit of the hinge displacement during the El-Centro and Eureka earthquakes.

3) The maximum relative movements at the hinges were sensitive to the input ground motion even through the PGA's of the inputs in all the cases were identical.

Using the number of the cables which were determined by the "Dynamic-Caltrans" method (Table 6-3), a nonlinear analysis of the San Gregorio Bridge was performed. The black circles in Figure 6.4 represent the analysis results which are designated as "Design". From the figure it can be seen, that the maximum relative displacements at hinges 2 and 3 exceeded the allowable displacement limit during the El-Centro and Eureka earthquakes. To reduce the displacements, the number of cables was increased to 6 cables at each hinge. This modification set up an identical stiffness of the restrainer system at all the intermediate hinges. Using these cables, a nonlinear analysis of the bridge was performed. The maximum relative displacements, which were designated as "Modify 1", are shown in Figure 6.4. Because the relative displacement at hinge 1 still exceeded the allowable displacement limit during the El-Centro earthquake, the number of cables at each hinge increased

from 6 to 8. Using this number of the cables, a dynamic analysis of the bridge was performed. The corresponding relative displacements, which are designated as "Modify 2", are also shown in Fig. 6.4.

It can be seen, that the maximum relative displacements at the intermediate hinges are less than the allowable displacement for all the cases considered. It should be noted that the final number of the cables after the two modifications is less than the existing cables in the San Gregorio Bridge. This means that the "Dynamic-Caltrans" procedure has the potential of producing a more cost effective restrainer design.

## Chapter 6 Summary and Conclusions

### 6.1 Summary

As part of a study to evaluate the effects of the longitudinal restrainer system on the earthquake response of bridges, a detailed parametric study of the nonlinear response of the San Gregorio bridge to the Loma Prieta earthquake was carried out and is described in this report. A linear and a nonlinear mathematical model of the San Gregorio bridge were developed based on the construction plans and the seismic retrofit design. The results discussed in this report are the response of the bridge with and without retrofit and the effects of the reduction in the restrainer gap on the bridge performance during the earthquake.

The San Gregorio Bridge is a five-span reinforced concrete structure with a total length of 265 feet and a height of 56 feet. The bridge elevation is higher at the south abutment than at the north abutment. The two end spans are 42 feet long and the three intermediate spans are 59 feet. The three columns at bent 2 are reverse-tapered rectangular columns while bents 3, 4 and 5 consist of three tapered columns resting on 15 feet high walls.

Three expansion joints in the two end spans and the third span separate the bridge into four portions. Two frames at spans 2 and

4 have cantilever sections at the end spans and the third span. The superstructure at each end span is supported on the expansion hinge and the abutment concrete seats.

The intermediate expansion hinges have a gap of 1 inch at the joint seat. Two sets of restrainer cables were installed at each hinge to prevent the superstructure from falling off the joint seats. Each restrainer set consists of seven cables of 0.75 inch diameter. Also two 3 inch diameter steel pipes filled with concrete were installed as transverse shear keys.

The seat-type abutments consist of a concrete seat 30-inch thick by 7 foot wide and one 12-inch thick, approximately 7.6 foot high concrete backwall. A 2 in. expansion joint gap exists between the abutment backwall and the bridge deck. Three reinforced concrete shear pedestals were installed under the girder end at each abutment. Each shear pedestal contains two shear blocks, one on either side of the deck girder. One 0.75 inch diameter cable was installed at each shear pedestal to connect the superstructure to the abutment concrete seat. An 1 inch expansion gap exists between the shear block and the girder.

The San Gregorio bridge modal and nonlinear earthquake analyses were performed using the computer programs Images-3D and NEABS, respectively. The linear model of the San Gregorio bridge for the Images-3D analysis consists of 77 nodes and 82 linear-

elastic beam elements. To simulate the concrete seat-type abutments, the deck end nodes were modelled as roller supports in the longitudinal direction. Three intermediate hinges which were located in the two end spans and the middle span were modelled by using pin connections at the corresponding nodes. The retrofit restrainers were not included in the Images-3D analysis.

The NEABS nonlinear analysis model of the San Gregorio Bridge consists of 85 nodes, 82 linear-elastic straight beam elements, 31 expansion joint elements and 3 five-spring nonlinear biaxial bending elements. The intermediate expansion hinges were modeled with several expansion joint elements: one element to model cable restrainers, and others to model the shear bolts and the pipe shear keys. The expansion joint elements were also used to model the abutment back fill soil, the abutment piles, the backwalls and the shear blocks at the abutment expansion joints. Five-spring elements representing the nonlinear behavior of concrete joints were used at the bottoms of bents 3, 4 and 5.

Accelerograms from the nearest strong-motion CSMIP station (station number 58378) were used as the ground motion input for the NEABS earthquake analyses of the San Gregorio Bridge. The north component of the acceleration record was applied longitudinally to the bridge and the east component was applied transversely. The earthquake records were normalized to three peak ground accelerations (PGA) combinations for the earthquake analysis: the

first PGA combination was 0.16g and 0.09g, the second PGA combination was 0.32g and 0.18g and the third was 0.60g and 0.34g. In all the cases, the ground motion component with the larger PGA was applied in the longitudinal direction of the bridge.

To evaluate the effectiveness of the seismic retrofit, two earthquake responses of the bridge were performed for each PGA combination: the first with the seismic retrofit present and the second case without the seismic retrofit. Initially, a 0.75 inch restrainer gap, which corresponds to a 1.0 inch hinge gap and a 2.0 inch abutment expansion joint gap, were used in these cases. To determine the influence of initial restrainer gap on the earthquake responses, the cases with zero restrainer gap were analyzed for each PGA level. In these cases the corresponding hinge and abutment joint gaps became 1.75 inch and 2.375 inch, respectively.

Finally, some design methods for the longitudinal restrainer system at intermediate hinges were evaluated. In this evaluation, three longitudinal cable restrainer systems were studied. The first system consists of the existing cables in the San Gregorio Bridge, the second consists of the cables based on the current Caltrans design method and the third consists of the cables designed based on the "Dynamic-Caltrans" procedure. In this procedure the relative longitudinal displacements at the hinges of the unrestrained bridge were calculated by using nonlinear analysis and then the number of cables was calculated by following the standard Caltrans cable

design procedure. In all the cases, a PGA of 0.7g was assumed. For dynamic analyses, three earthquake records were used.

## 6.2 Conclusions

1. Based on the bridge responses, the force level of the intermediate hinges and the abutment damage, the earthquake analysis of the San Gregorio bridge due to a PGA combination of 0.32g and 0.18g was more consistent with the observed damage of the bridge during the Loma Prieta earthquake. The earthquake analysis for a PGA combination of 0.60g and 0.34g can be used to predict the response and serious structural damage of the bridge in a stronger earthquake. In this case the longitudinal relative displacement at hinge 2 was very close to the allowable displacement limit and both abutment forces reached the yield level.

2. The maximum displacements were sensitive to the location of the segment in the superstructure. The simply supported segments at each end span had larger responses than the bridge frames.

3. The maximum transverse relative displacements at hinges 1 and 3 were larger than the displacements at hinge 2 for the all PGA combination cases, because the movements of the end span segments can be restrained only by the friction between the superstructure and the abutment and the retrofit elements at the hinge. The

maximum longitudinal relative displacements at hinges 1 and 3, however, were not always larger than those at hinge 2.

4. The maximum transverse relative displacements at the intermediate hinges were larger than the longitudinal relative displacements in all the cases studied, because the latter were reduced by the closure of the hinge gaps in the longitudinal direction of the bridge.

5. Both the longitudinal and the transverse displacement responses of the bridge superstructure were insensitive to the seismic retrofit, except for the transverse displacements at the end span segments. The seismic retrofit at the abutment and the intermediate hinge reduced the transverse displacements at the end span segments and changed low frequency response to high frequency response. This is because the seismic retrofit is the primary resisting mechanism for the end span movement in addition to the friction between the abutment and the superstructure.

6. The longitudinal relative hinge displacements were sensitive to the seismic retrofit. The cable restrainers effectively reduced the longitudinal relative displacements at the hinges regardless of the PGA combination of the input ground motion. Especially due to a PGA combination of 0.60g and 0.34g, the longitudinal relative displacement at hinge 2 in the case without the seismic retrofit exceeded the permissible limit and would

potentially lead to the collapse of the superstructure. For the same case, the relative displacements at hinges 1 and 3 were also very close to the relative displacement limit. However, all longitudinal relative displacements at the intermediate hinges with the restrainer cables were less than the allowable relative displacement limit.

7. The pipe restrainers were also effective in reducing the transverse relative displacement at the intermediate hinges. The restrainer pipes in cases with higher PGA input, were more effective than in the cases with a lower PGA input.

8. The seismic retrofit reduced the abutment back fill forces and the abutment pile forces. In the cases with 0.60g and 0.34g PGA combination, however, the abutment back fill and the piles reached the yield force regardless of the retrofit condition except for the pile force at abutment 6 in the case with the seismic retrofit present.

9. The transverse relative displacements at the abutment expansion joints were sensitive to the seismic retrofit. The shear blocks and the cables connecting the girder to the abutment concrete seats effectively reduced the transverse relative displacements, especially, in the cases of higher level PGA combinations of the input ground motion.

10. The maximum cable restrainer forces were sensitive to the restrainer gap. A reduction in the restrainer gap, generally, increased the magnitude of the cable forces regardless of the PGA combination. The most critical relative hinge movements corresponded to the zero restrainer gap, because the size of the available hinge seat in the zero restrainer gap case is smaller than the seat size in the non-zero restrainer gap case.

11. The larger gap at the abutment expansion joints in the zero restrainer gap generally resulted in smaller forces in the abutment back fill soil and the abutment piles. Considering that the pile force at abutment 6 in the zero restrainer case due to 0.60g and 0.34g PGA level was less than the force in the non-zero restrainer case, conditions 10 and 11 indicate that it is necessary to analyze the bridge for both the extreme cold and extreme high ambient temperature conditions.

12. The analyses of the bridge with the existing cable system in the San Gregorio Bridge show conservative results for three earthquake inputs with a PGA of 0.7g. On the other hand, the analyses with a cable system based on the current Caltrans cable design method show some problems at the hinges. Therefore, a modified "Dynamic-Caltrans" procedure, which was preliminarily tested in this study, may be a more promising method for designing restrainers.

13. The modified "Dynamic-Caltrans" design procedure tested in this study consists of the following steps: a) The nonlinear analyses of the unrestrained bridge are performed using selected earthquake inputs in order to calculate the maximum relative displacements of the hinges; b) Based on the maximum displacements calculated from the step a, the required number of cables at the hinge is calculated using the current Caltrans method; c) The nonlinear analyses of the bridge with the restrainers calculated at step b are performed again; d) The maximum displacements calculated in step c are compared to the allowable limit; e) if the displacements exceed the limit the number of cables is increased and steps c - e are repeated. For simplicity purposed it is recommended that the same number of cables be used in all the hinges.

## References

1. Horold Herr, 1989. "San Grogorio Bridge Supplementary Bridge Report". Sacramento, California Department of Transportation.
2. Images-3D, 1985. Berkeley, California: Celestial Software.
3. Saiddi M., G. Ghusn, and Y. Jiang, "Five-Spring Element for Biaxially Bent R/C Columns" Journal of Structural Engineering, ASCE, Vol. 115, No. 2, February 1989.
4. Division of Structures. 1991. "Seismic Design Reference: Sacramento, California Department of Transportation.
5. Manual of Steel Construction, 8th Edition, 1980, Chicago, American Institute of Steel Construction.
6. Shakal, A., M. Huang, M. Reichle, C. Venture, T. Cao, R. Sherburne, M. Savage, R. Darrah, and C. Peterson. 1989 "CSMIP Strong-Motion Records from the Santa Cruz Mountains (Lowa Priesta), California Earthquake of 17 October 1989" Report No. OSMS-89-06. Sacramento. California Department of Conservation, Division of Mines and Geology.
7. Imbsen, R. A., and R. A. Schamber, 1983. "Earthquake Resistant Bridge Bearing" Report No. FHWA/RD-82/166, Vol. 2, Washington, D.C., U.S. Department of Transportation, Federal Highway Administration.
8. Clough, R. W., and J. Penzien, 1975. "Dynamics of Structures", McGraw-Hill, Inc.

Table 3-1. Material Properties for San Gregorio Bridge

Properties	Value
compressive Strength, $f'_c$	360 ksf (2500 psi)
Modulus of Elasticity, $E_c$	410,000 ksf ( $2.85 \times 10^6$ psi)
Poisson's Ratio, $\nu$	0.20
Mass Density, $\rho$	0*

\* Mass density is zero to bypass Images-3D and NEABS internal dead load calculations; dead loads are applied as discrete nodal loads.

Table 3-2 Beam Element Cross-Sectional Properties

Member Type	Cross-Sectional Area (ft <sup>2</sup> )	Bending Inertia about Weak-Axis (ft <sup>4</sup> )	Bending Inertia about Strong-Axis (ft <sup>4</sup> )	Torsional inertia (ft <sup>4</sup> )
Deck Element 1*	40.73	79.84	3155.1	19.11
Deck Element 2	38.97	63.50	3025.3	17.48
Deck Element 3	41.27	85.32	3194.9	19.61
Deck Element 4	46.84	155.9	3605.7	24.76
Deck Element 5	54.51	300.3	4171.6	31.87
Deck Element 6	53.34	274.4	4085.2	30.79
Deck Element 7	44.14	118.5	3406.9	22.27
Deck Element 8	39.54	68.58	3067.7	18.01
Deck Element 9	40.26	75.28	3120.7	18.67
Column/Bent 2,3,4,5	7.00	3.18	5.25	6.48
Column/Bent 2,3,4,5	7.13	3.35	5.34	6.72
Column/Bent 2	5.21	1.94	2.65	3.58
Column/Bent 2	5.76	2.62	2.93	4.23
Column/Bent 3	4.94	1.76	2.35	3.21
Column/Bent 3	5.58	2.53	2.66	3.90
Column/Bent 4	5.24	1.95	2.69	3.62
Column/Bent 4	5.79	2.63	2.97	4.28
Column/Bent 5	5.52	2.14	3.01	4.01
Column/Bent 5	5.97	2.71	3.26	4.62
Wall/Bent 3	36.08	8.16	1069.0	31.09
Wall/Bent 4	40.45	11.31	1240.0	42.89
Wall/Bent 5	44.43	14.77	1419.0	55.72

\* The deck elements 1,2,3,4,5 were used for both the end spans from the abutment to the bent; the deck elements 6,7,8,8,7,6 were used for spans 2,4 from left to right; the deck elements 6,7,9,2,3,4,5 were used for span 3 from left to right.

Table 3-3 NEABS Five-Spring Element Properties

Property	Value
Concrete Compressive Strength, $f_c'$	360 ksf
Reinforcing Steel Yield Strength, $f_y'$	5760 ksf
Gross Cross-Sectional Area of Column, $A_g$	31.63 ft <sup>2</sup>
Area of Longitudinal Reinforcing in Column, $A_s$	0.092 ft <sup>2</sup>
Development Length of Longitudinal Reinforcing Steel, $L_d$	0.89 ft
Balanced Condition average Axial Capacity, $P_{b(ave.)}$	5708.0 kips
Balanced Moment Capacity, $M_{by}$	28103.0 k-ft
Stiffness Degradation Factor for Tension	0.4
Stiffness Degradation Factor for Compression	0.4

Table 3-4 NEABS Expansion Joint Restrainer Properties

	Stiffness, K (k/ft)	Yield Force, $F_y$ (kips)	Number of Restrainers
Restrainer Cables, Longitudinal	907.5	273.7	2
Restrainer Bolts, Longitudinal	$1.58 \times 10^4$	2.21	5
Restrainer Bolts, Transverse	$7.91 \times 10^4$	11.04	1
Restrainer Pipes, Transverse	$1.26 \times 10^5$	128	1
Abutments, Longitudinal	$3.3 \times 10^4$	1996	1
Piles, Longitudinal	5760	480	1
Backwalls, Longitudinal	9552	19.86	1
Shear Blocks, Transverse	$2.5 \times 10^5$	105.2	1

**Table 4-1 San Grogorio Bridge Modal Analysis Results**

Mode	Period, T (sec.)	Frequency, $\omega$ (rad./sec.)
Mode 1	1.133	5.545
Mode 2	0.463	13.559
Mode 3	0.412	15.233

**Table 4-2  $\alpha$  and  $\beta$  Factors for San Grogorio Bridge**

Mass-proportional damping factor	0.5556
Stiffness-proportional damping factor	0.00435

**Table 4-3 Displacement Ductilities of Bents**

Input PGA	Bent 3	Bent 4	Bent 5
0.16g and 0.09g	0.710	0.580	0.660
0.32g and 0.18g	1.270	0.870	1.100
0.60g and 0.34g	2.120	1.380	1.930

**Table 5-1. Number of Cables for San Gregorio Bridge**

Study Case	Hinge 1	Hinge 2	Hinge 3
Existing Cables	2x7	2x7	2x7
Caltrans Method	2x6	2x1	2x5
Dynamic-Caltrans Procedure	2x3	2x1	2x2

**Table 5-2. Number of Cables (Current Caltrans Method)**

Hinge No.	$D_{eq}$ (in)	$D_r$ (in)	Required No. of Cable	Recommended No. of Cable
1	9.07	4.0	10.7	12
2	3.24	4.0	-	2
3	8.54	4.0	9.01	10

**Table 5-3. Number of Cables (Dynamic-Caltrans Procedure)**

Hinge No.	$D_{eq}$ (in)	$D_r$ (in)	Required No. of Cable	Recommended No. of Cable
1	5.25	3.25	4.1	6
2	4.06	3.25	0.8	2
3	4.56	3.25	2.3	4

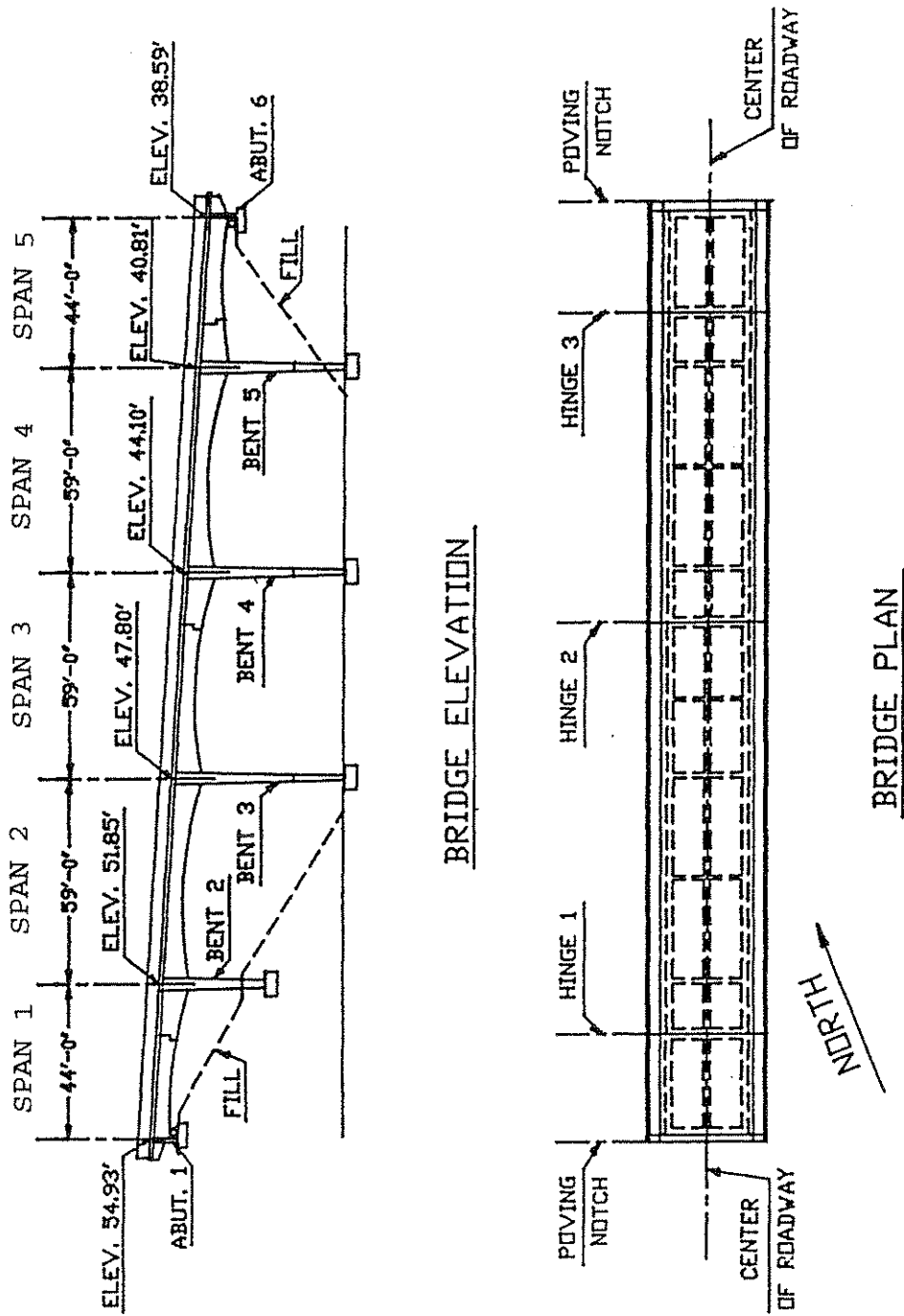


Figure 2.1 San Gregorio Bridge

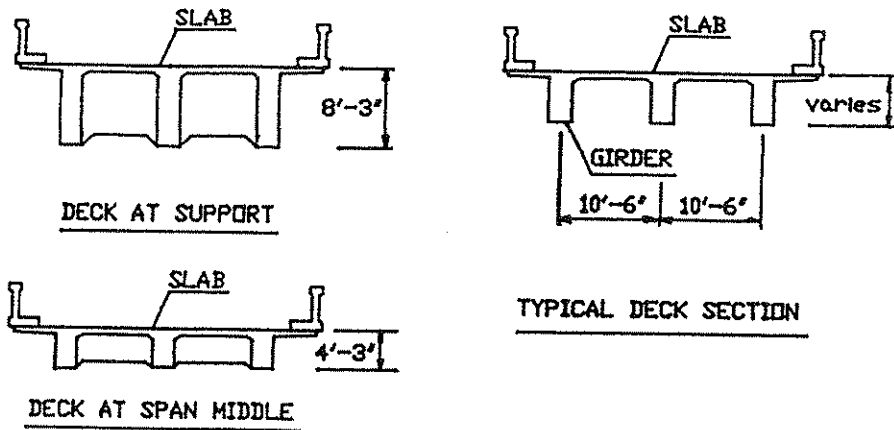


Figure 2.2 Deck Sections of San Gregorio Bridge

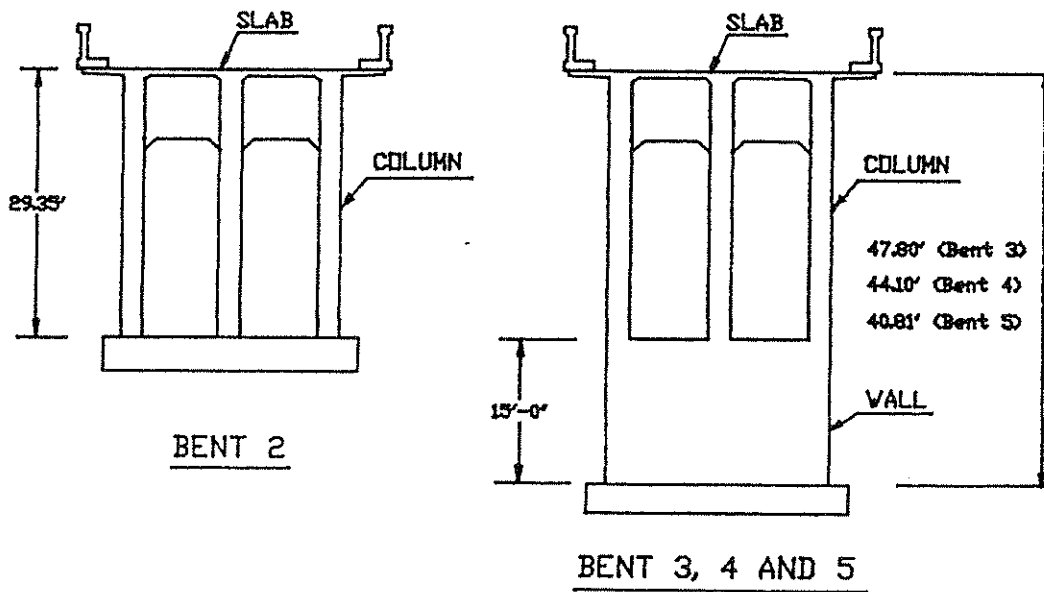


Figure 2.3 Bent Elevations of San Gregorio Bridge

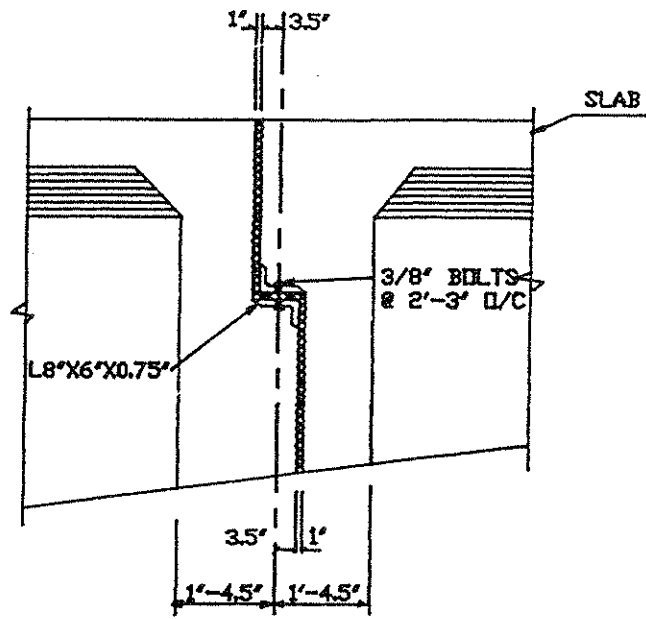


Figure 2.4 Detail of Intermediate Hinge

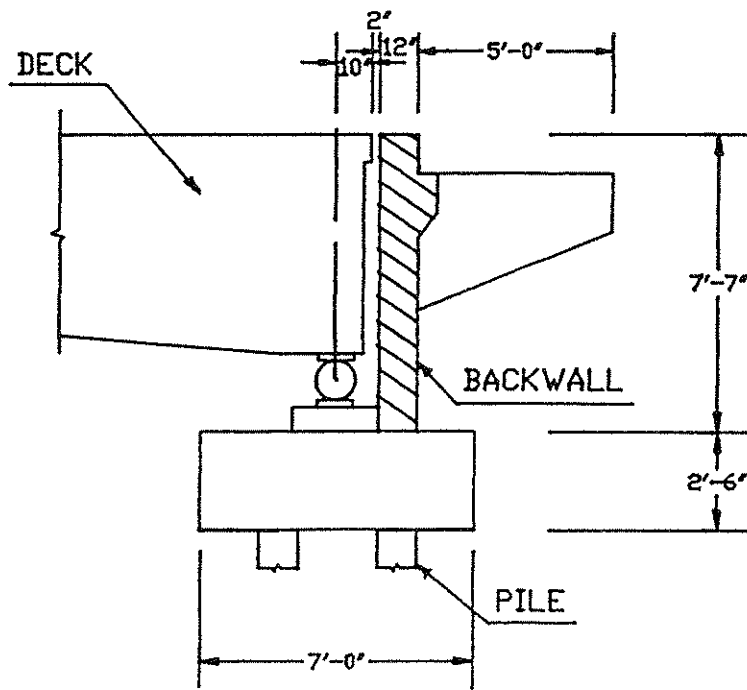


Figure 2.5 Detail of Abutment

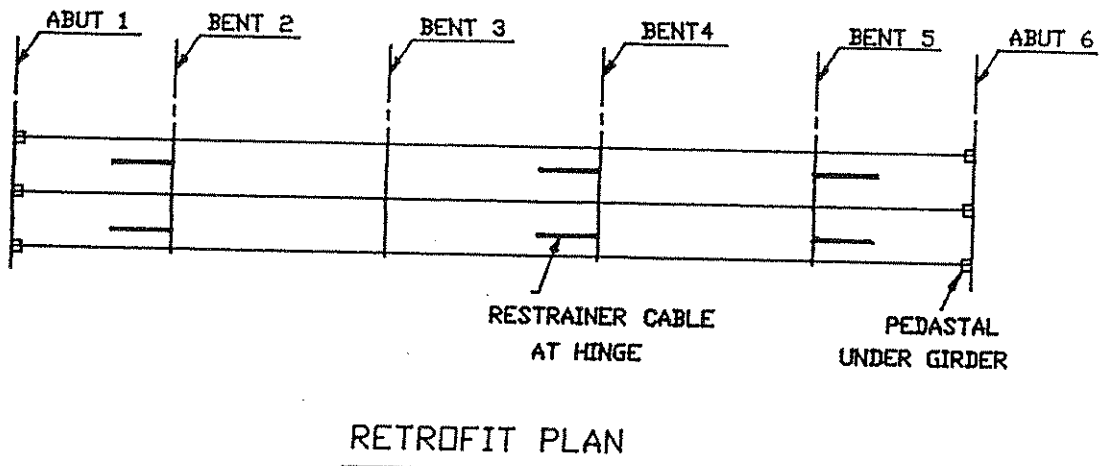


Figure 2.6 Seismic Retrofit of San Gregorio Bridge

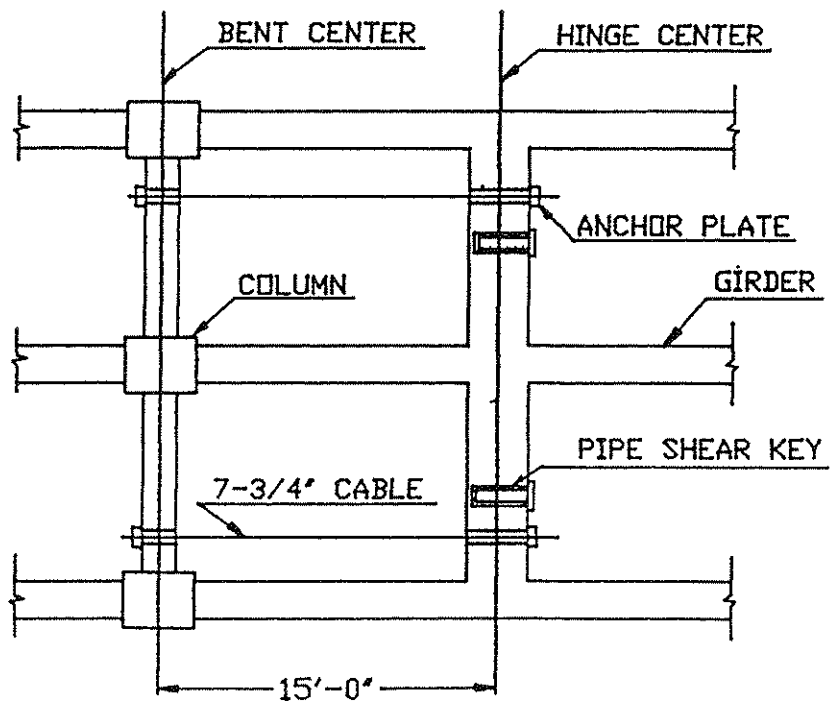


Figure 2.7 Intermediate Hinge Retrofit

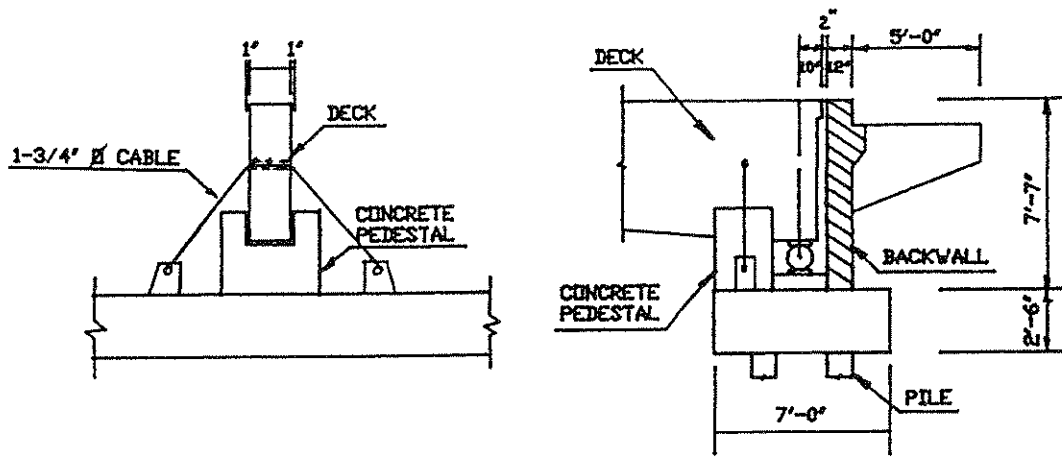


Figure 2.8 Abutment Retrofit

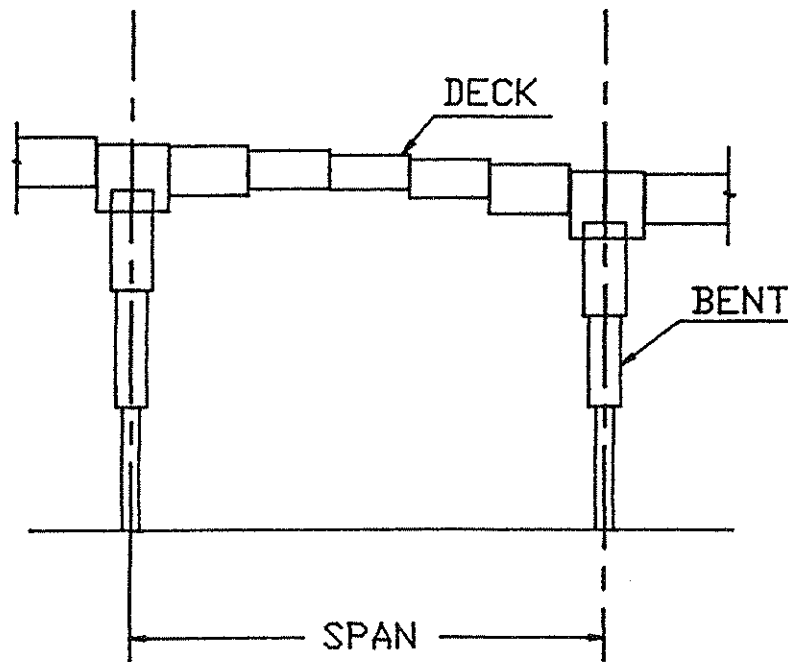


Figure 3.1 Straight Beam Model for Irregular Sections

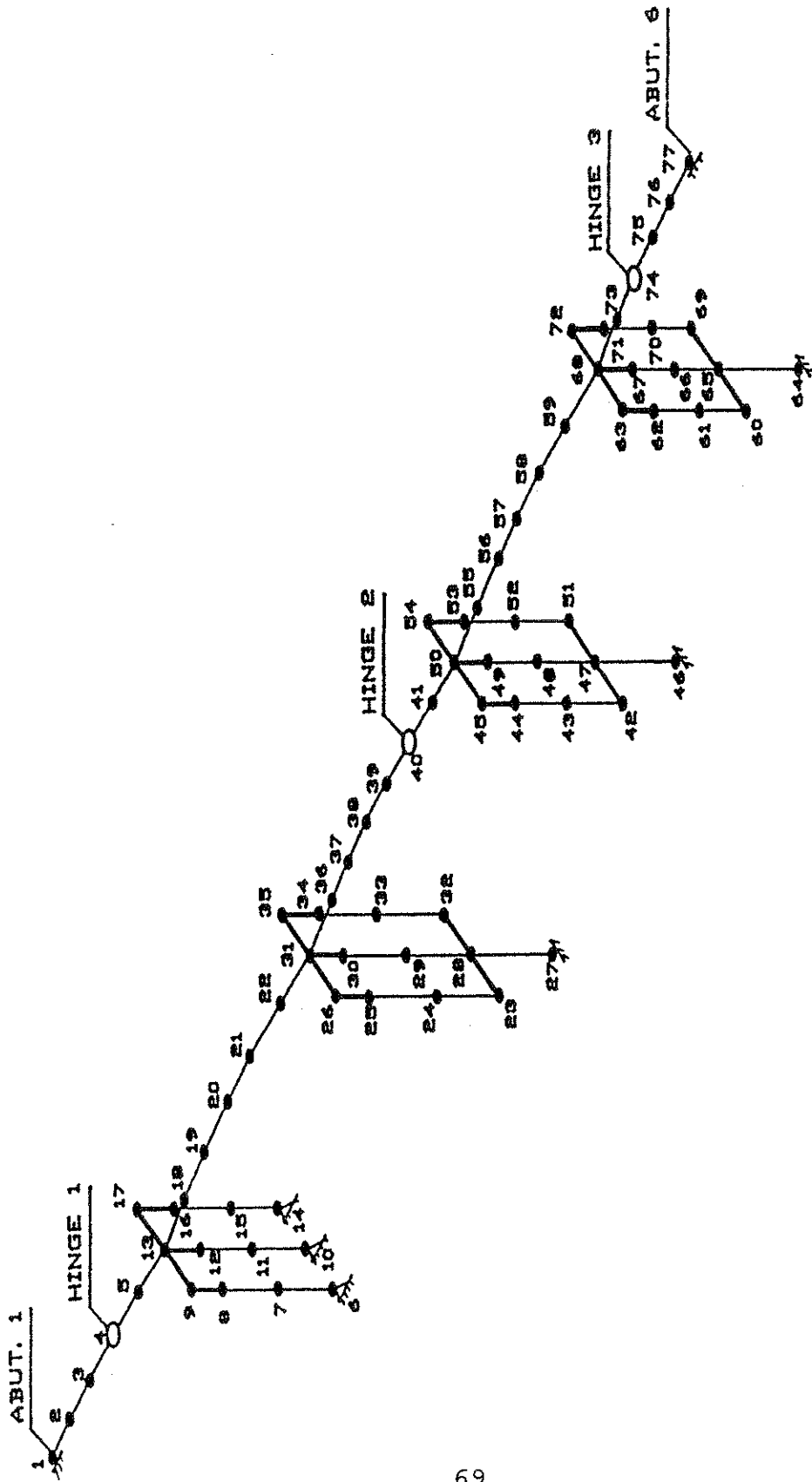


Figure 3.2 Images-3D Finite Element Model for San Gregorio Bridge

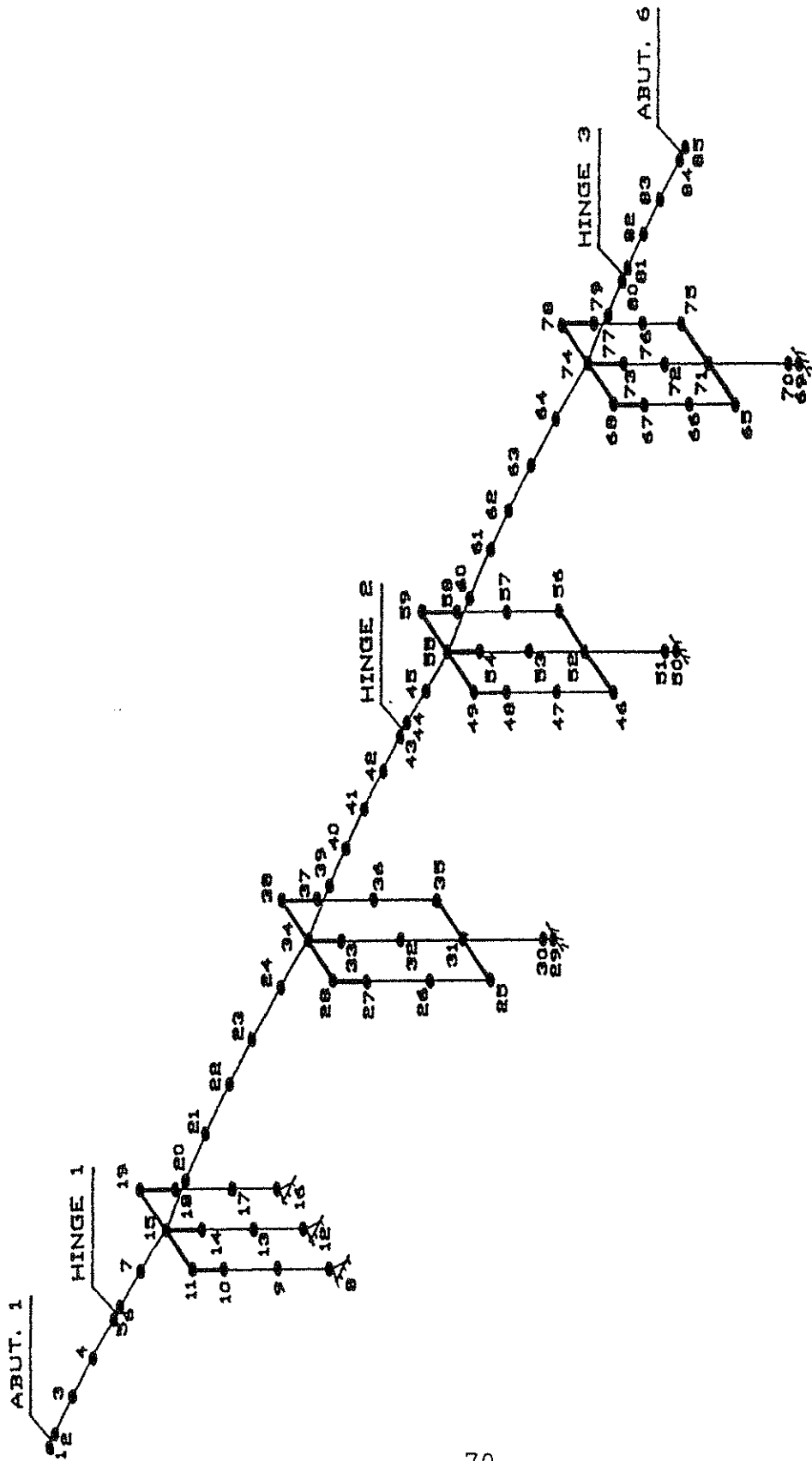


Figure 3.3 NEABS Finite Element Model for San Gregorio Bridge

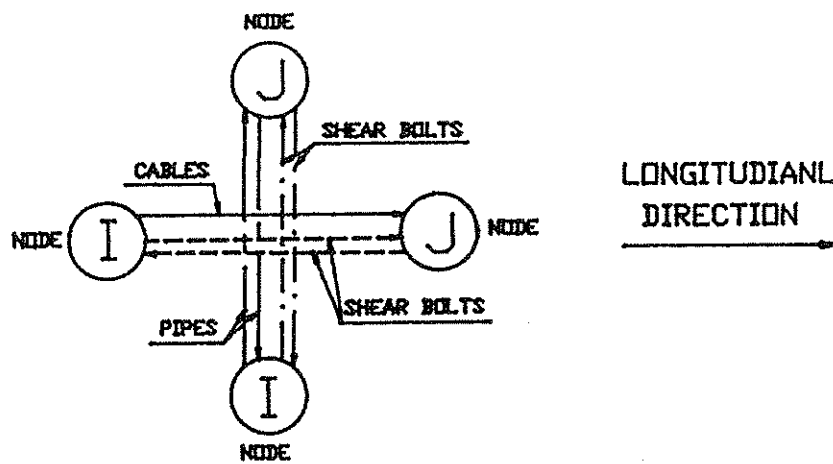


Figure 3.4 Hinge Element Model for Cables, Shear Bolts and Pipe Shear Keys at Hinge

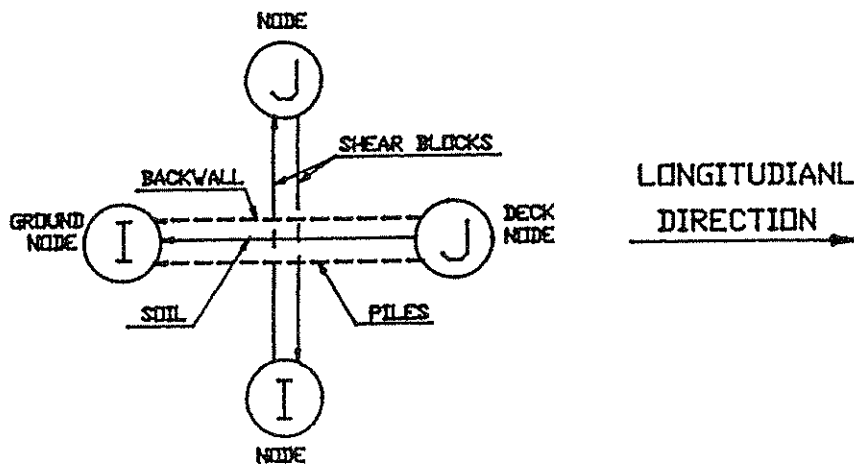


Figure 3.5 Hinge Element Model for Abutment Soil, Backwall and Shear Blocks at Abutment

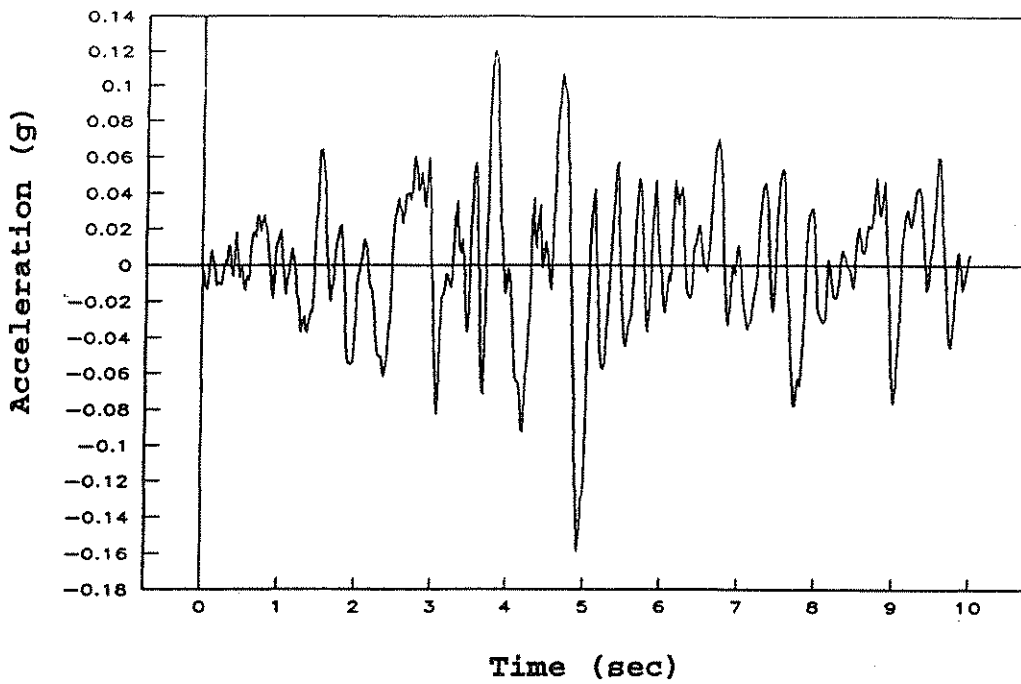


Figure 3.6 Accelerogram of the Loma Prieta Earthquake  
(Upper Crystal Station, North Component)

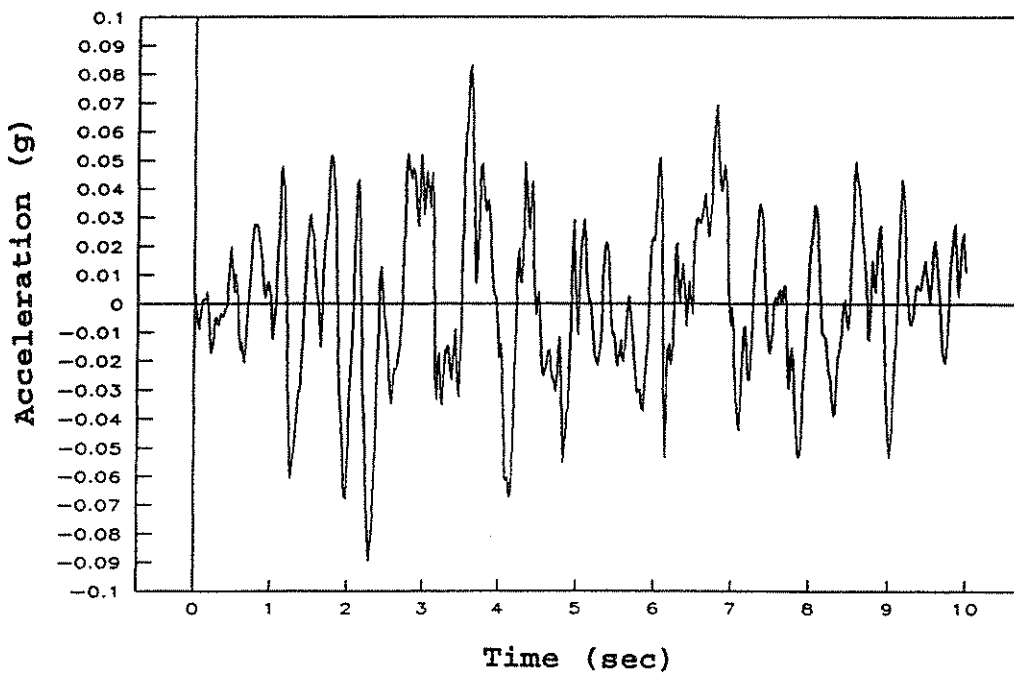
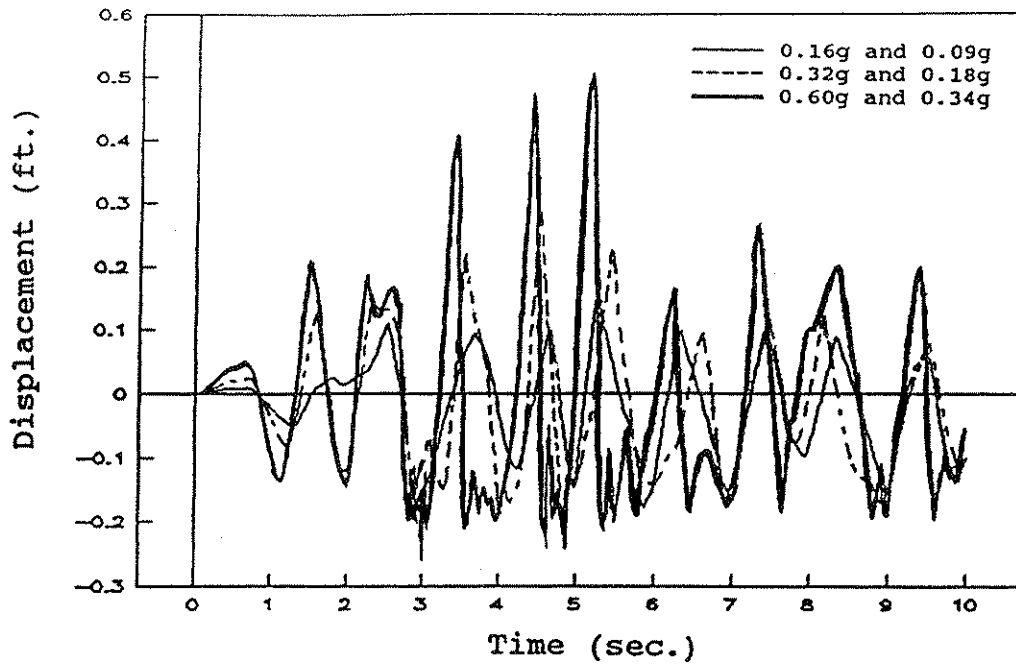
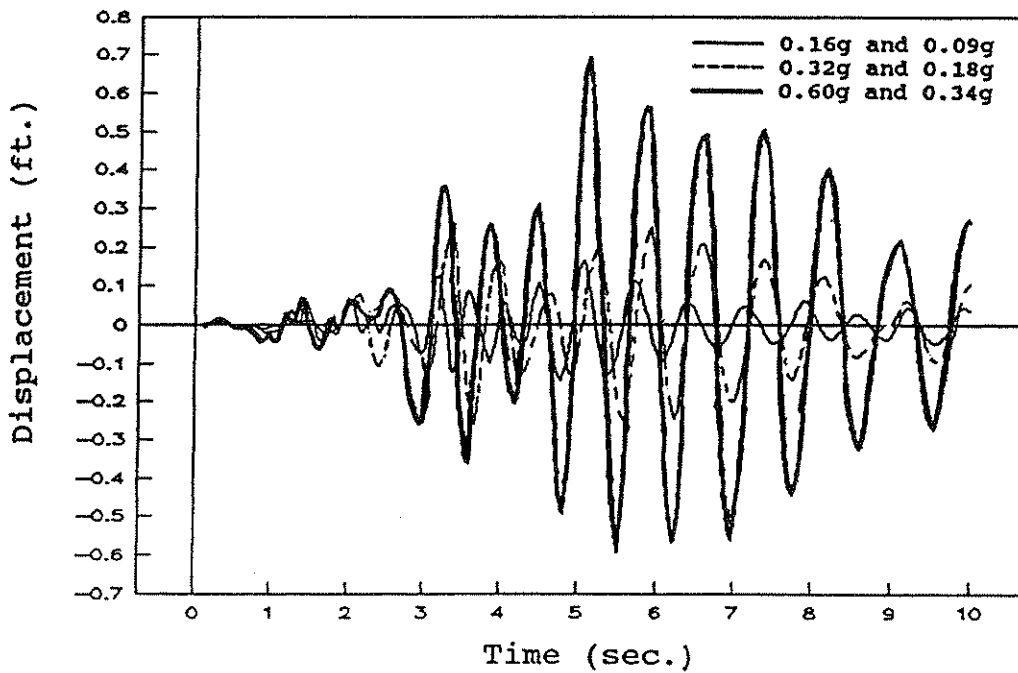


Figure 3.7 Accelerogram of the Loma Prieta Earthquake  
(Upper Crystal Station, East Component)

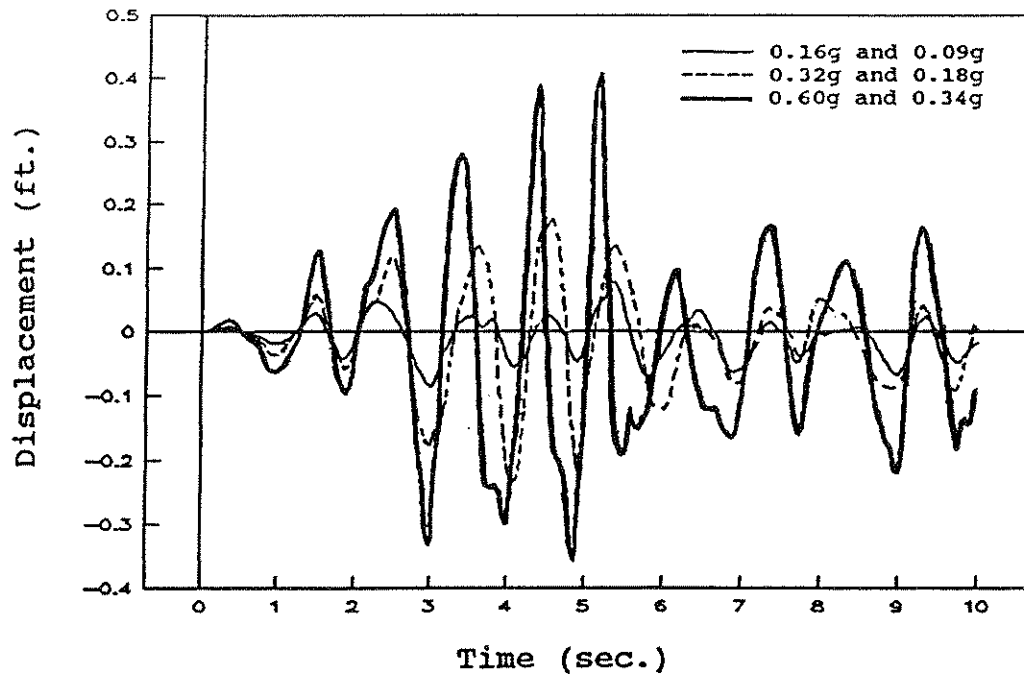


(a) Longitudinal Displacements

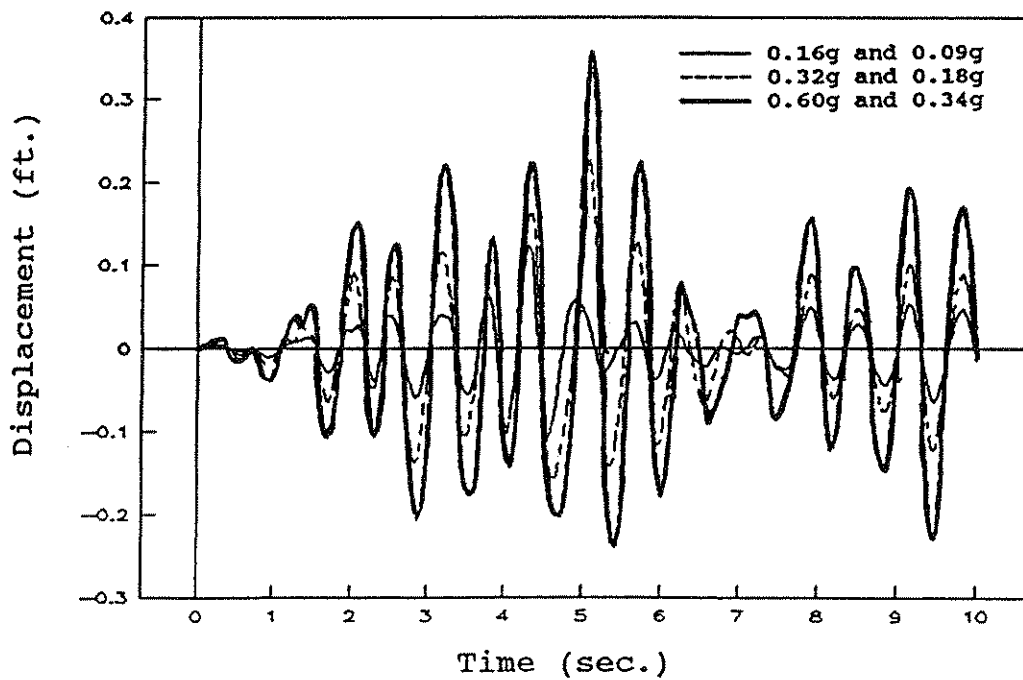


(b) Transverse Displacements

Figure 4.1 Displacement Responses of Node 4  
for the Three PGA Combinations

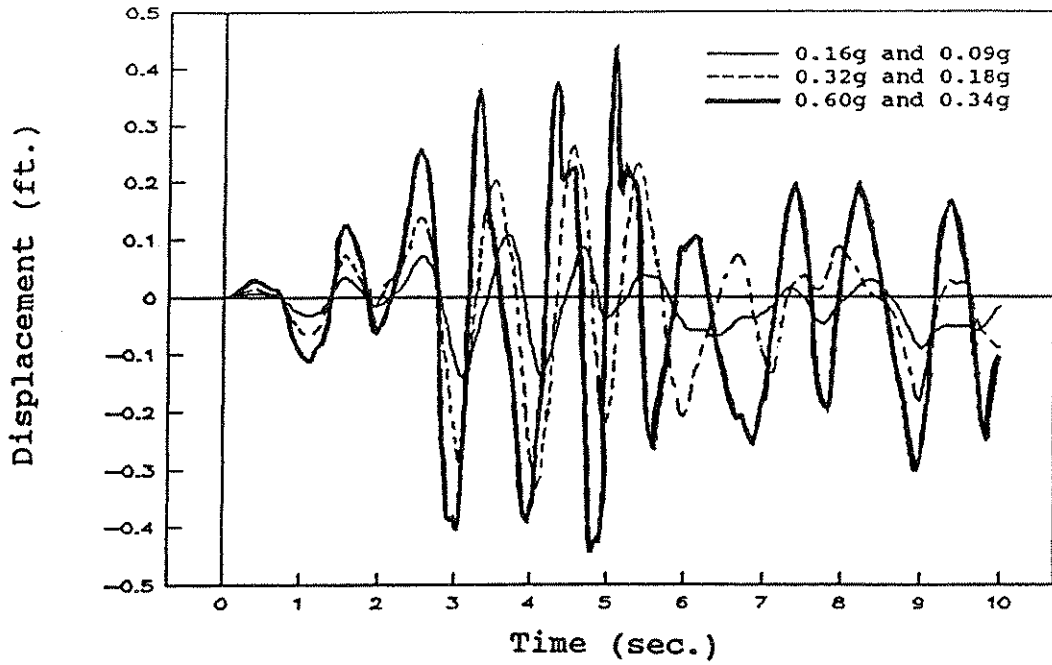


(a) Longitudinal Displacements

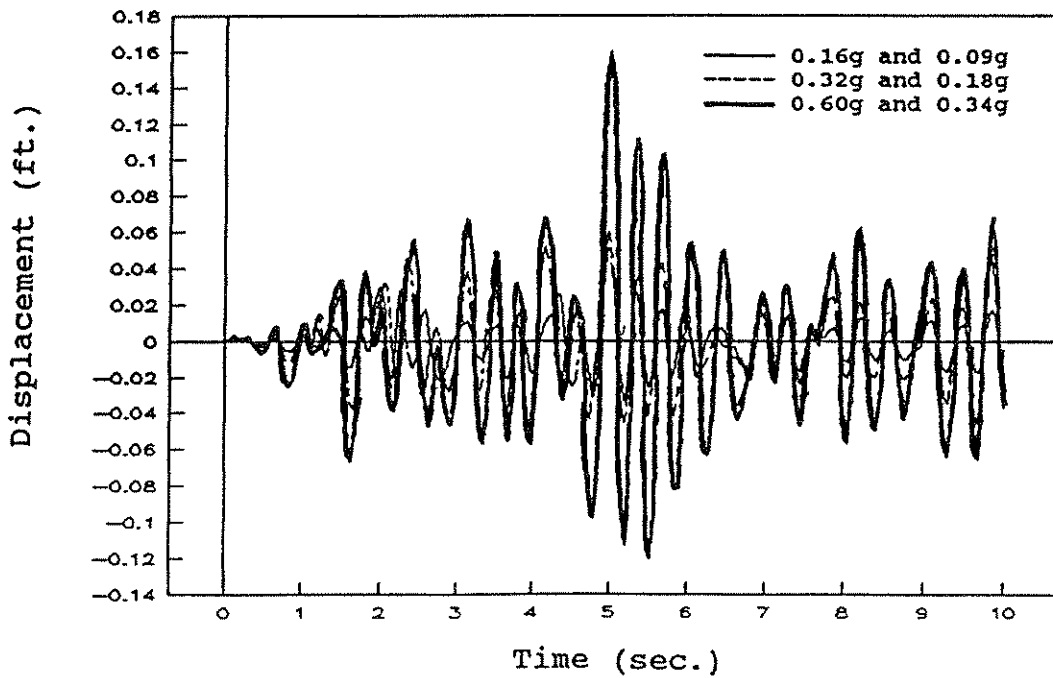


(b) Transverse Displacements

Figure 4.2 Displacement Responses of Node 22 for the Three PGA Combinations

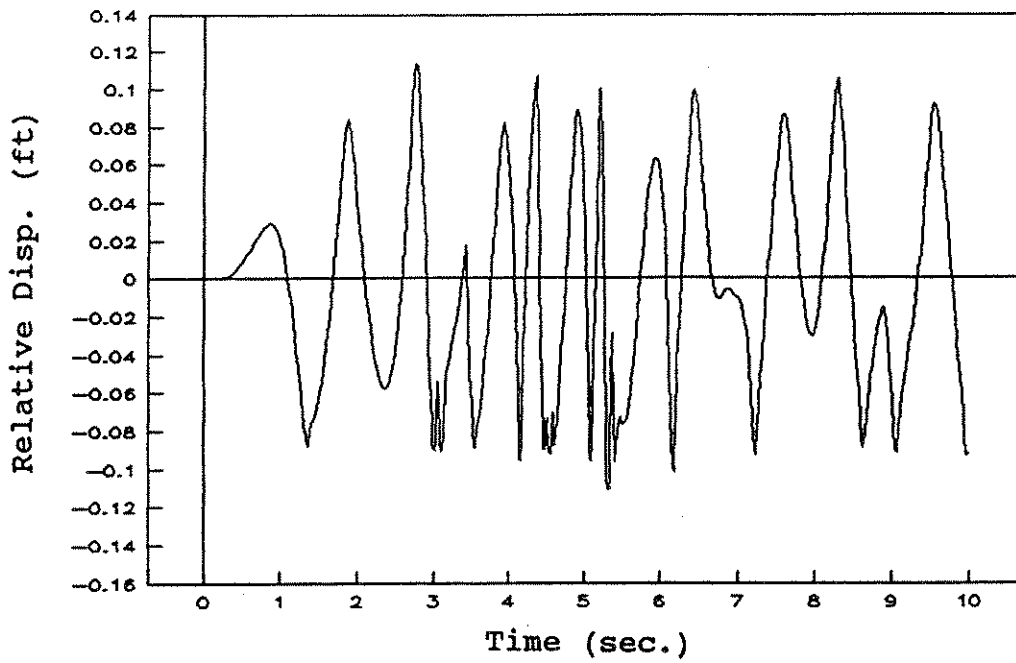


(a) Longitudinal Displacements

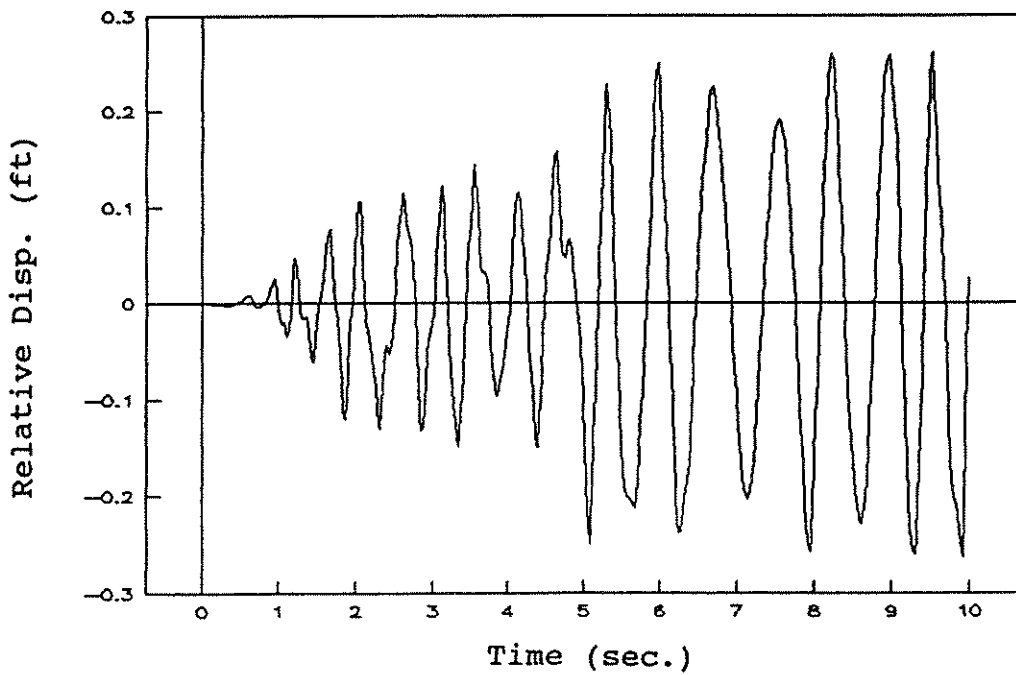


(b) Transverse Displacements

Figure 4.3 Displacement Responses of Node 62 for the Three PGA Combinations

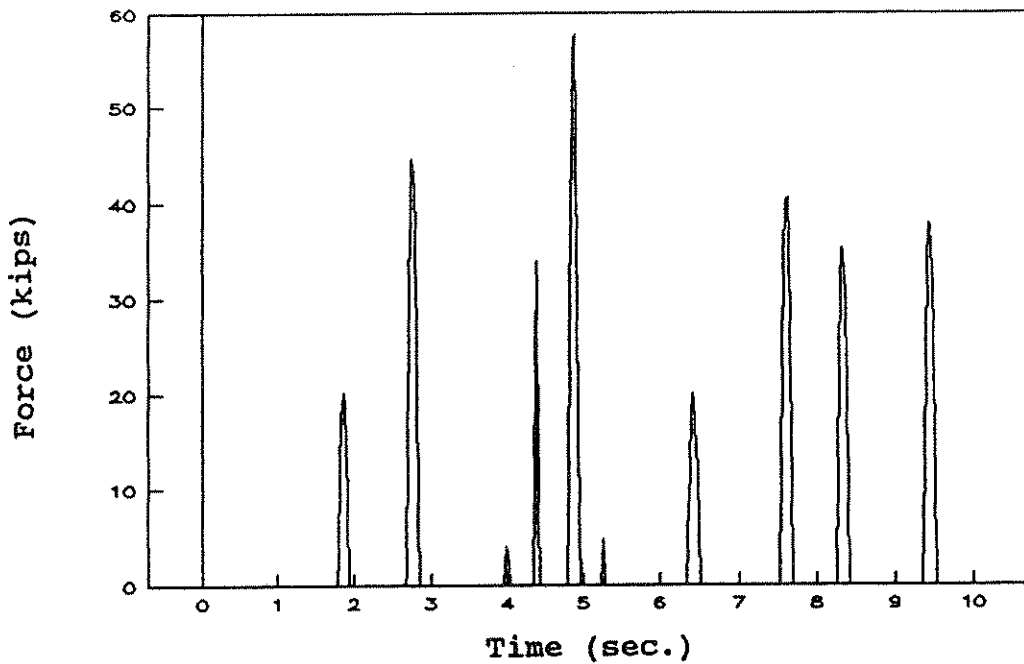


(a) Longitudinal Relative Displacements

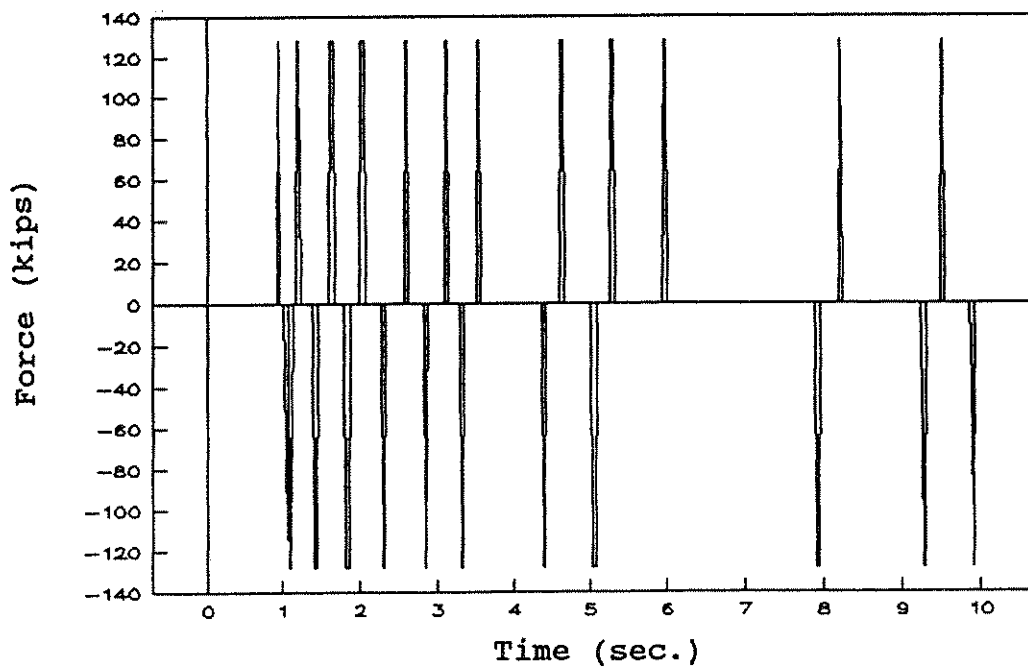


(b) Transverse Relative Displacements

Figure 4.4 Relative Displacements at Hinge 3 due to 0.32g and 0.18g Combination

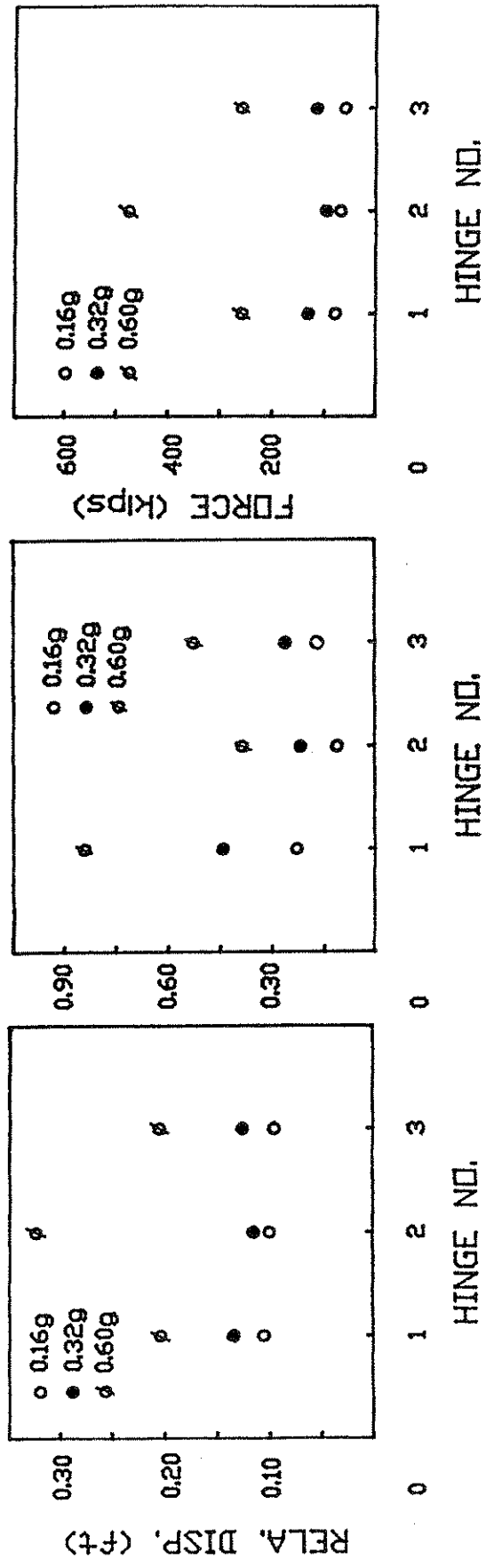


(a) Force of Restrainer Cable



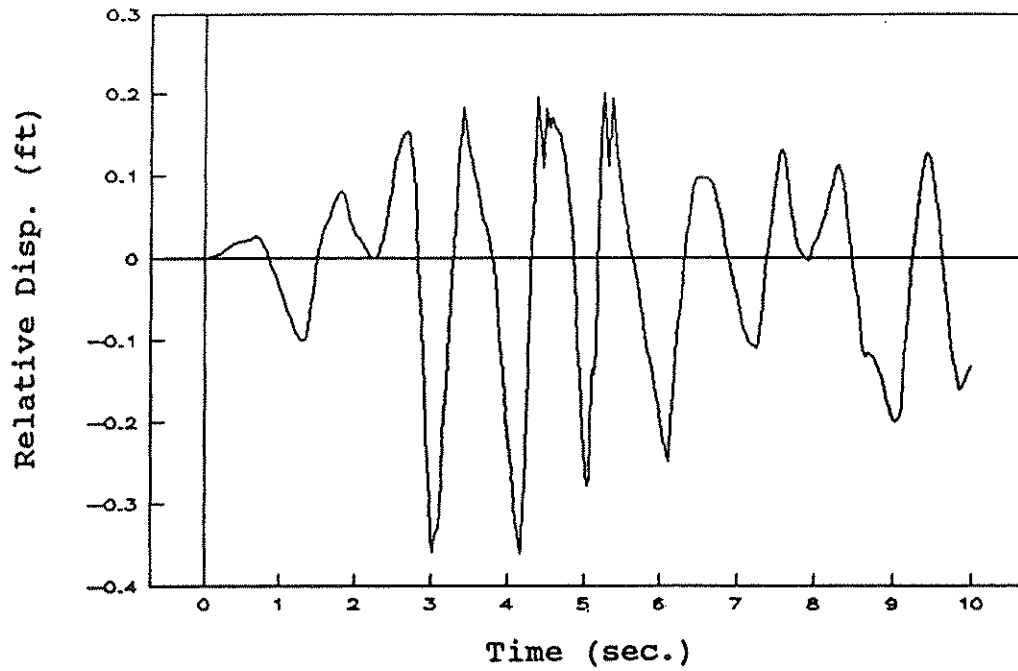
(b) Force of Pipe Shear Key

Figure 4.5 Force Responses at Hinge 3  
due to 0.32g and 0.18g Combination

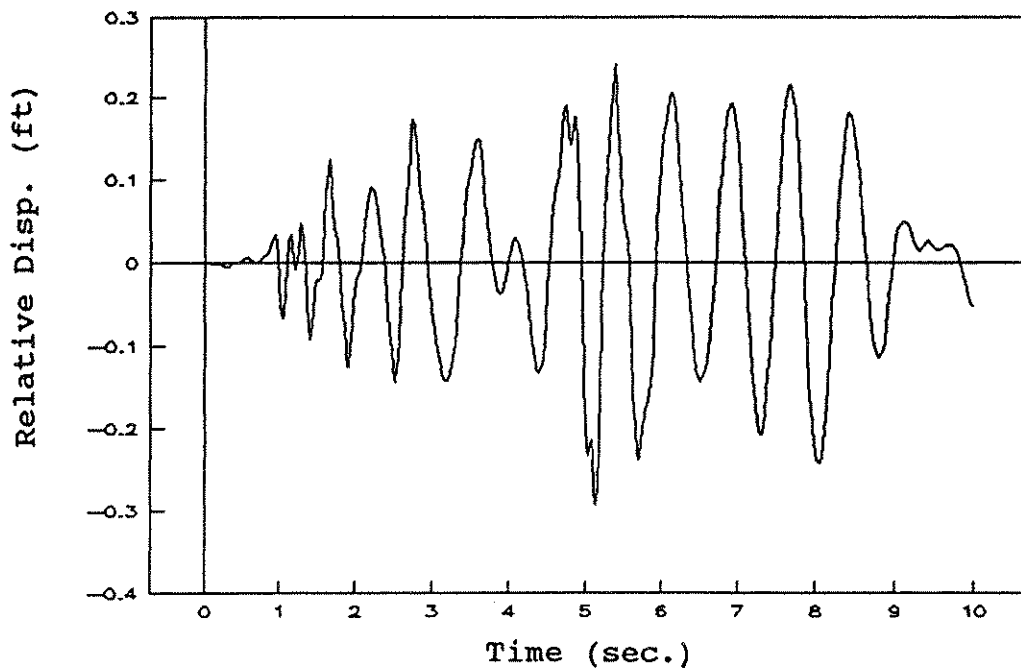


a) Maximum Longitudinal Relative Displacements      b) Maximum Transverse Relative Displacements      c) Maximum Cable Forces

Figure 4.6 Maximum Responses at the Hinges for the Three PGA Combinations

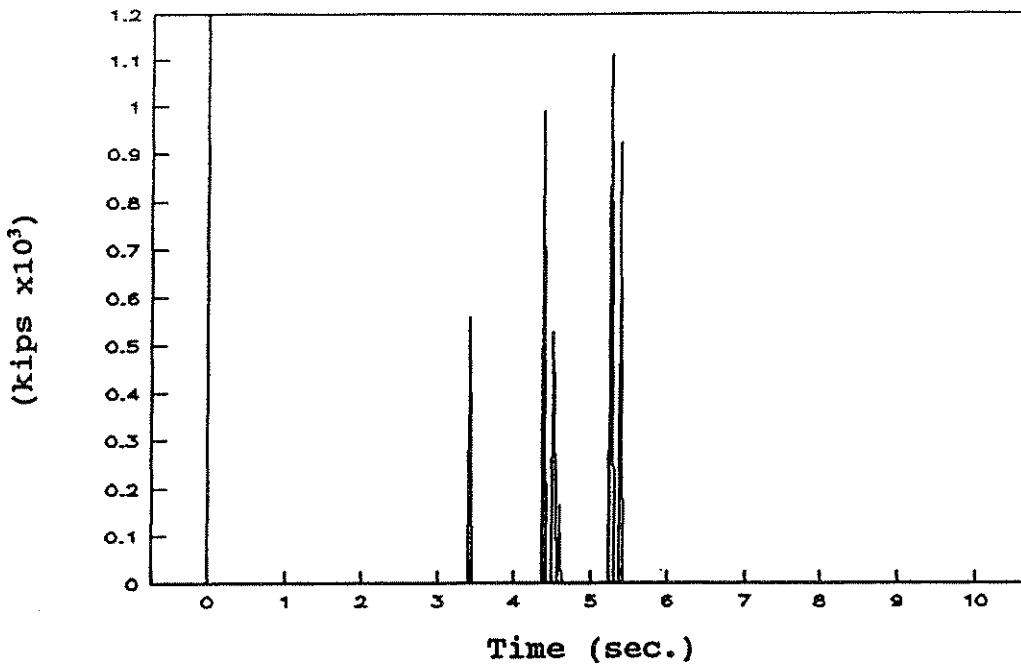


(a) Longitudinal Relative Displacements

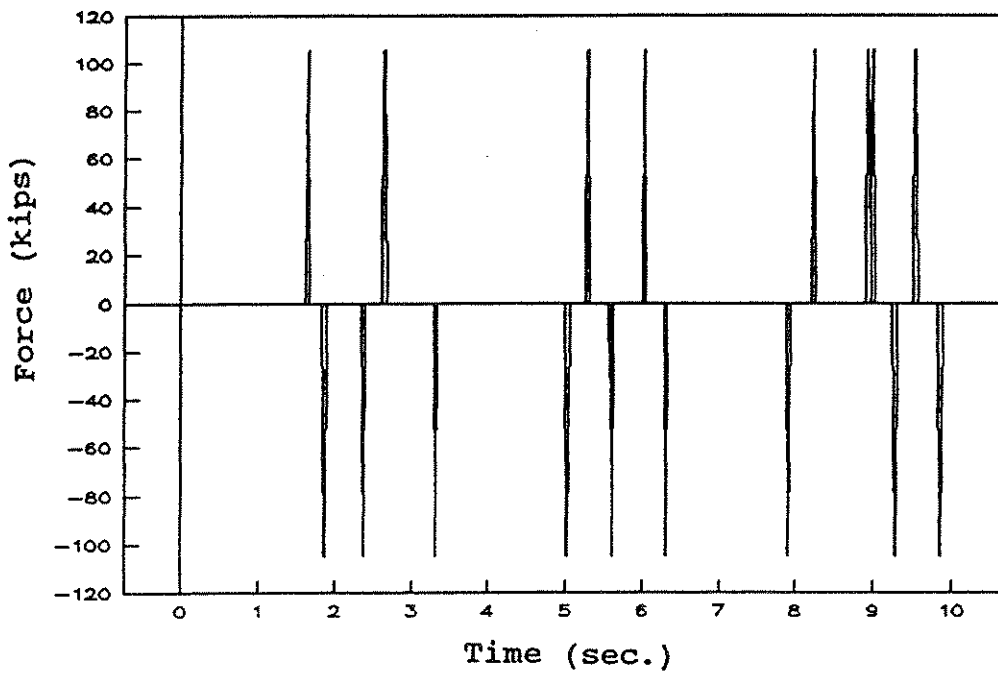


(b) Transverse Relative Displacements

Figure 4.7 Relative Displacements at Abutment 6 due to 0.32g and 0.18g Combination

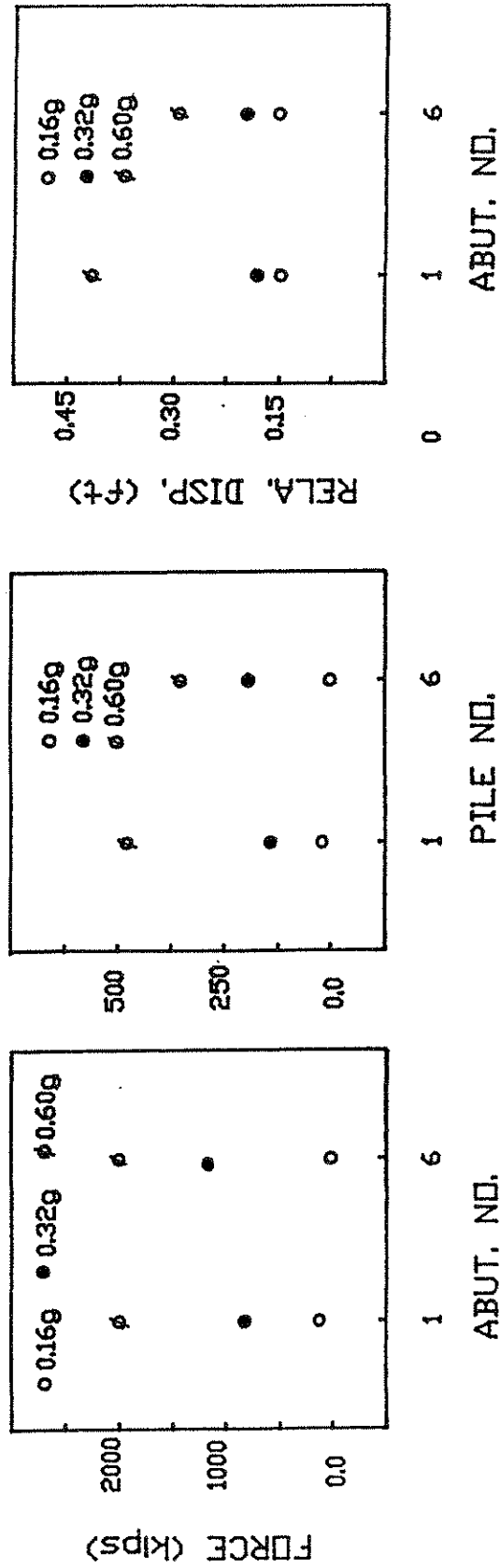


(a) Force of Abutment Back Fill



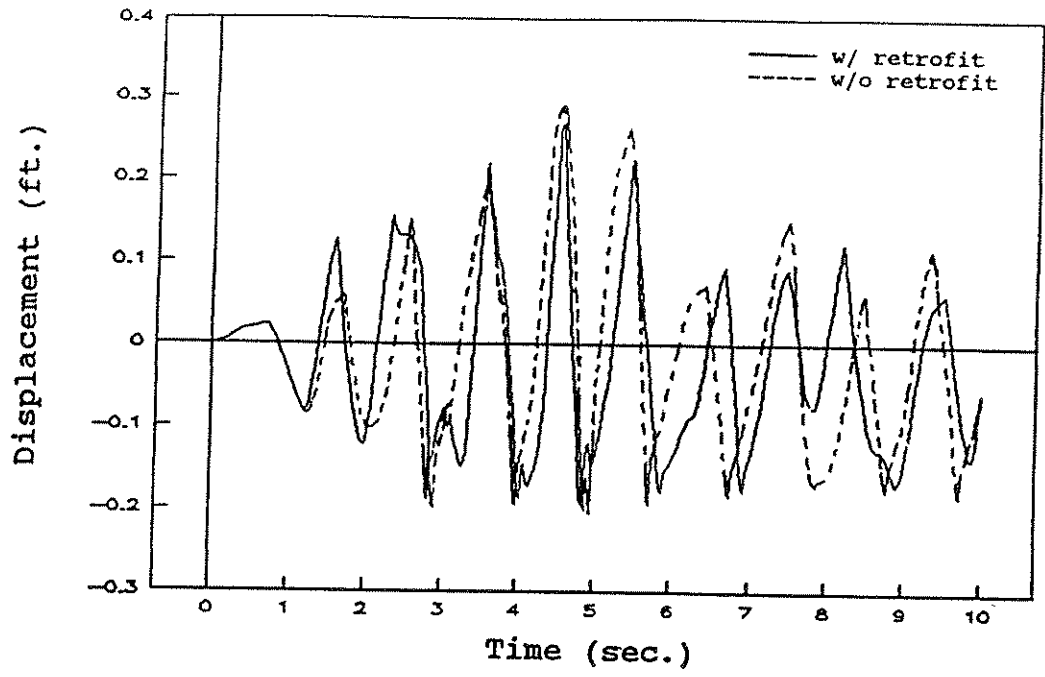
(b) Force of Shear Block at Abutment

Figure 4.8 Force Responses at Abutment 6  
due to 0.32g and 0.18g Combination

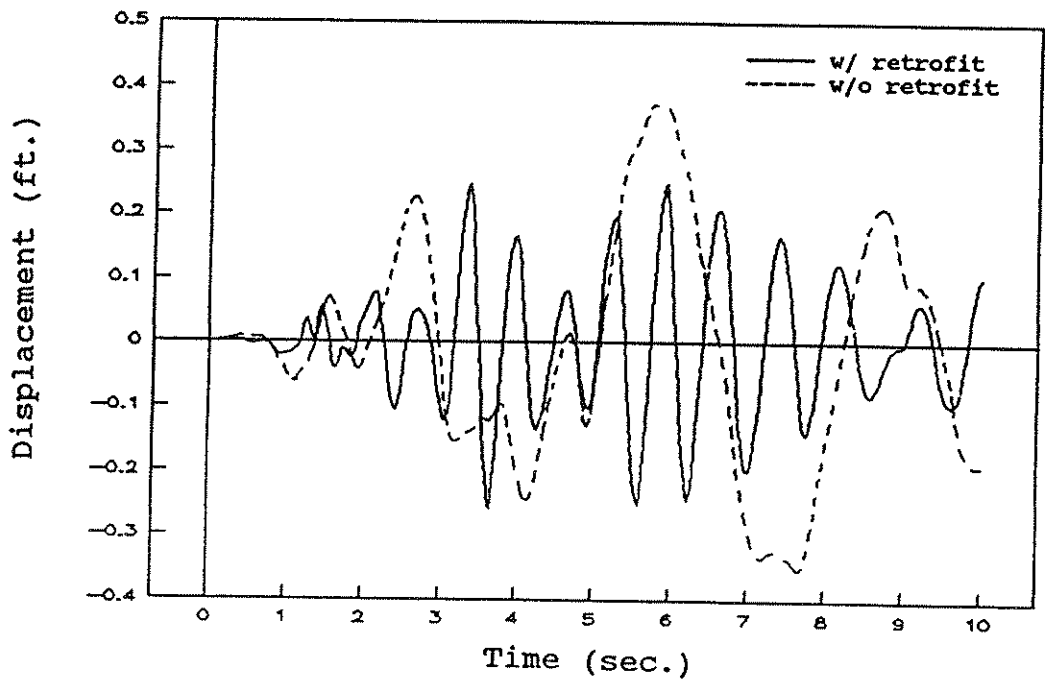


a) Force of Abutment Back Fill (b) Force of Abutment Piles (c) Transverse Relative Displacements

Figure 4.9 Maximum Responses at Abutments for the Three PGA Combinations

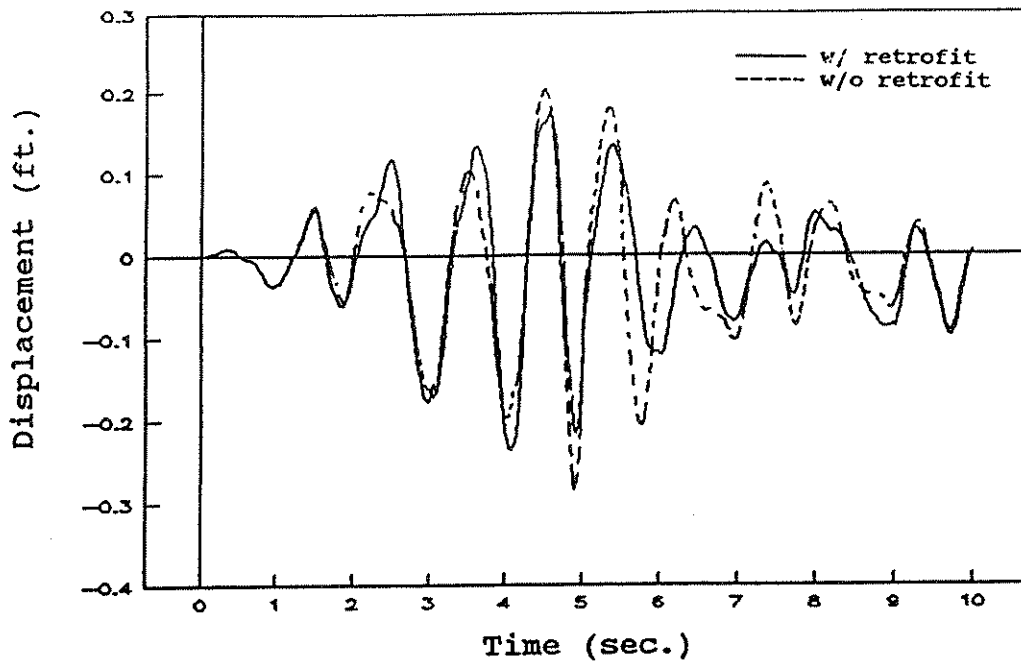


(a) Longitudinal Displacements

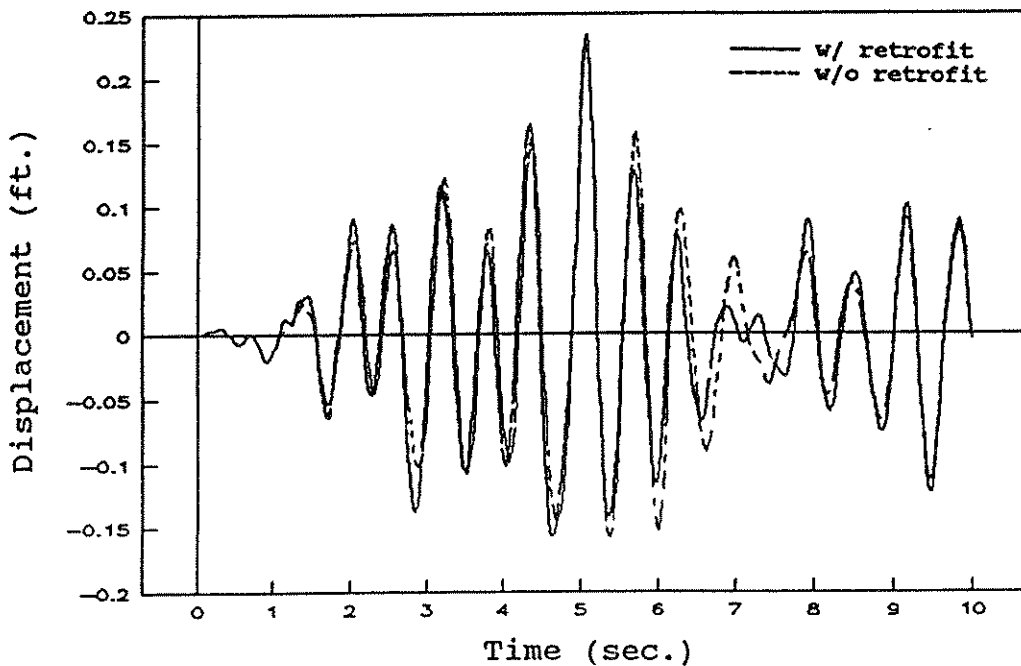


(b) Transverse Displacements

Figure 4.10 Displacement Responses of Node 4 with Retrofit and without Retrofit

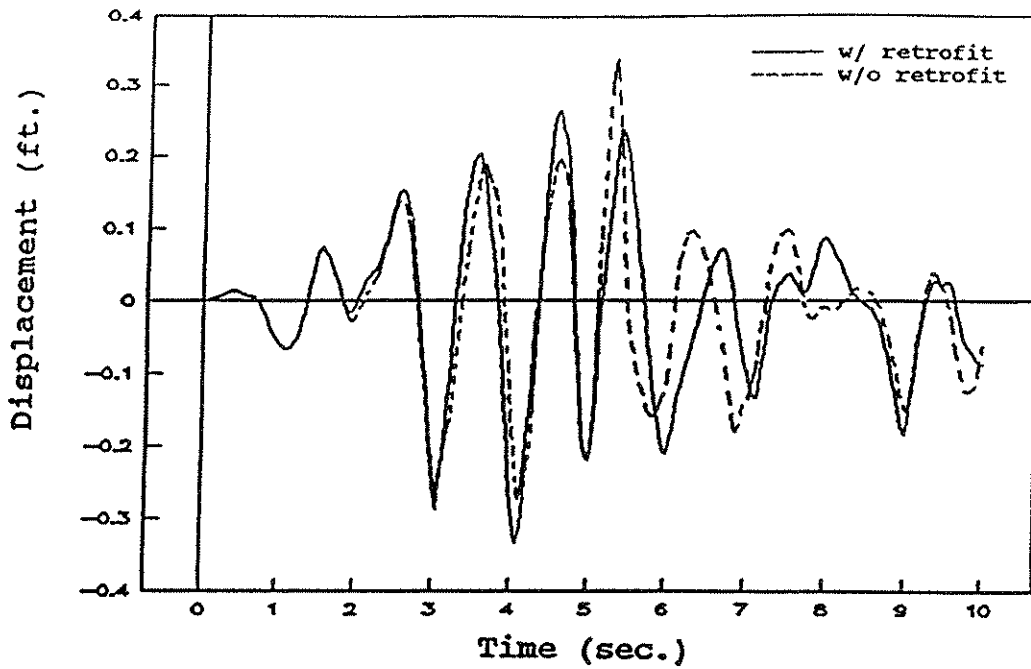


(a) Longitudinal Displacements

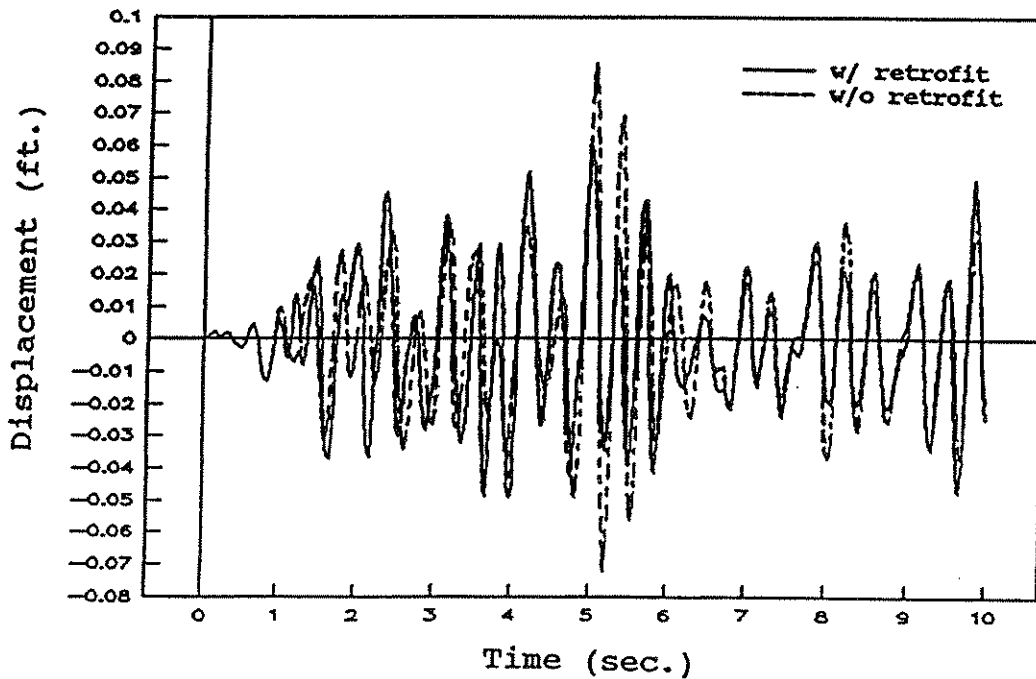


(b) Transverse Displacements

Figure 4.11 Displacement Responses of Node 22 with Retrofit and without Retrofit

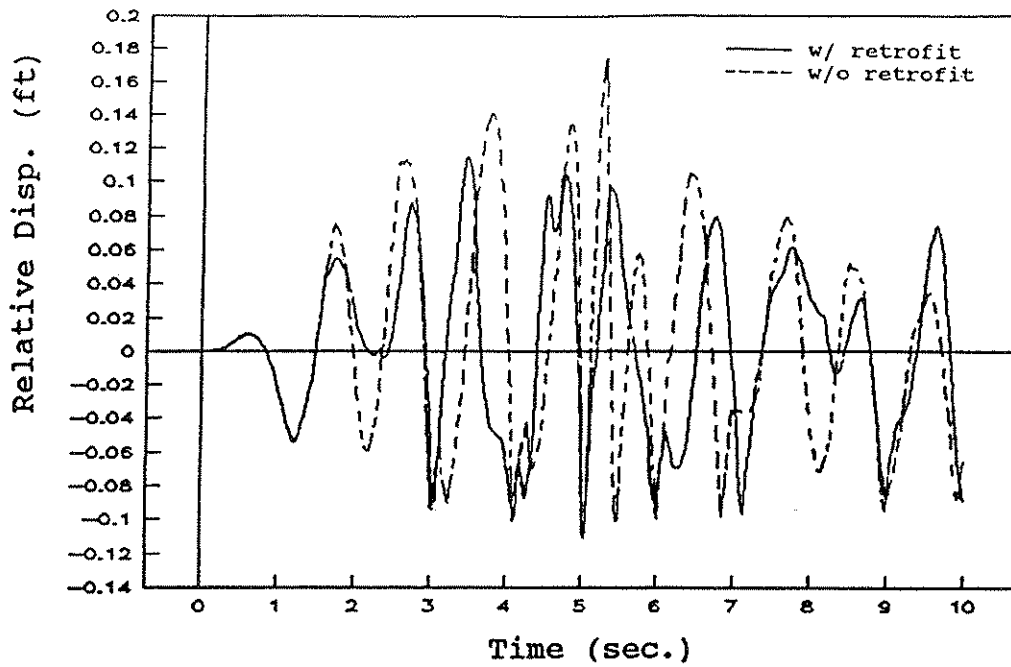


(a) Longitudinal Displacements

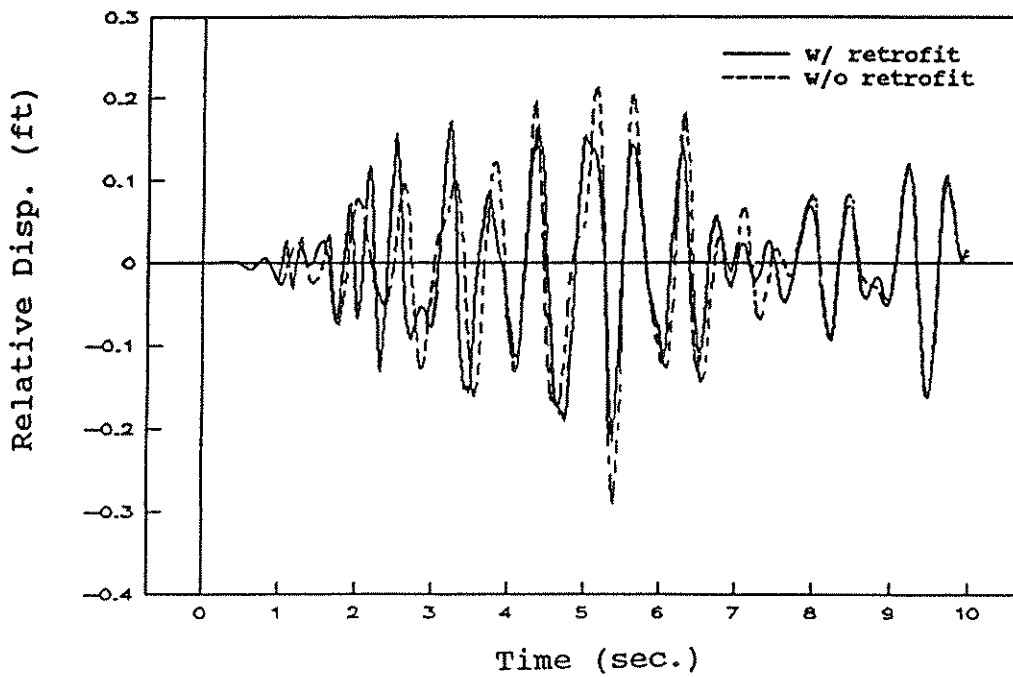


(b) Transverse Displacements

Figure 4.12 Displacement Responses of Node 62 with Retrofit and without Retrofit

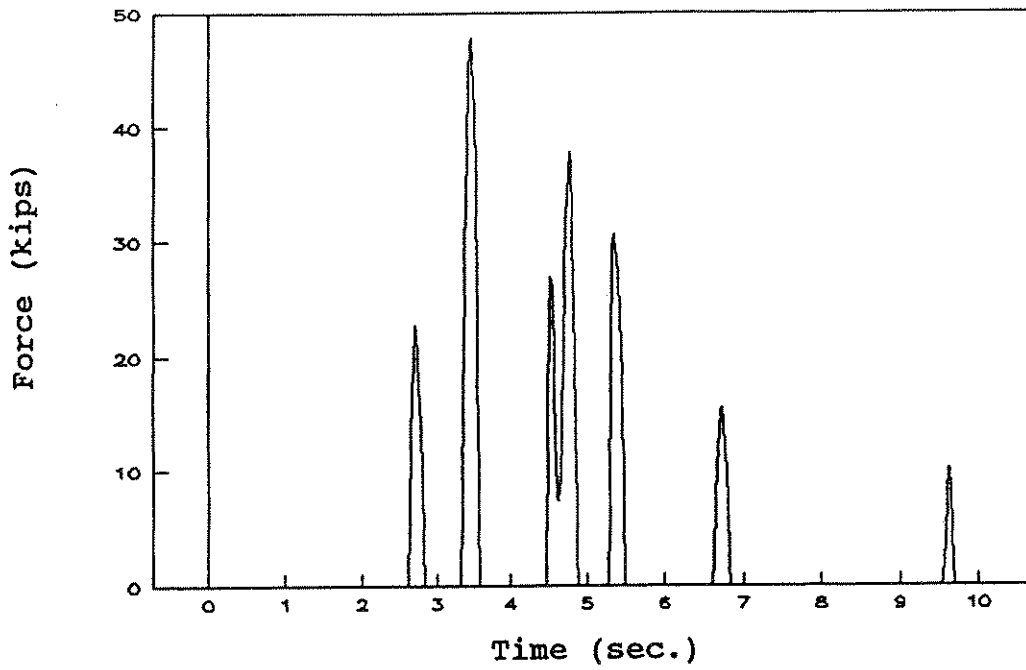


(a) Longitudinal Relative Displacements

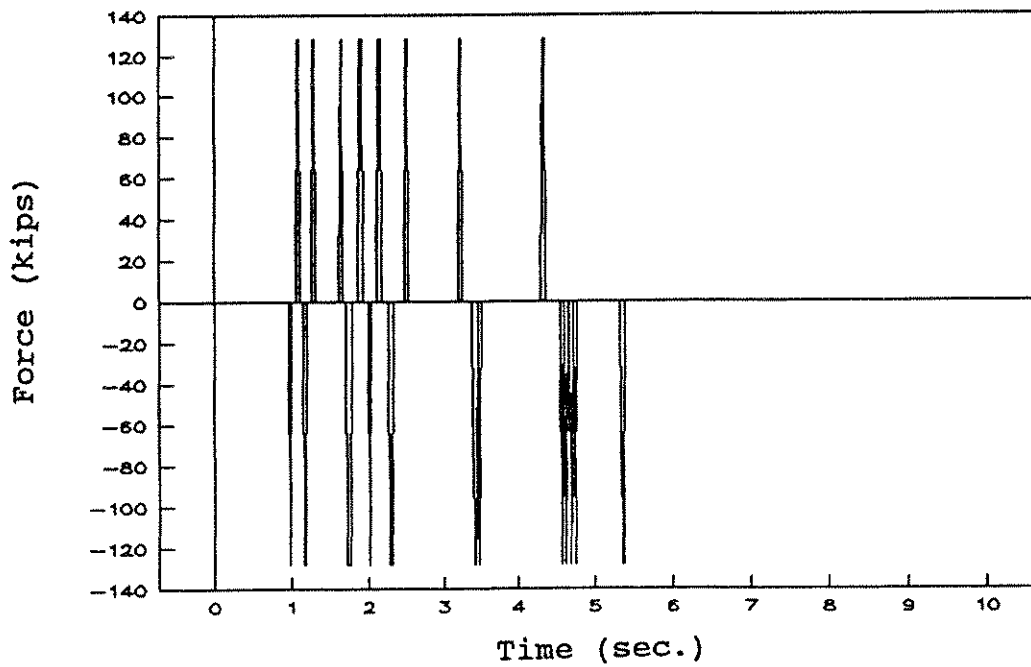


(b) Transverse Relative Displacements

Figure 4.13 Relative Displacements at Hinge 2 with Retrofit and without Retrofit

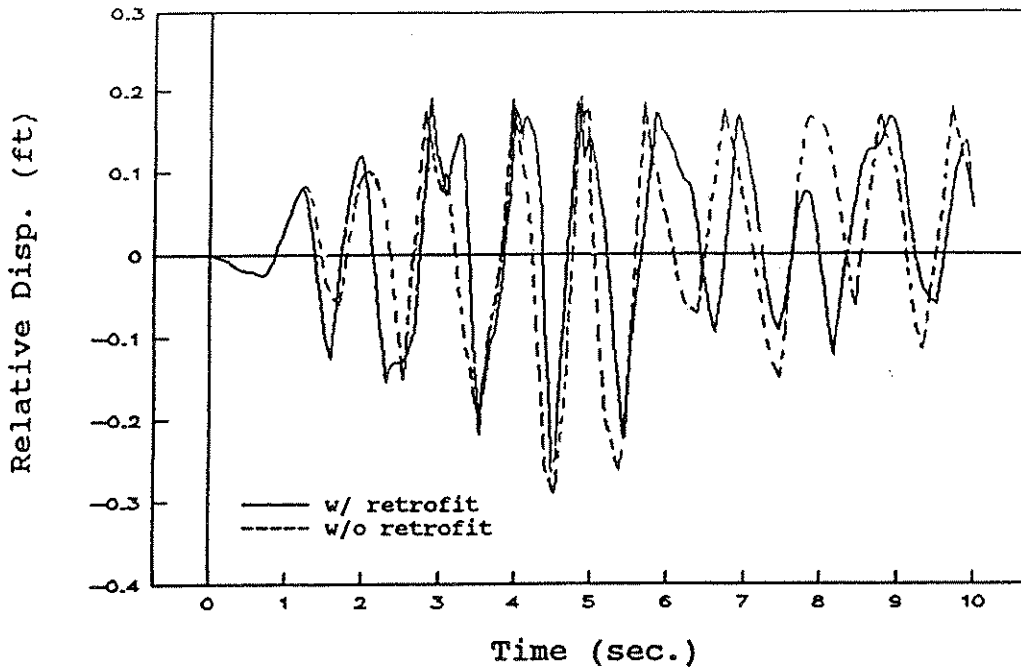


(a) Force of Restrainer Cable

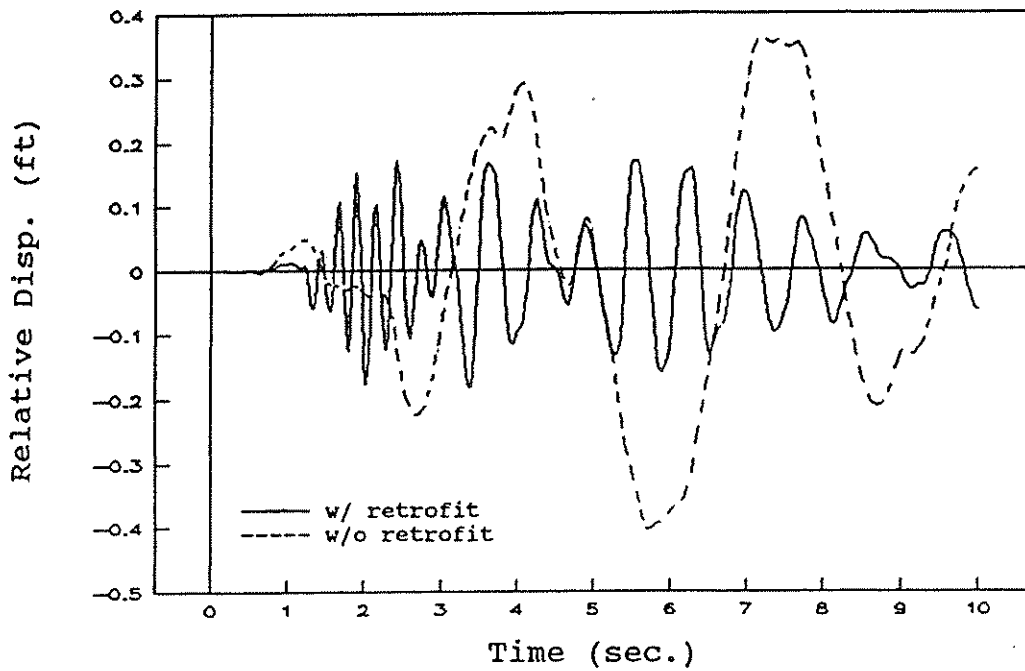


(b) Force of Pipe Shear Key

Figure 4.14 Force Responses at Hinge 2  
with Retrofit and without Retrofit

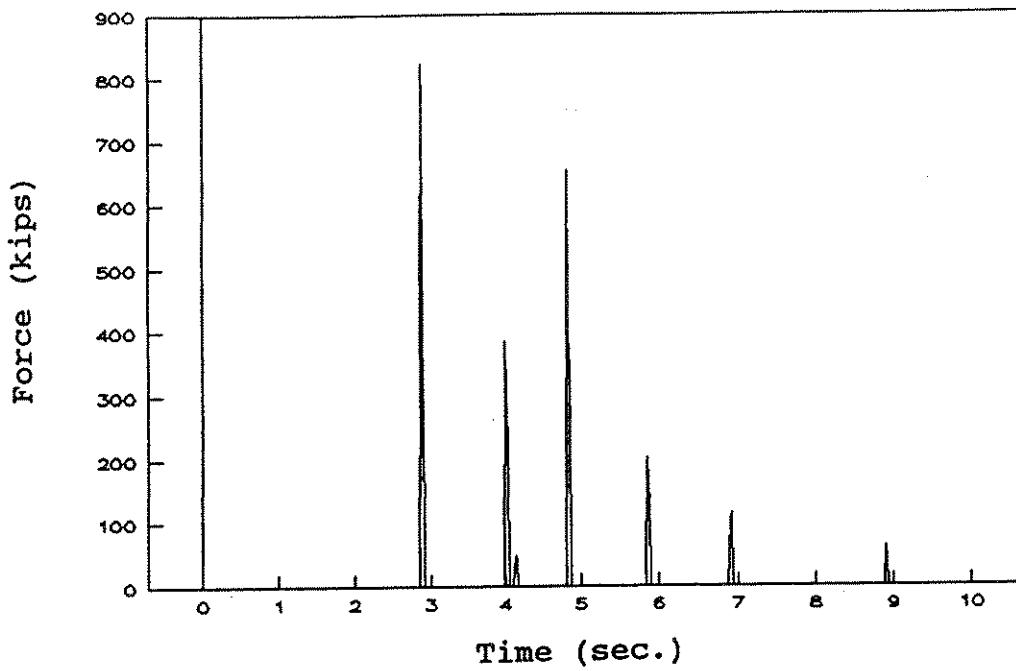


(a) Longitudinal Relative Displacements

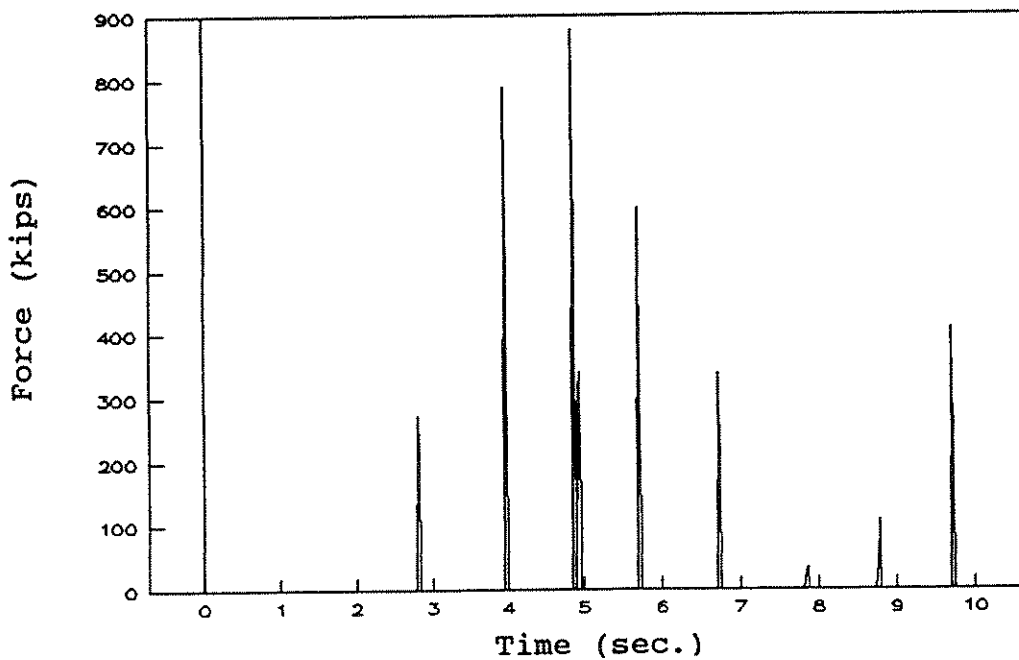


(b) Transverse Relative Displacements

Figure 4.15 Relative Displacements at Abutment 1 with Retrofit and without Retrofit



(a) Abutment Force for Case w\ Retrofit



(b) Abutment Force for Case w\o Retrofit

Figure 4.16 Forces of Abutment Back Fill at Abutment 1 with Retrofit and without Retrofit

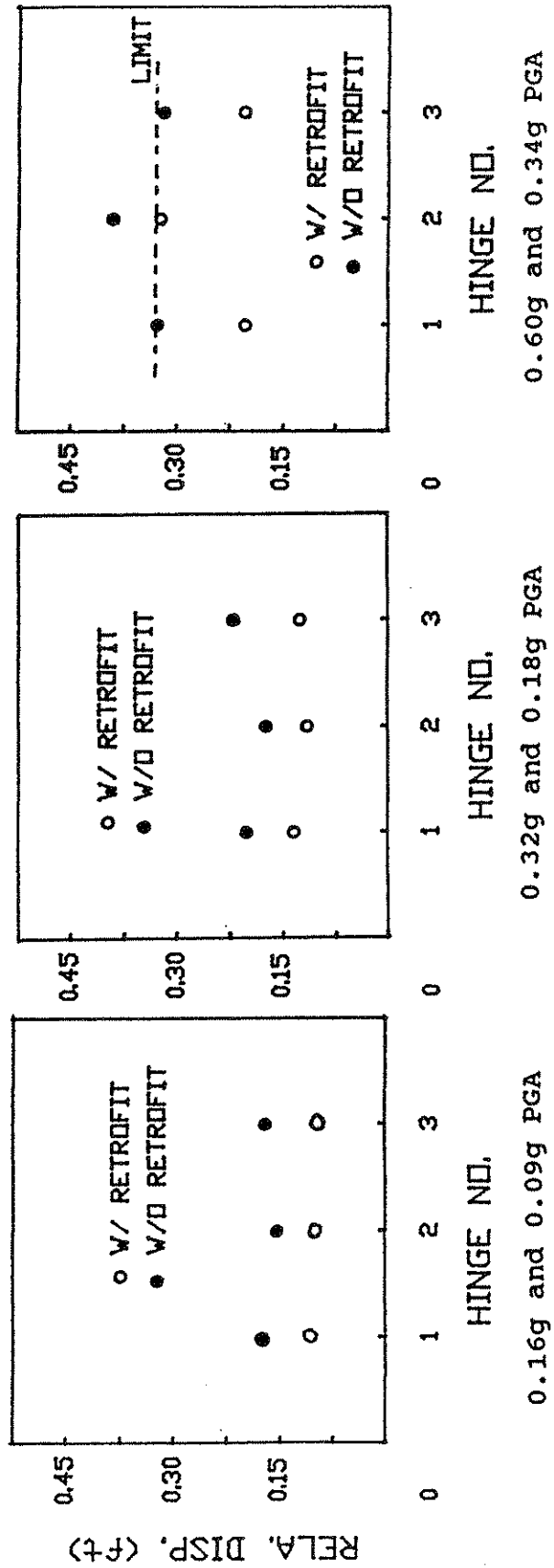


Figure 4.17 Maximum Longitudinal Relative Displacements at Hinges with Retrofit and without Retrofit

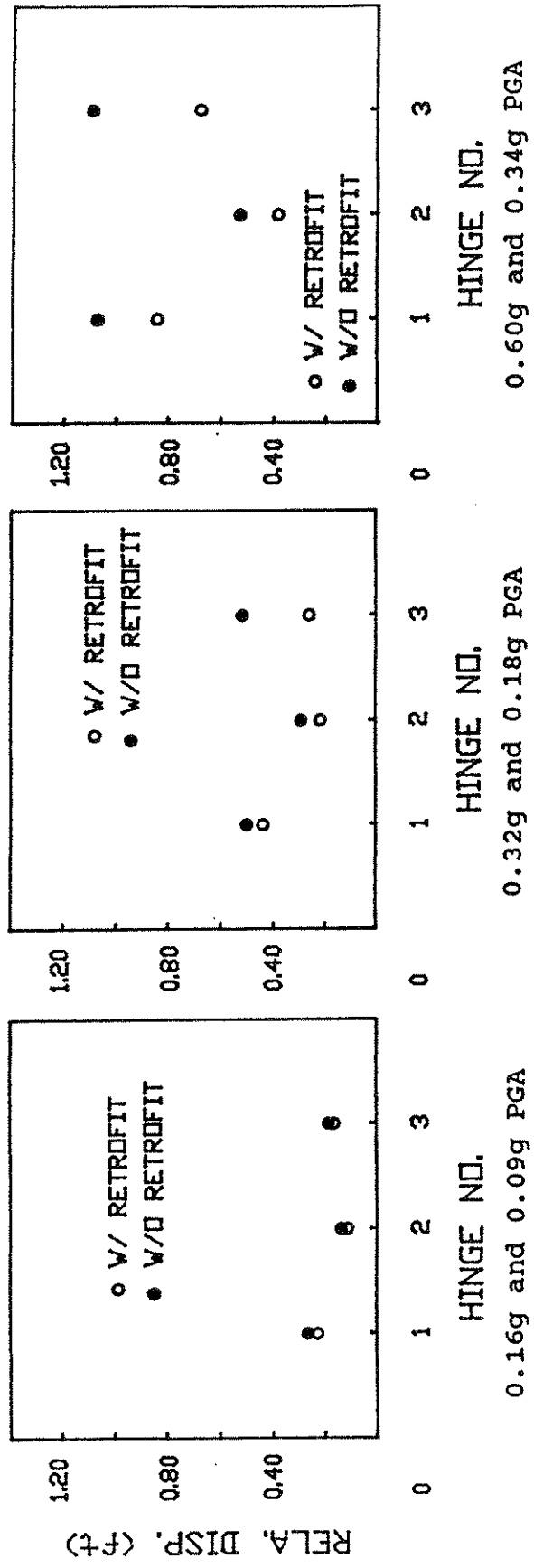


Figure 4.18 Maximum Transverse Relative Displacements at Hinges with Retrofit and without Retrofit

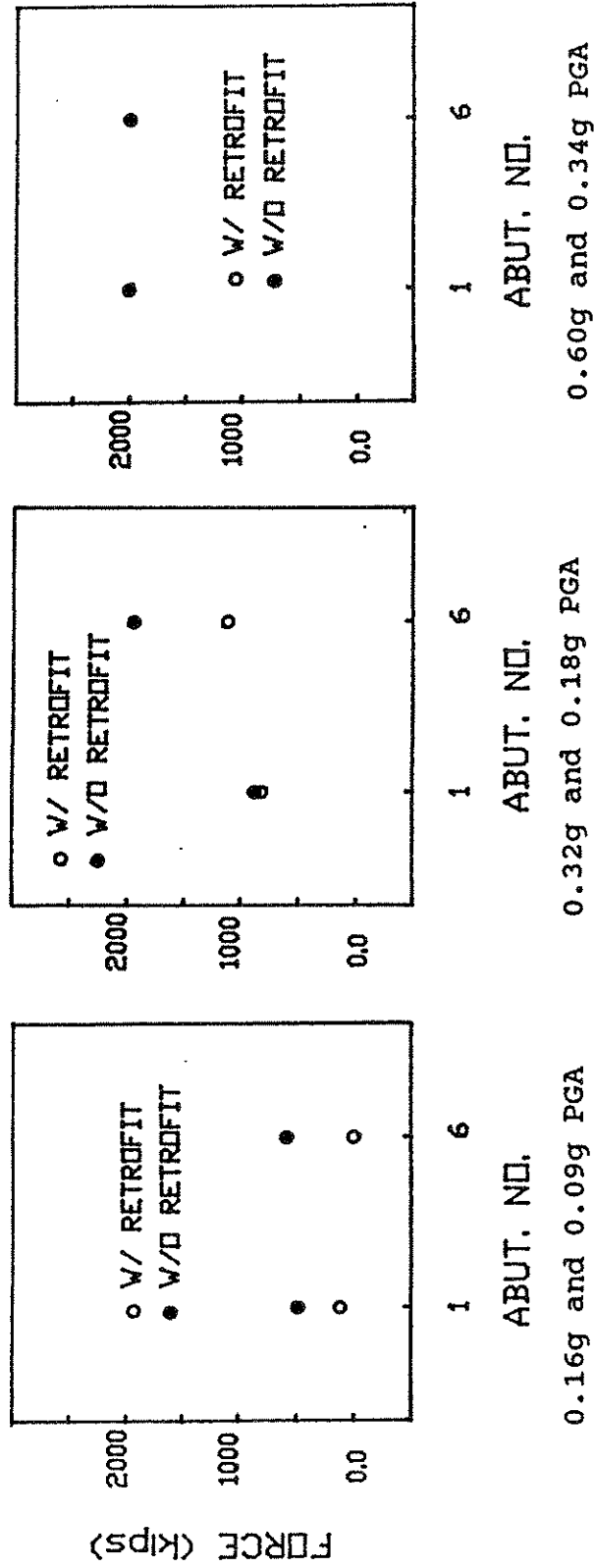


Figure 4.19 Maximum Abutment Back Fill Forces with Retrofit and without Retrofit

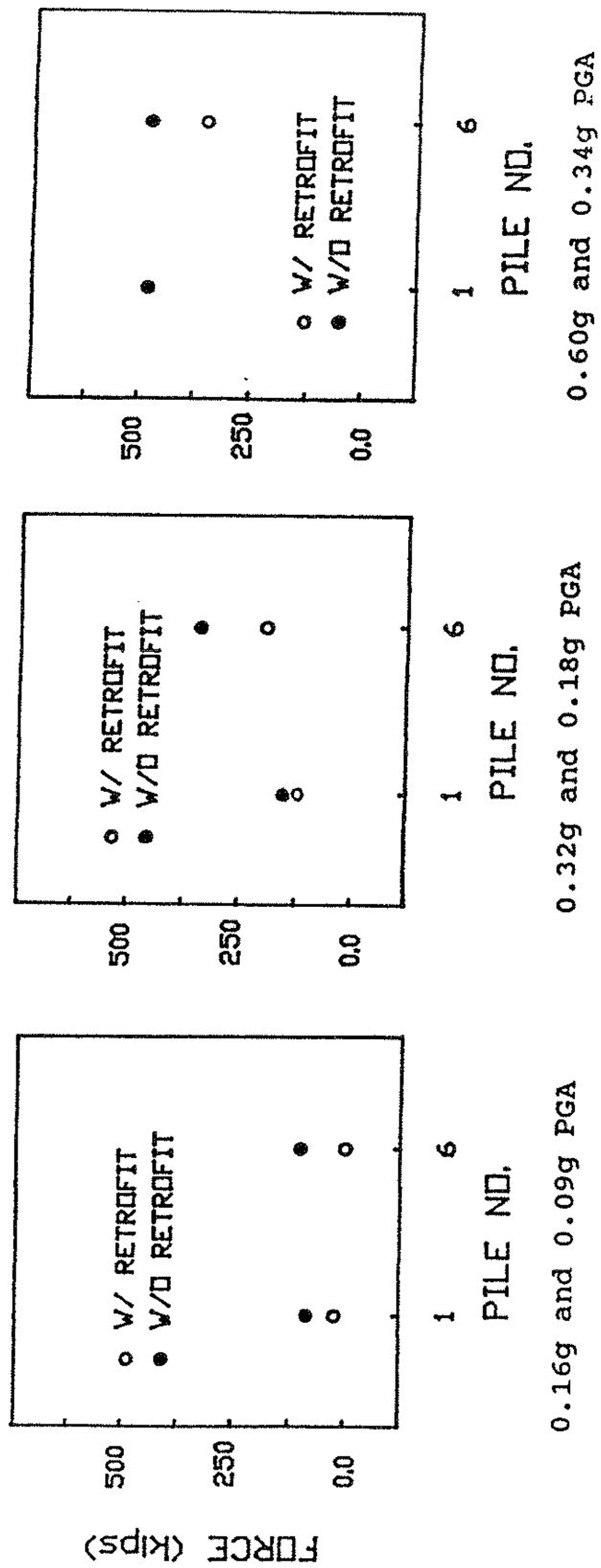


Figure 4.20 Maximum Abutment Pile Forces with Retrofit and without Retrofit

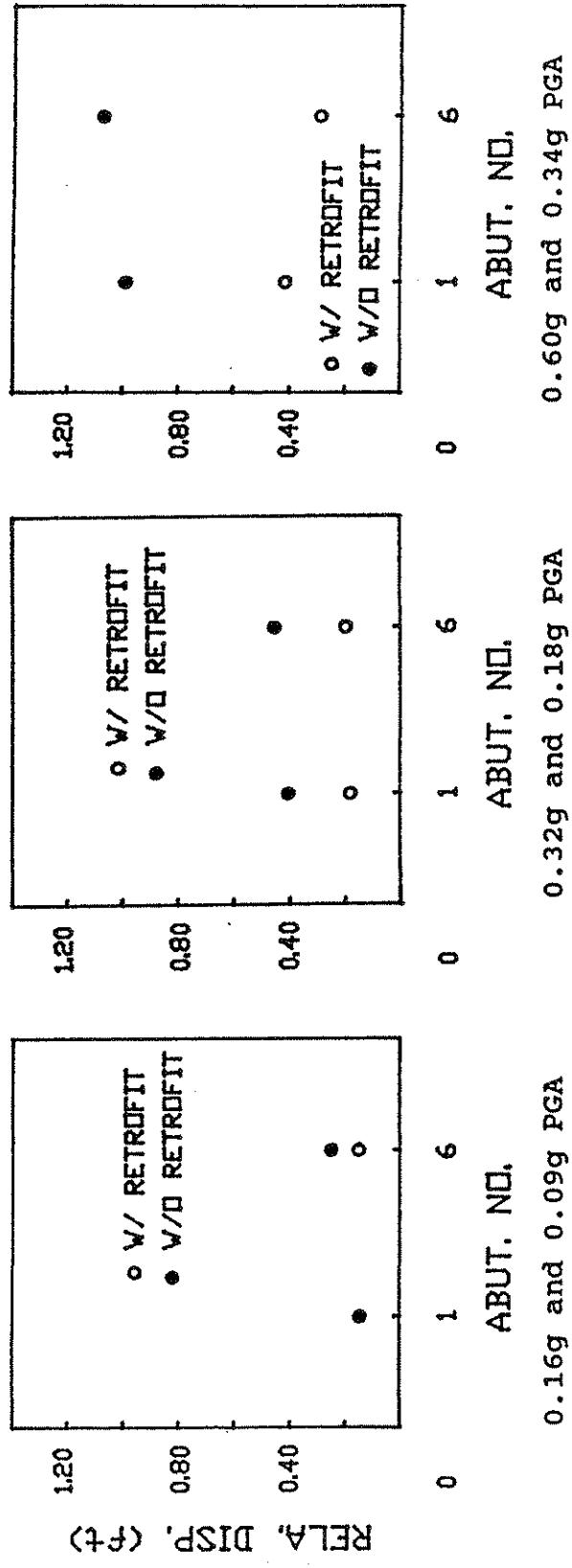
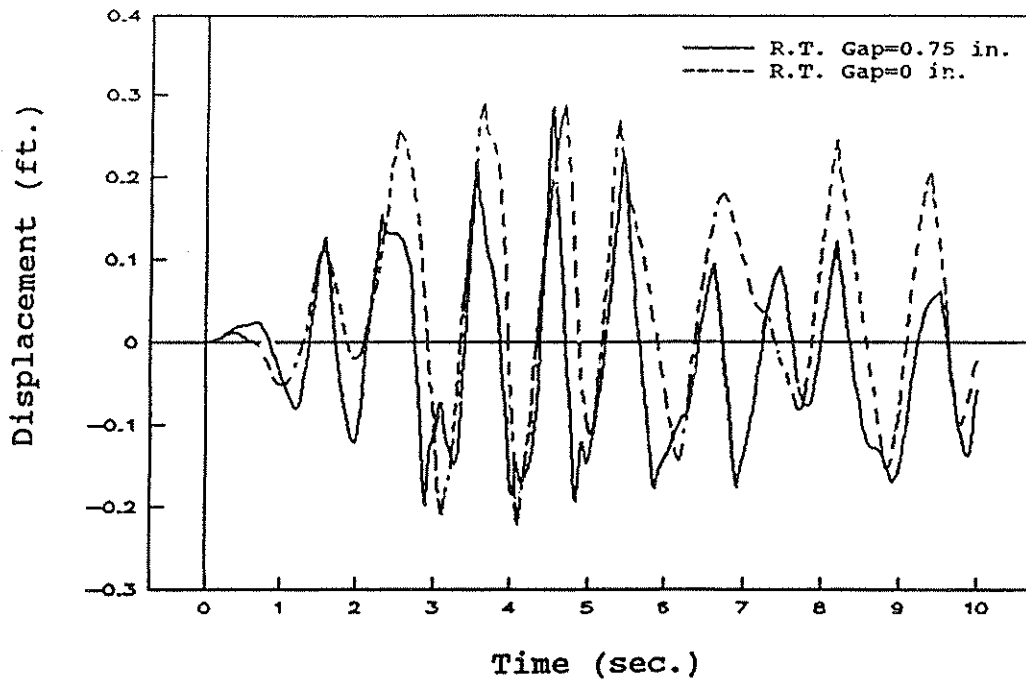
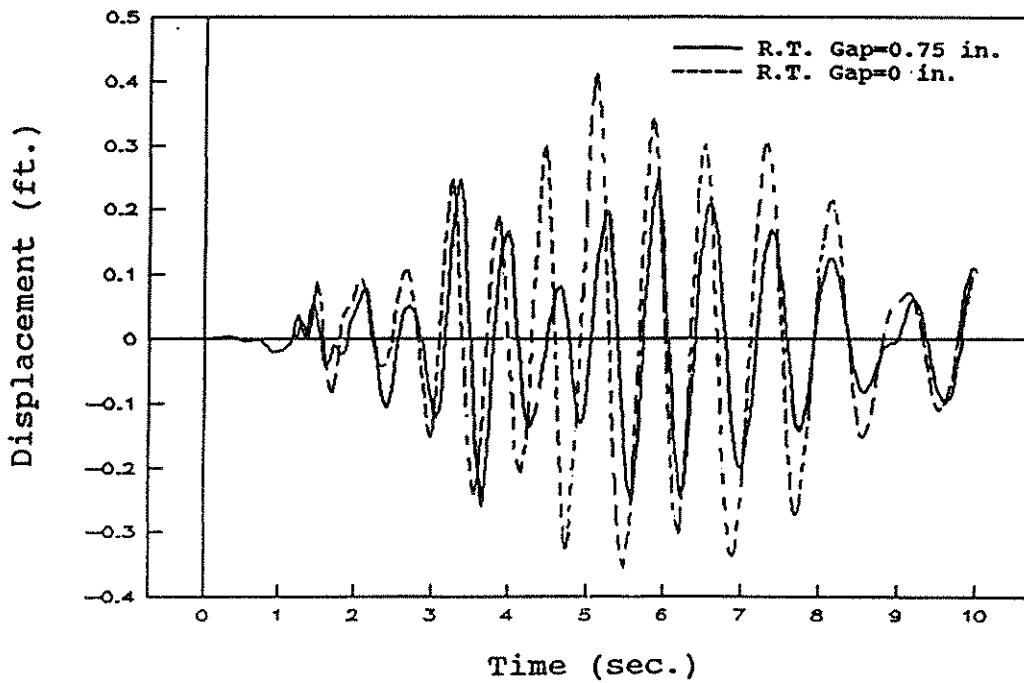


Figure 4.21 Maximum Transverse Relative Displacements at Abutments with Retrofit and without Retrofit

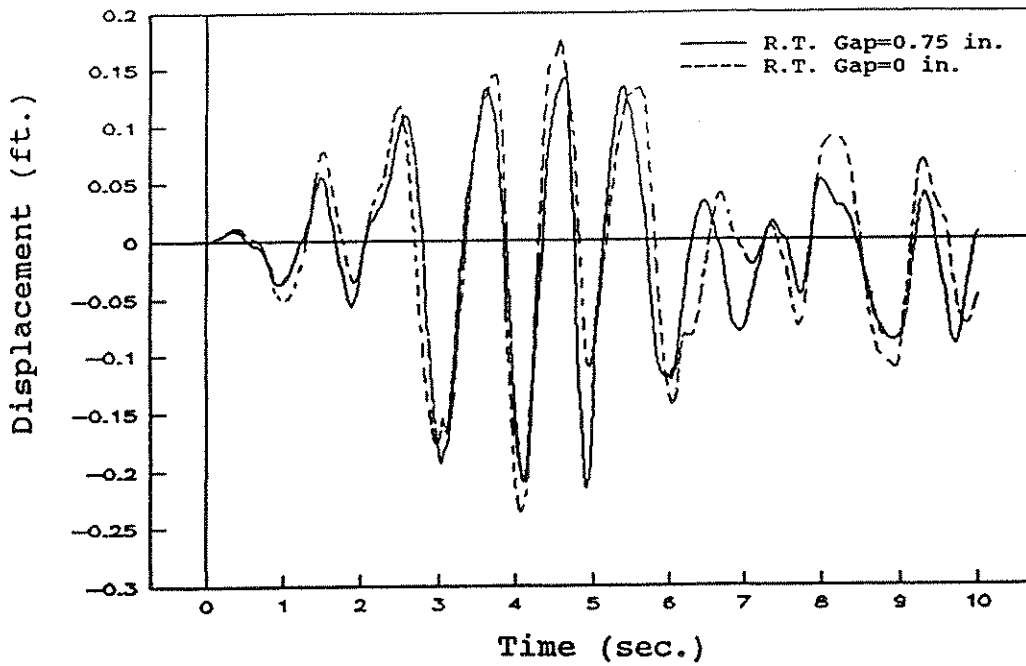


(a) Longitudinal Displacements

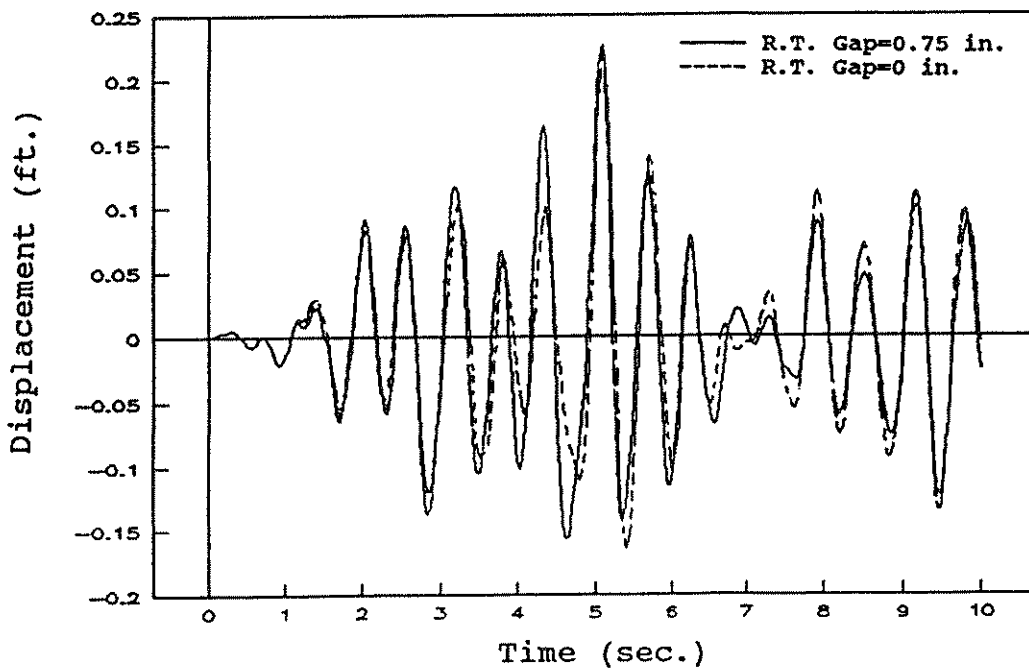


(b) Transverse Displacements

Figure 4.22 Displacement Responses of Node 4  
Zero and Non-Zero Restrainer Gaps

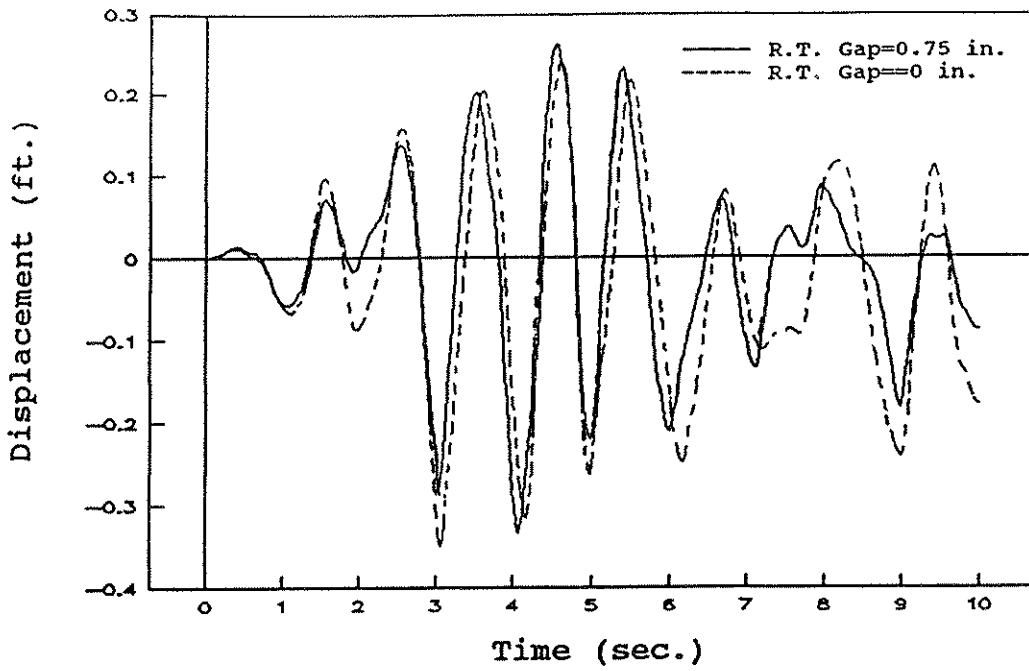


(a) Longitudinal Displacements

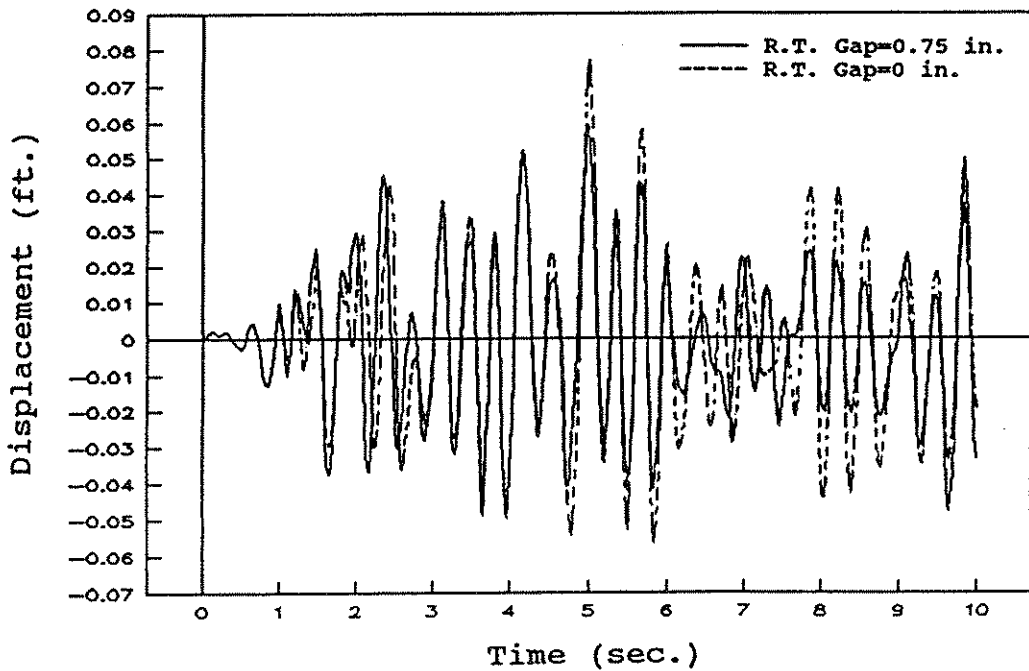


(b) Transverse Displacements

Figure 4.23 Displacement Responses of Node 22  
Zero and Non-Zero Restrainer Gaps

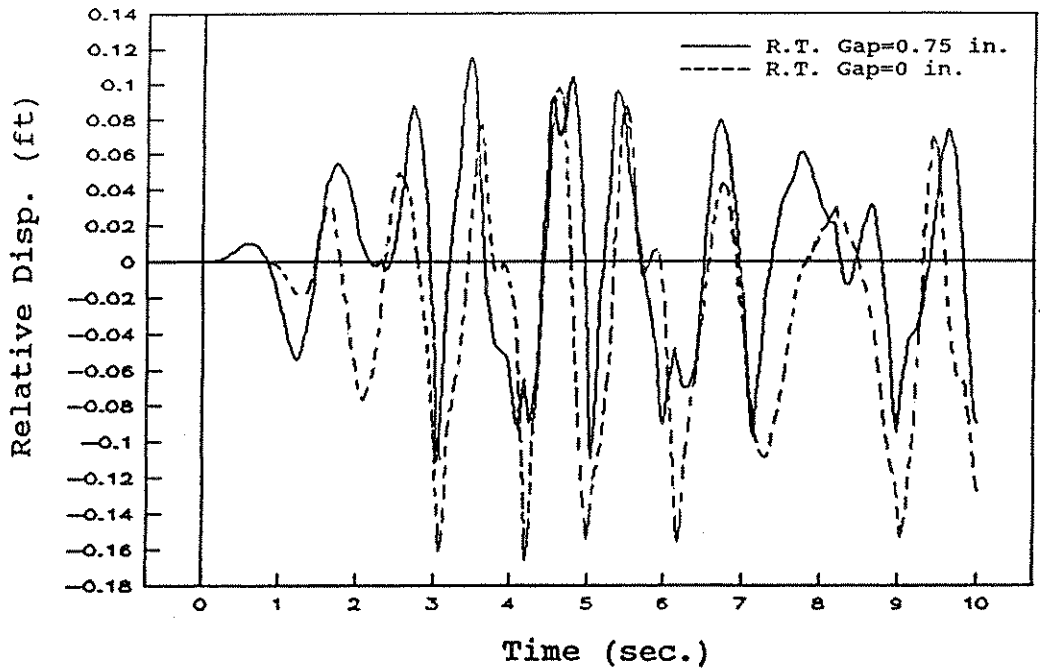


(a) Longitudinal Displacements

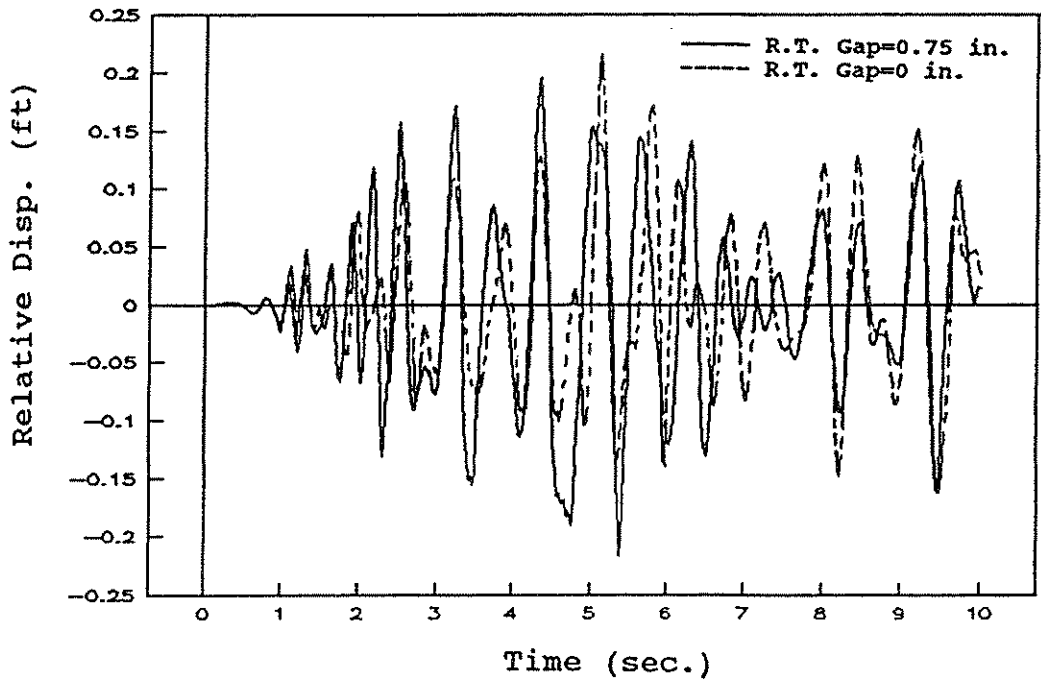


(b) Transverse Displacements

Figure 4.24 Displacement Responses of Node 62  
Zero and Non-Zero Restrainer Gaps

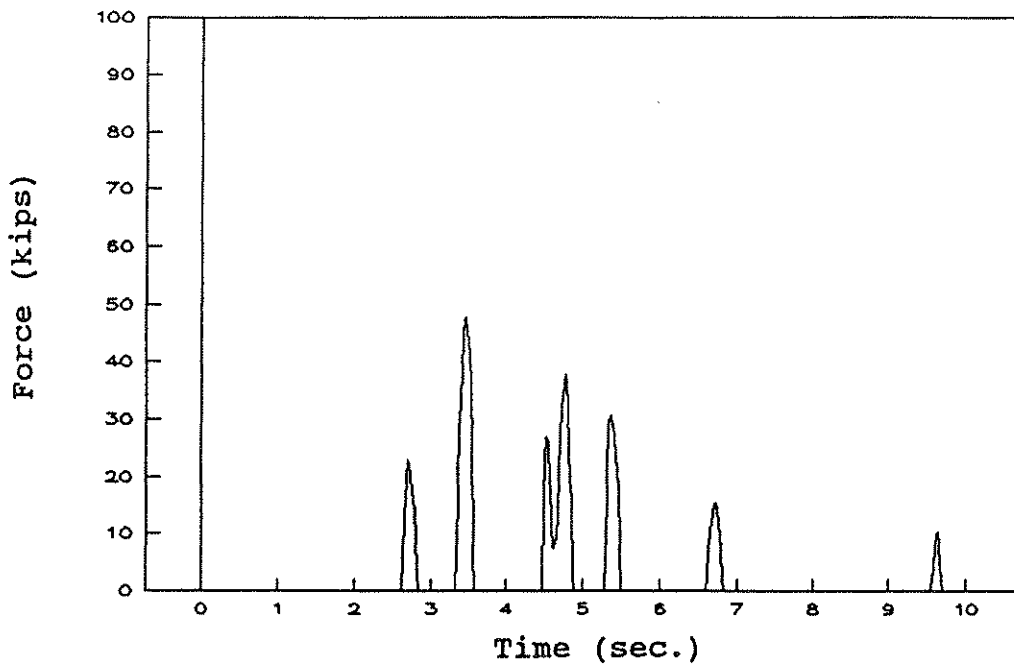


(a) Longitudinal Relative Displacements

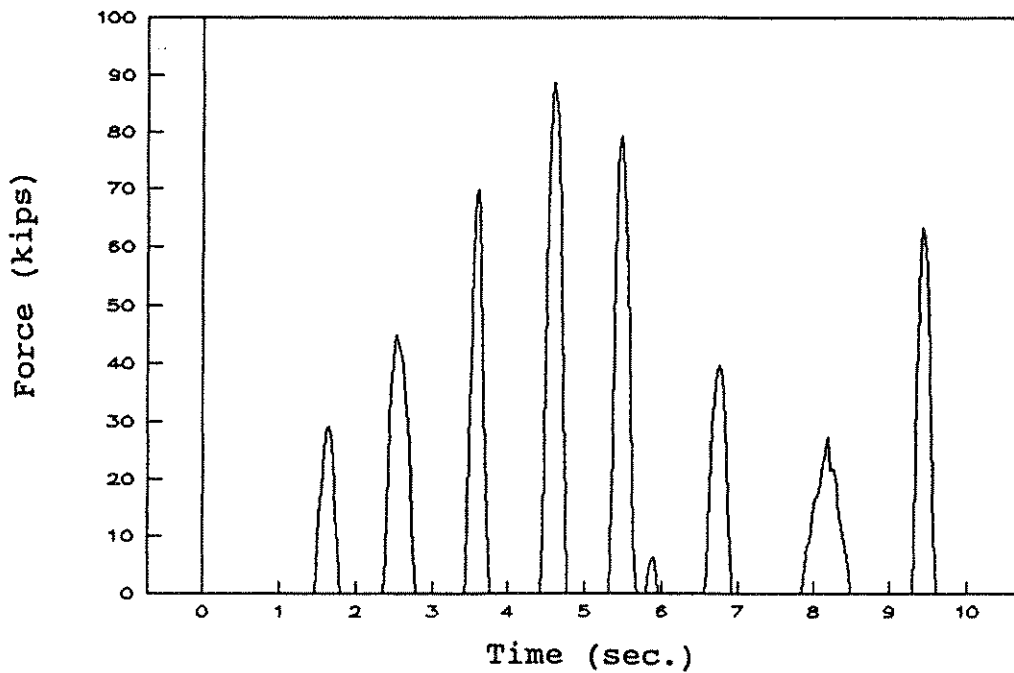


(b) Transverse Relative Displacements

Figure 4.25 Relative Displacement at Hinge 2  
Zero and Non-Zero Restrainer Gaps

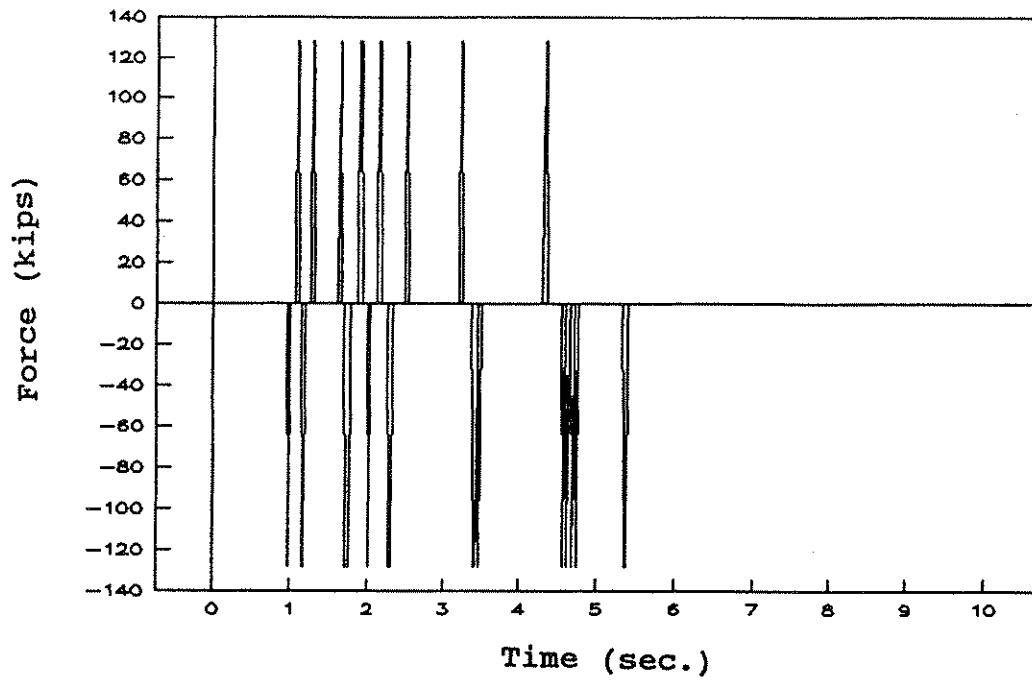


(a) Force for 0.75 in. Restrainer Gap

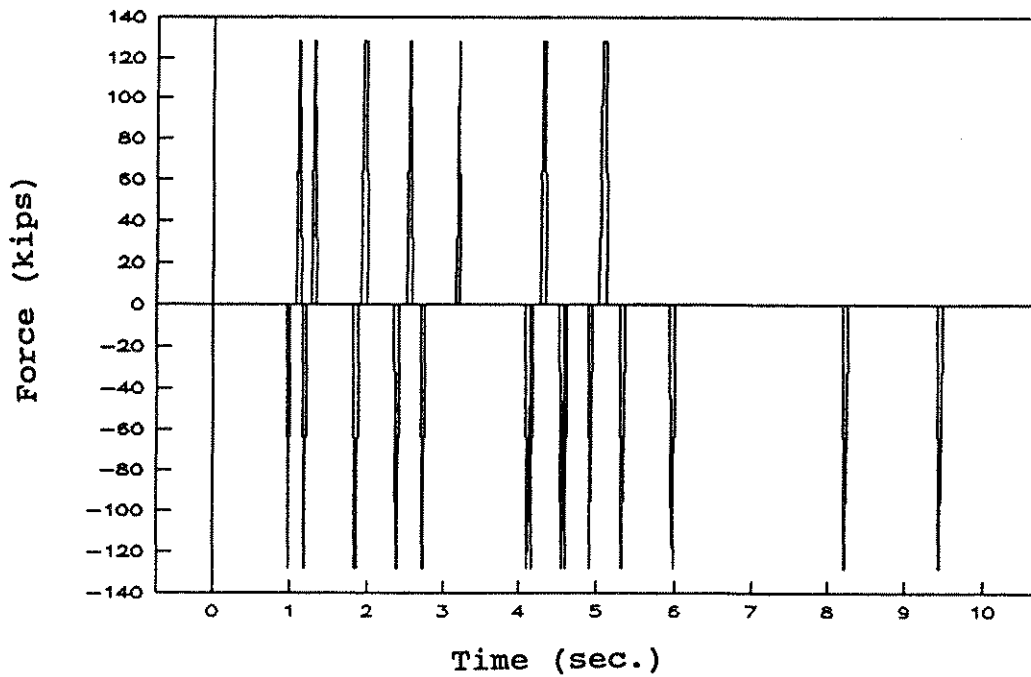


(b) Force for 0 in. Restrainer Gap

Figure 4.26 Cable Force Responses at Hinge 2  
Zero and Non-Zero Restrainer Gaps

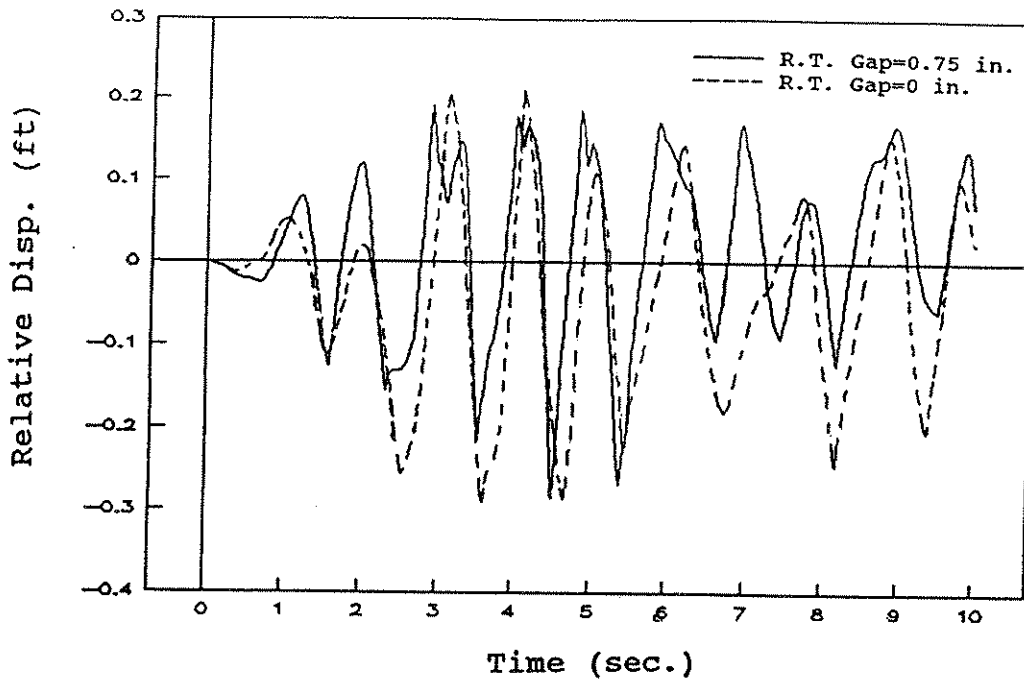


(a) Force for 0.75 in. Restrainer Gap

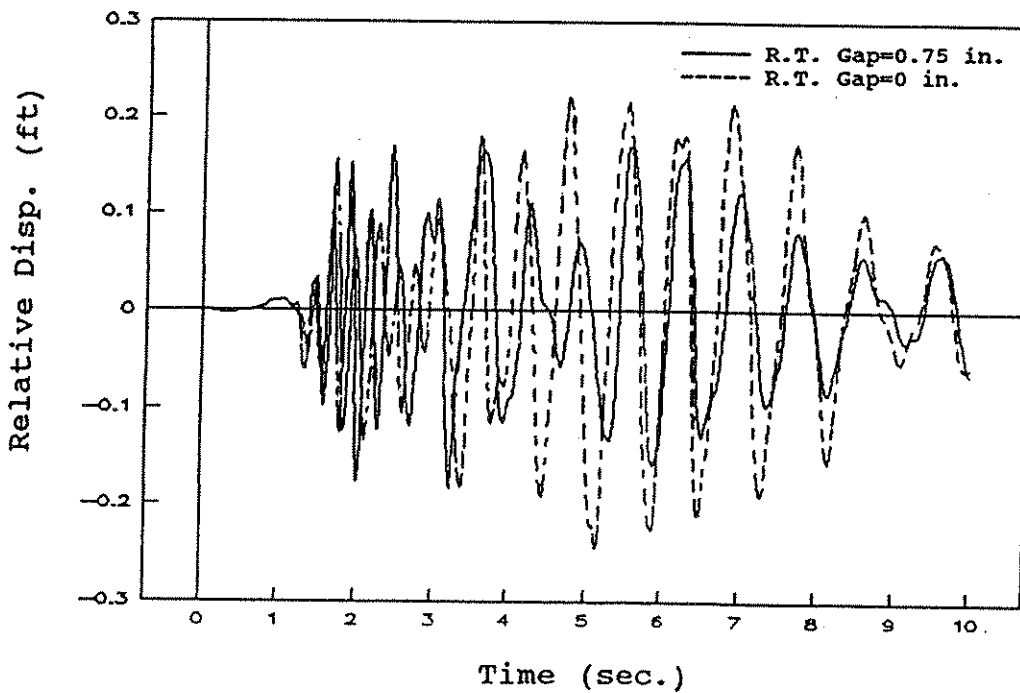


(b) Force for 0 in. Restrainer Gap

Figure 4.27 Pipe Force Responses at Hinge 2  
Zero and Non-Zero Restrainer Gaps

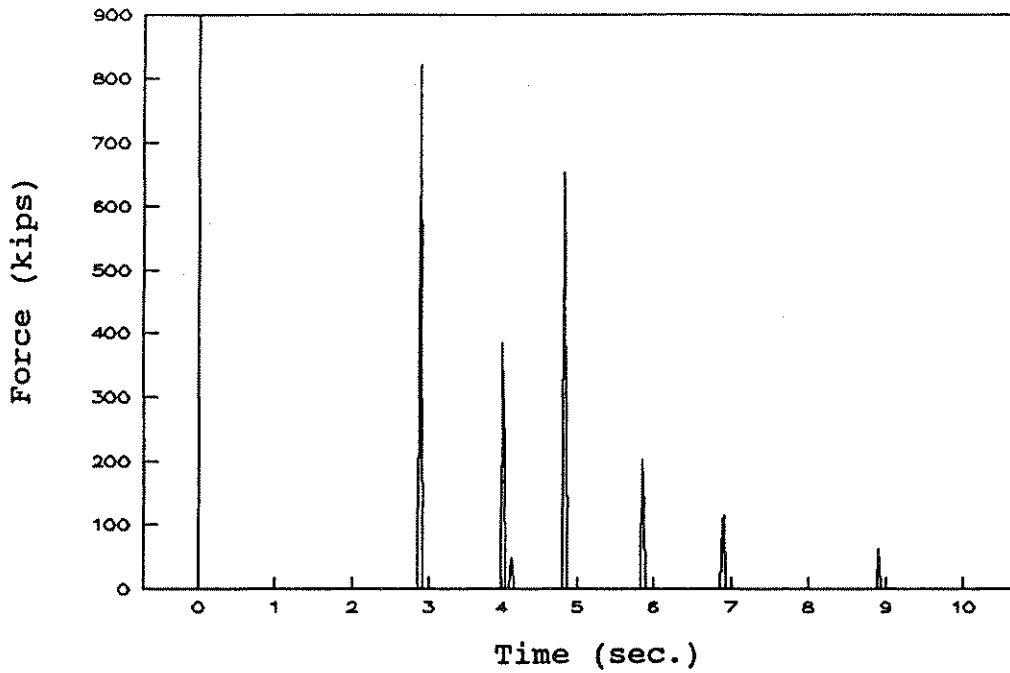


(a) Longitudinal Relative Displacements

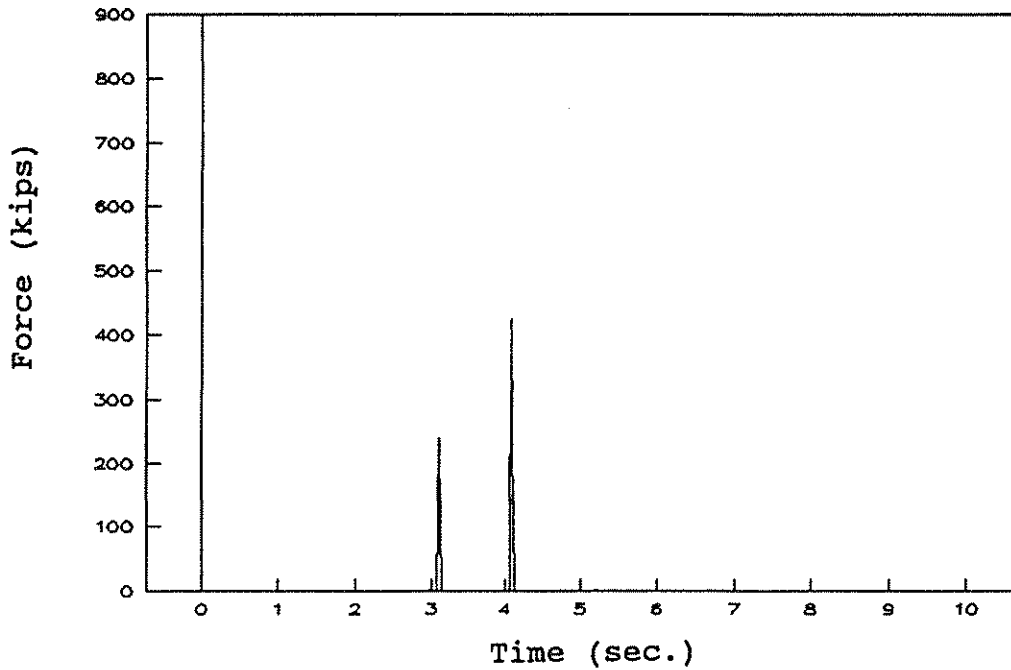


(b) Transverse Relative Displacements

Figure 4.28 Relative Displacements at Abutment 1  
Zero and Non-Zero Restrainer Gaps



(a) Force for 0.75 inch Restrainer Gap



(b) Force for 0 inch Restrainer Gap

Figure 4.29 Forces of Abutment Back Fill at Abutment 1  
Zero and Non-Zero Restrainer Gaps

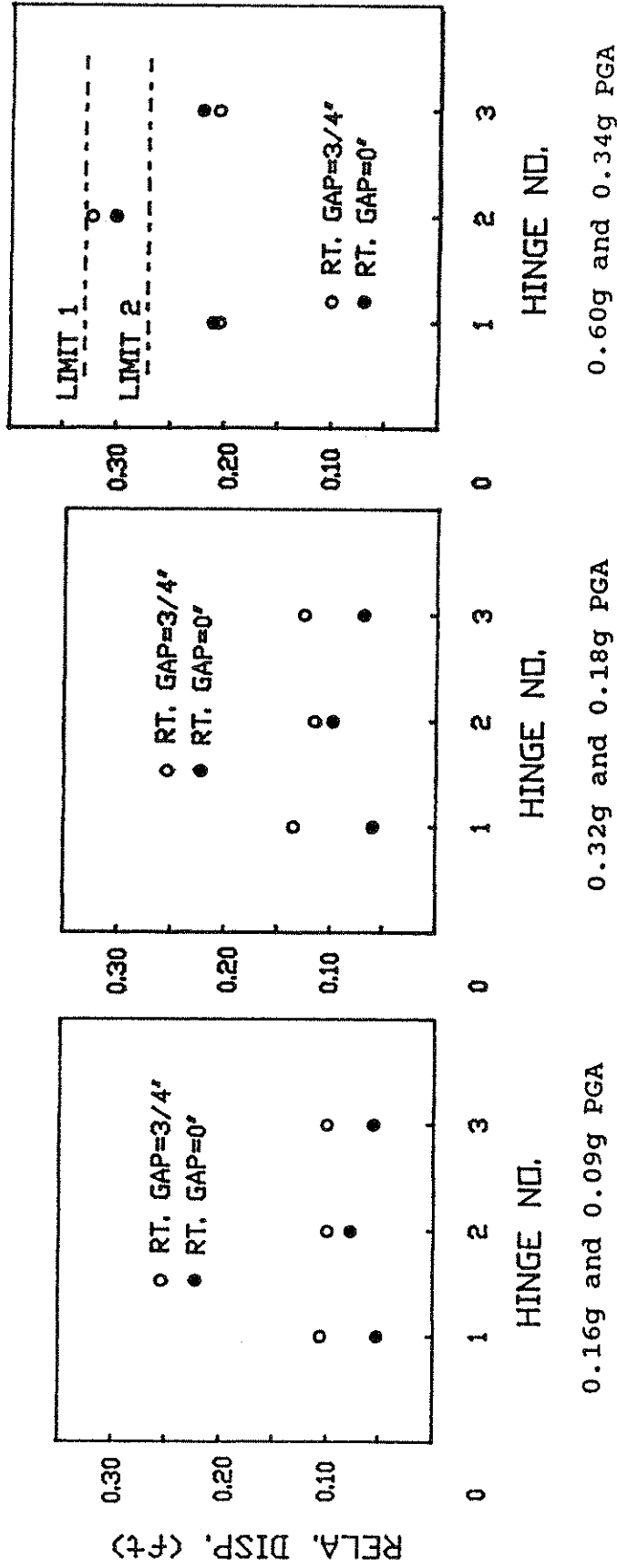


Figure 4.30 Maximum Longitudinal Relative Displacements at Hinges  
Zero and Non-Zero Restrainer Gaps

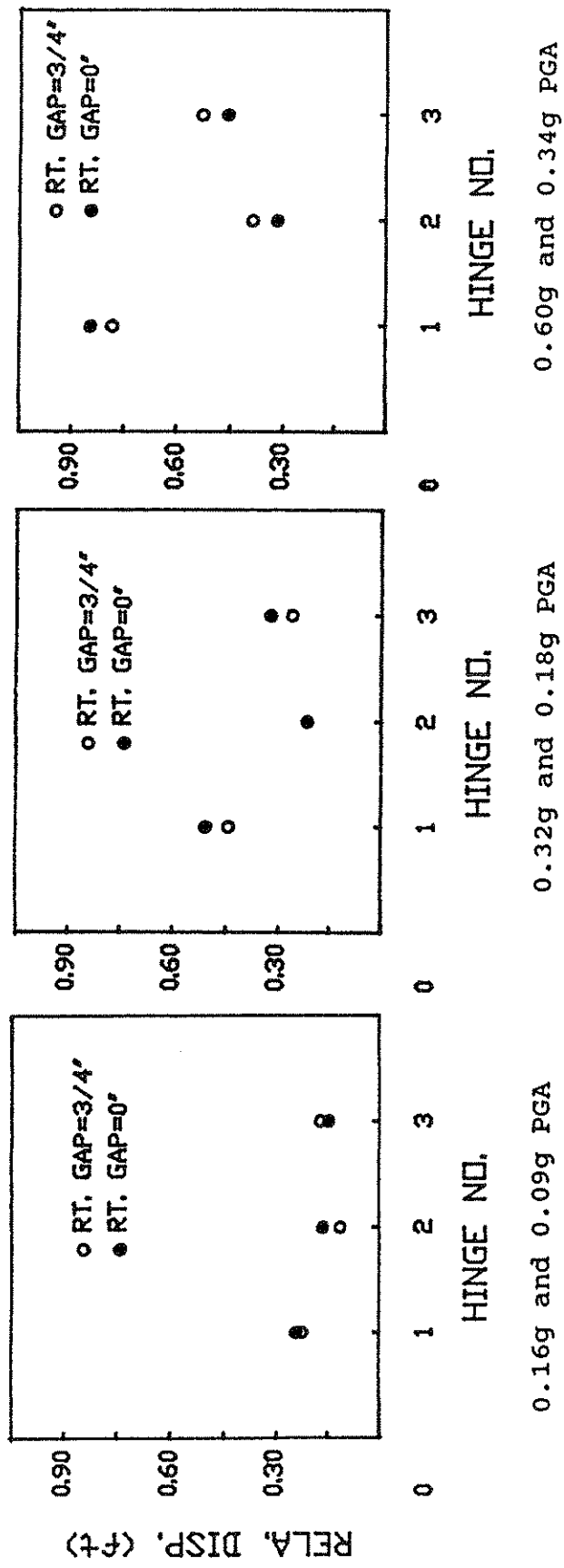


Figure 4.31 Maximum Transverse Relative Displacements at Hinges  
Zero and Non-Zero Restrainer Gaps

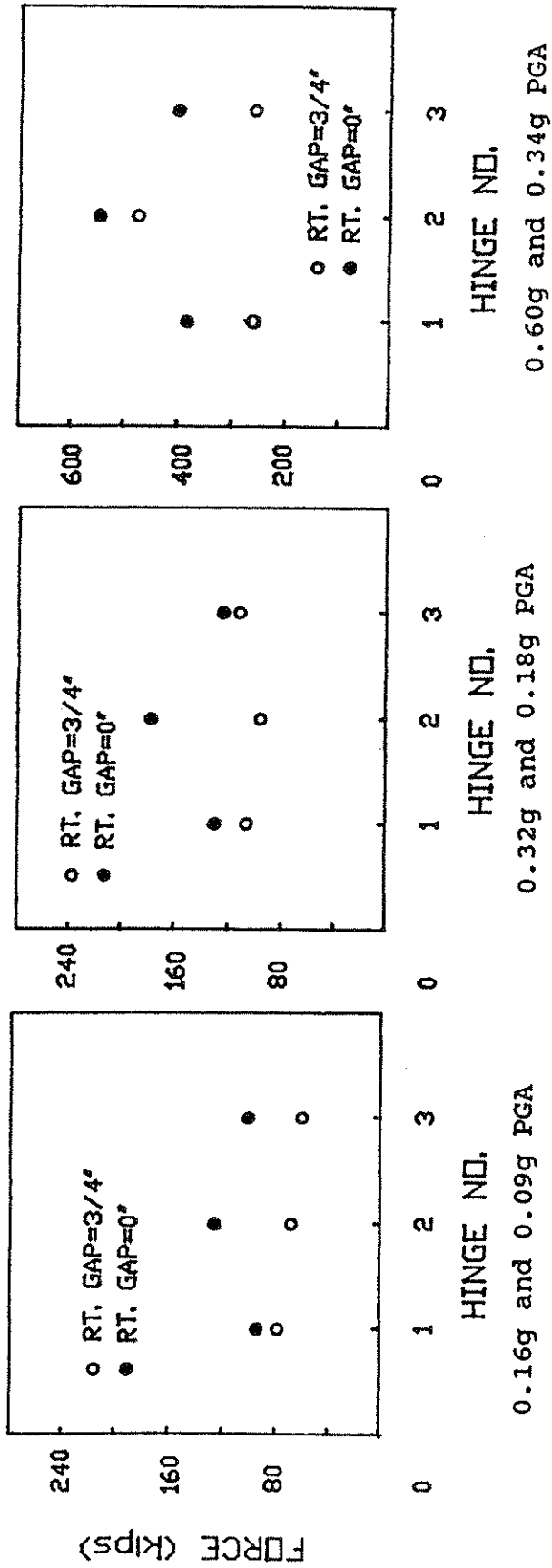


Figure 4.32 Maximum Cable Forces at Hinges  
Zero and Non-Zero Restrainer Gaps

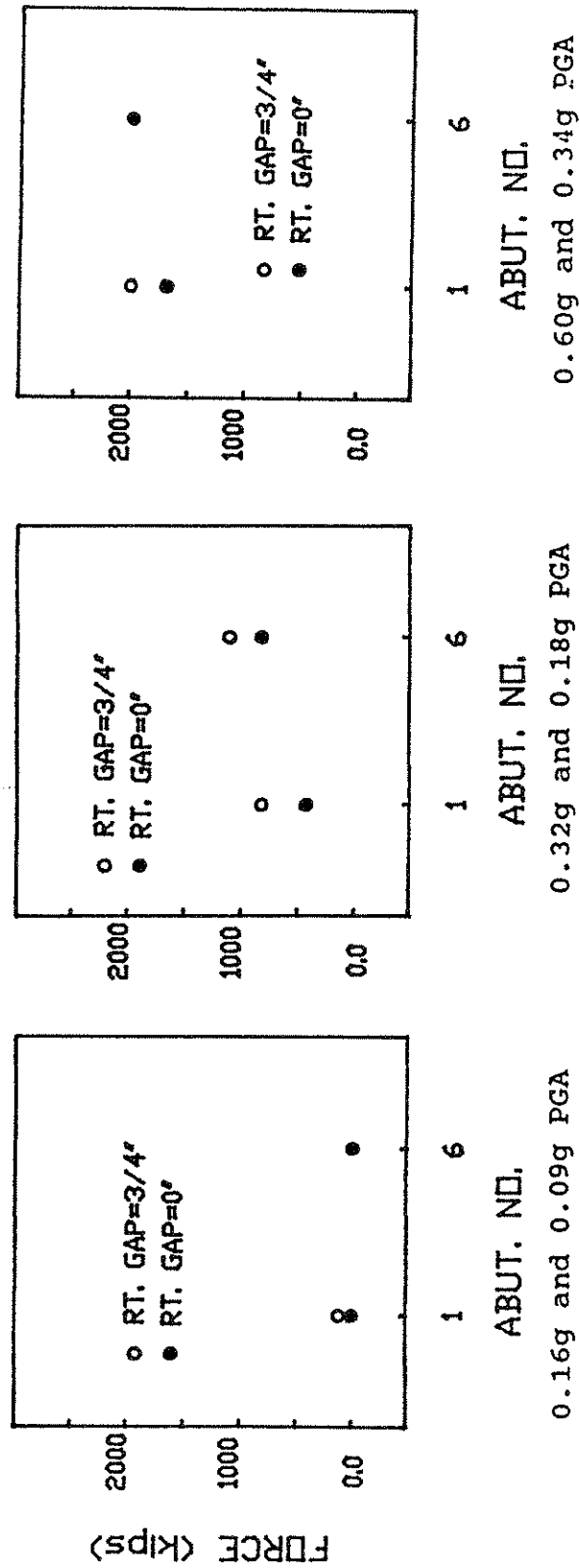


Figure 4.33 Maximum Abutment Back Fill Forces  
Zero and Non-Zero Restrainer Gaps

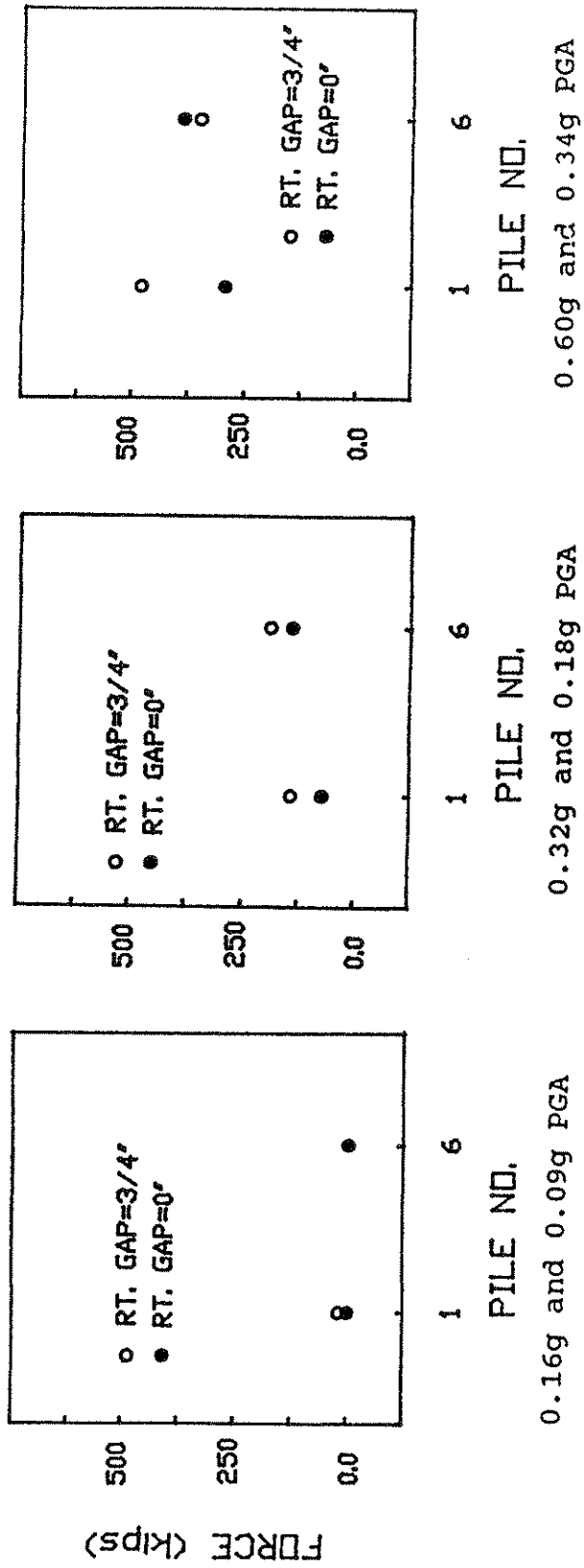


Figure 4.34 Maximum Abutment Pile Forces  
Zero and Non-Zero Restrainer Gaps

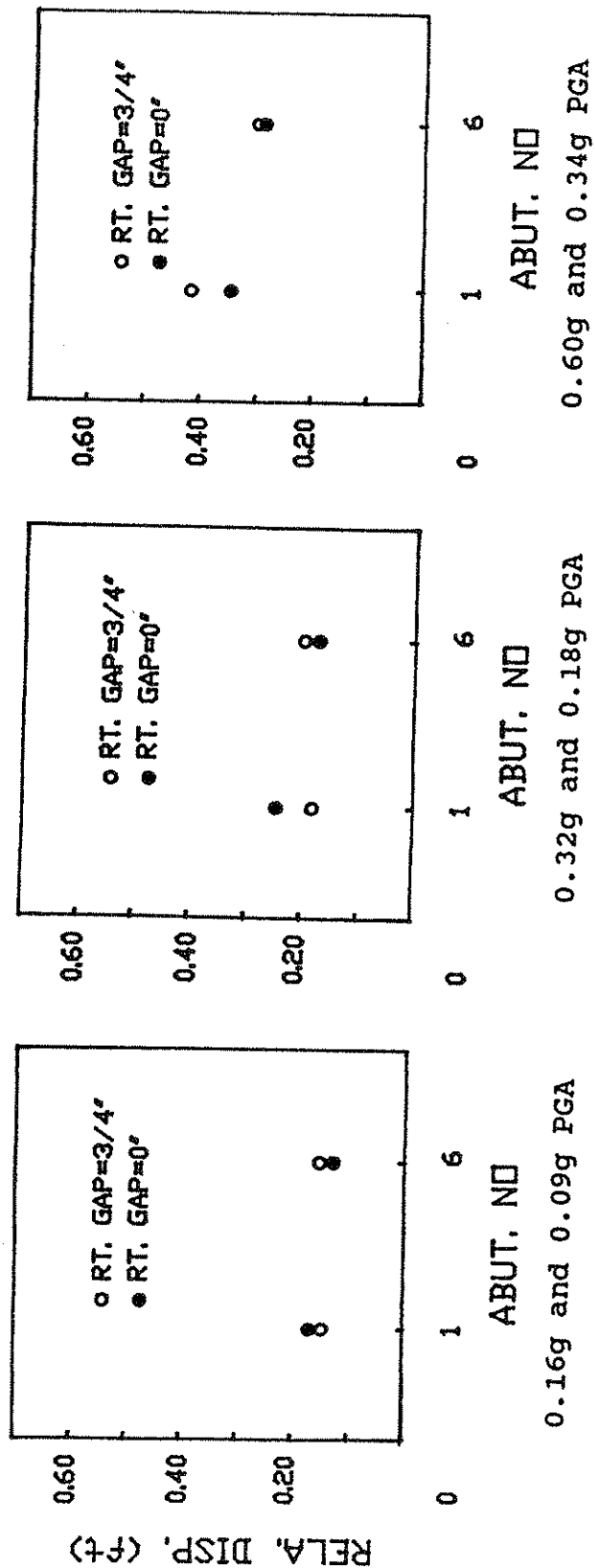


Figure 4.35 Maximum Transverse Relative Displacements at Abutments  
Zero and Non-Zero Restrainer Gaps

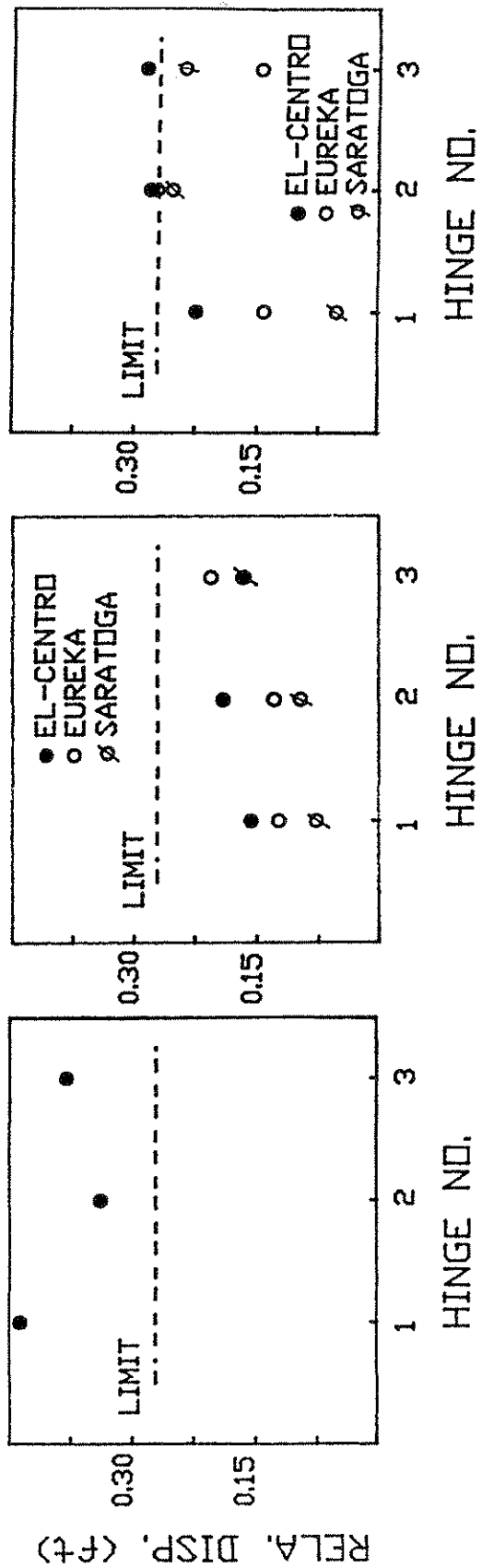


Figure 5.1 Maximum Response of Unrestrained San Gregorio Bridge  
 Figure 5.2 Maximum Response of Existing Cables  
 Figure 5.3 Maximum Response of Caltrans Design Cables

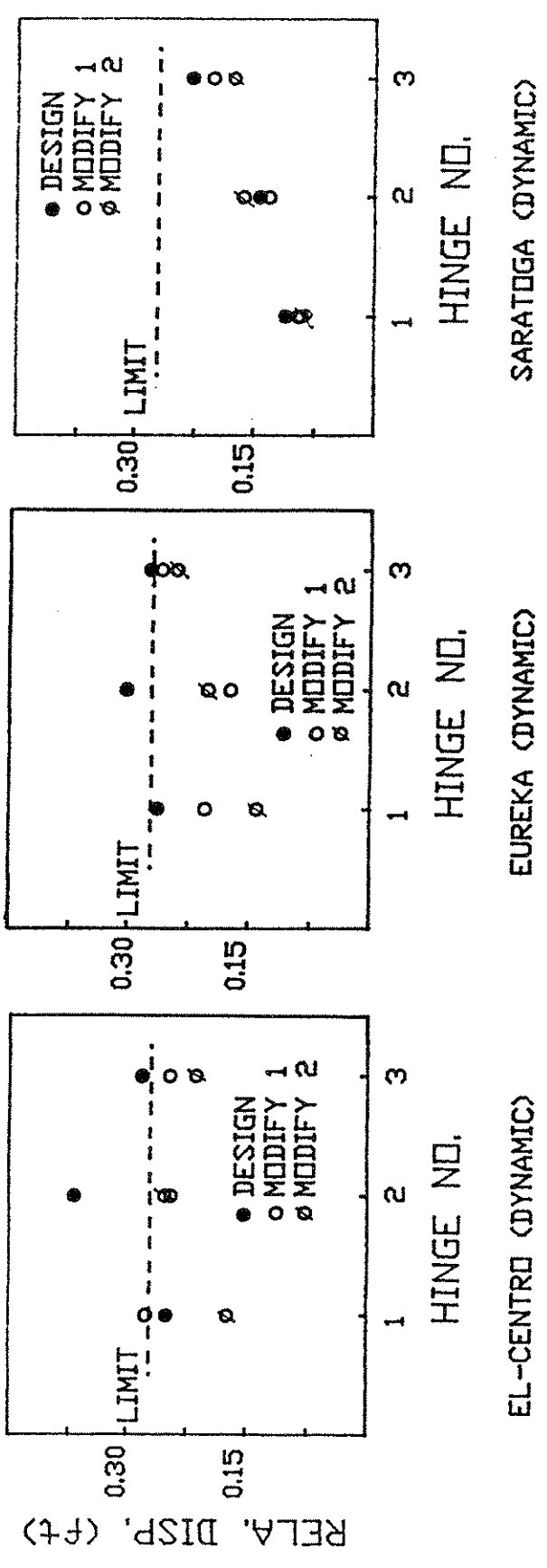


Figure 5.4 Maximum Dynamic Response of San Gregorio Bridge  
(Cables based on Dynamic-Caltrans Procedure)

## List of CCEER Publications

<u>Report No.</u>	<u>Publication</u>
CCEER-84-1	Saiidi, M., and R. A. Lawver. "User's manual for LZAK-C64, a computer program to implement the Q-model on Commodore 64." <i>Report number CCEER-84-1</i> . Reno: University of Nevada, Department of Civil Engineering. January 1984.
CCEER-84-2	Douglas, B. M., and T. Iwasaki. "Proceedings of the first USA-Japan bridge engineering workshop," held at the Public Works Research Institute, Tsukuba, Japan. <i>Report number CCEER-84-2</i> . Reno: University of Nevada, Department of Civil Engineering. April 1984.
CCEER-84-3	Saiidi, M., J. D. Hart, and B. M. Douglas. "Inelastic static and dynamic analysis of short R/C bridges subjected to lateral loads." <i>Report number CCEER-84-3</i> . Reno: University of Nevada, Department of Civil Engineering. July 1984.
CCEER-84-4	Douglas, B. "A proposed plan for a national bridge engineering laboratory." <i>Report number CCEER-84-4</i> . Reno: University of Nevada, Department of Civil Engineering. December 1984.
CCEER-85-1	Norris, G. M., and P. Abdollahiaee. "Laterally loaded pile response: Studies with the strain wedge model." <i>Report number CCEER-85-1</i> . Reno: University of Nevada, Department of Civil Engineering. April 1985.
CCEER-86-1	Ghusn, G. E., and M. Saiidi. "A simple hysteretic element for biaxial bending of R/C columns and implementation in NEABS-86." <i>Report number CCEER-86-1</i> . Reno: University of Nevada, Department of Civil Engineering. July 1986.
CCEER-86-2	Saiidi, M., R. A. Lawver, and J. D. Hart. "User's manual of ISADAB and SIBA, computer programs for nonlinear transverse analysis of highway bridges subjected to static and dynamic lateral loads." <i>Report number CCEER-86-2</i> . Reno: University of Nevada, Department of Civil Engineering. September 1986.
CCEER-87-1	Siddharthan, R. "Dynamic effective stress response of surface and embedded footings in sand." <i>Report number CCEER-87-1</i> . Reno: University of Nevada, Department of Civil Engineering. June 1987.
CCEER-87-2	Norris, G., and R. Sack. "Lateral and rotational stiffness of pile groups for seismic analysis of highway bridges." <i>Report number CCEER-87-2</i> . Reno: University of Nevada, Department of Civil Engineering. June 1987.
CCEER-88-1	Orie, J., and M. Saiidi. "A preliminary study of one-way reinforced concrete pier hinges subjected to shear and flexure." <i>Report number CCEER-88-1</i> . Reno: University of Nevada, Department of Civil Engineering. January 1988.
CCEER-88-2	Orie, D., M. Saiidi, and B. Douglas. "A micro-CAD system for seismic design of regular highway bridges." <i>Report number CCEER-88-2</i> . Reno: University of Nevada, Department of Civil Engineering. June 1988.

- CCEER-88-3      Orié, D., and M. Saiidi. "User's manual for Micro-SARB, a microcomputer program for seismic analysis of regular highway bridges." *Report number CCEER-88-3*. Reno: University of Nevada, Department of Civil Engineering. October 1988.
- CCEER-89-1      Douglas, B., M. Saiidi, R. Hayes, and G. Holcomb. "A comprehensive study of the loads and pressures exerted on wall forms by the placement of concrete." *Report number CCEER-89-1*. Reno: University of Nevada, Department of Civil Engineering. February 1989.
- CCEER-89-2a      Richardson, J., and B. Douglas. "Dynamic response analysis of the Dominion Road Bridge test data." *Report number CCEER-89-2*. Reno: University of Nevada, Department of Civil Engineering. March 1989.
- CCEER-89-2b      Vrontinos, S., M. Saiidi, and B. Douglas. "A simple model to predict the ultimate response of R/C beams with concrete overlays." *Report number CCEER-89-2*. Reno: University of Nevada, Department of Civil Engineering. June 1989.
- CCEER-89-3      Ebrahimpour, A., and P. Jagadish. "Statistical modeling of bridge traffic loads: A case study." *Report number CCEER-89-3*. Reno: University of Nevada, Department of Civil Engineering. December 1989.
- CCEER-89-4      Shields, J., and M. Saiidi. "Direct field measurement of prestress losses in box girder bridges." *Report number CCEER-89-4*. Reno: University of Nevada, Department of Civil Engineering. December 1989.
- CCEER-90-1      Saiidi, M., E. Maragakis, G. Ghusn, Jr., Y. Jiang, and D. Schwartz. "Survey and evaluation of Nevada's transportation infrastructure, task 7.2—highway bridges, final report." *Report number CCEER-90-1*. Reno: University of Nevada, Department of Civil Engineering. October 1990.
- CCEER-90-2      Abdel-Ghaffar, S., E. Maragakis, and M. Saiidi. "Analysis of the response of reinforced concrete structures during the Whittier earthquake of 1987." *Report number CCEER-90-2*. Reno: University of Nevada, Department of Civil Engineering. October 1990.
- CCEER-91-1      Saiidi, M., E. Hwang, E. Maragakis, and B. Douglas. "Dynamic testing and analysis of the Flamingo Road Interchange." *Report number CCEER-91-1*. Reno: University of Nevada, Department of Civil Engineering. February 1991.
- CCEER-91-2      Norris, G., R. Siddharthan, Z. Zafir, S. Abdel-Ghaffar, and P. Gowda. "Soil-foundation-structure behavior at the Oakland Outer Harbor Wharf." *Report number CCEER-91-2*. Reno: University of Nevada, Department of Civil Engineering. July 1991.
- CCEER-91-3      Norris, G. M. "Seismic lateral and rotational pile foundation stiffness at Cypress." *Report number CCEER-91-3*. Reno: University of Nevada, Department of Civil Engineering. August 1991.
- CCEER-91-4      O'Connor, D. N., and M. Saiidi. "A study of protective overlays for highway bridge decks in Nevada, with emphasis on polyester-styrene polymer concrete." *Report number CCEER-91-4*. Reno: University of Nevada, Department of Civil Engineering. October 1991.

- CCEER-91-5 O'Connor, D. N., and M. Saiidi. "Laboratory studies of polyester-styrene polymer concrete engineering properties." *Report number CCEER-91-5*. Reno: University of Nevada, Department of Civil Engineering. November 1991.
- CCEER-92-1 Straw, D. L., and M. "Saiid" Saiidi. "Scale model testing of one-way reinforced concrete pier hinges subjected to combined axial force, shear and flexure." *Report number CCEER-92-1*, ed. by D. N. O'Connor. Reno: University of Nevada, Department of Civil Engineering. March 1992.
- CCEER-92-2 Wehbe, N., M. Saiidi, and F. Gordaninejad. "Basic behavior of composite sections made of concrete slabs and graphite epoxy beams." *Report number CCEER-92-2*. Reno: University of Nevada, Department of Civil Engineering. August 1992.
- CCEER-92-3 Saiidi, M., and E. Hutchens. "A study of prestress changes in a post-tensioned bridge during the first 30 months." *Report number CCEER-92-3*. Reno: University of Nevada, Department of Civil Engineering. April 1992.
- CCEER-92-4 Saiidi, M., B. Douglas, S. Feng, E. Hwang, and E. Maragakis. "Effects of axial force on frequency of prestressed concrete bridges." *Report number CCEER-92-4*. Reno: University of Nevada, Department of Civil Engineering. August 1992.
- CCEER-92-5 Siddharthan, R., and Zafir, Z. "Response of layered deposits to traveling surface pressure waves." *Report number CCEER-92-5*. Reno: University of Nevada, Department of Civil Engineering. September 1992.
- CCEER-92-6 Norris, G., and Zafir, Z. "Liquefaction and residual strength of loose sands from drained triaxial tests." *Report number CCEER-92-6*. Reno: University of Nevada, Department of Civil Engineering. September 1992.
- CCEER-92-7 Douglas, B. "Some thoughts regarding the improvement of the University of Nevada, Reno's national academic standing." *Report number CCEER-92-7*. Reno: University of Nevada, Department of Civil Engineering. September 1992.
- CCEER-92-8 Saiidi, M., E. Maragakis, and S. Feng. "An evaluation of the current Caltrans seismic restrainer design method." *Report number CCEER-92-8*. Reno: University of Nevada, Department of Civil Engineering. October 1992.
- CCEER-92-9 O'Connor, D. N., M. Saiidi, and E. A. Maragakis. "Effect of hinge restrainers on the response of the Madrone Drive Undercrossing during the Loma Prieta earthquake." *Report number CCEER-92-9*. Reno: University of Nevada, Department of Civil Engineering. February 1993.
- CCEER-92-10 O'Connor, D. N., and M. Saiidi. "Laboratory studies of polyester concrete: Compressive strength at elevated temperatures and following temperature cycling, bond strength to portland cement concrete, and modulus of elasticity." *Report number CCEER-92-10*. Reno: University of Nevada, Department of Civil Engineering. December 1992.